*G*eological *F*ield *T*rips

Igneous evolutions across the Ivrea crustal section: the Permian Sesia Magmatic System and the Triassic Finero intrusion and mantle

Società Geologica Italiana

ISPRA
Istituto Superiore per la Protezione
e la Ricerca Ambientale

SERVIZIO GEOLOGICO D'ITALIA
Organo Cartografico dello Stato (legge N°68 del 2-2-1960)
Dipartimento Difesa del Suolo

GFT - *Geological Field Trips*

Igneous evolutions across the Ivrea crustal section: the Permian Sesia Magmatic System and the Triassic Finero intrusion and mantle

Goldschmidt Conference – Florence, Italy – 2013 August 25th-30th

Maurizio Mazzucchelli[1], James E. Quick[2], Silvano Sinigoi[3], Alberto Zanetti[4], Tommaso Giovanardi[1]

[1] Dipartimento di Scienze Chimiche e Geologiche, Università degli Studi di Modena e Reggio Emilia, Modena (Italy)
[2] Southern Methodist University, Dallas, Texas, USA
[3] Dipartimento di Matematica e Geoscienze, Università degli Studi di Trieste, Trieste (Italy)
[4] Istituto di Geoscienze e Georisorse, CNR, Pavia (Italy)

Corresponding Author e-mail address: maurizio.mazzucchelli@unimore.it

INDEX

Information

Excursion notes

Itinerary

References

Safety

The aim of this document is to collate key information into a simple format for use by field and on-call staff in the event of an incident. Safety in the field is closely related to awareness of potential difficulties, fitness and use of appropriate equipment. Safety is a personal responsibility and all participants should be aware of the following issues.
- The excursion takes place at relatively low altitude (between 300 and 600 meters above sea level in the first two days and between 800 and 1100 meters a.s.l. in the third day). Most of the outcrops are along the road and we will not make long walks. However, some downhills from roads through paths into creek beds are scheduled. The walk along creeks can become difficult in case of rain.

- All participants require comfortable walking boots. Trainer or running shoes are unsuitable footwear in the field.

- A waterproof coat/jacket is essential. The average weather conditions are the following: Spring: T min = 5 °C, T max = 25 °C, Rainfall = 104 mm per month, Humidity = 75 %; Summer: T min = 12 °C, T max = 28 °C, Rainfall = 71 mm per month, Humidity = 75 %, Sudden storms can be frequent;

Fall: T min = 2 °C, T max = 12 °C, Rainfall = 88 mm per month, Humidity = 80 %.

- Vehicle will carry one basic first aid kit.

- Mobile/cellular phone coverage is good although in some places it can be absent.

Local emergency services

Outline what is available with contact Number:
- Medical Emergency/Ambulance (valid all over Italy): 118 - Police (valid all over Italy): 113 or 112
- Fire Brigade (valid all over Italy): 115
- Local Medical Facilities: see nearest medical centre below.
Arrival day, 1st and 2nd days: Ospedale SS.Pietro e Paolo, Piazzale Lora, Borgosesia (VC), Tel.: 0163-203111.
3rd day: Ospedale San Biagio, Via Caduti 1, Domodossola (VB), Tel.: 0324-491233.

Informazioni generali

Durata: 4 giorni (giorno di arrivo a Varallo Sesia + 3 giorni di escursione).
Programma dell'escursione (Figg. B, C, D, E, F).
Giorno di arrivo – Fig. B) E' consigliabile alloggiare a Varallo Sesia. Un elenco degli Hotel di Varallo Sesia è disponibile all'indirizzo: www.comune.varallo.vc.it
Varallo Sesia è facilmente raggiungibile in auto, o in treno sia dall'Aeroporto di Milano Malpensa che dalla Stazione Ferroviaria di Milano Rogoredo.
1° giorno – Fig. C) Varallo Sesia (VC), Scopa (VC), Balmuccia (VC), Isola (VC), Varallo Sesia (VC), Agnona (VC), Postua (VC), Prato Sesia (VC), Varallo Sesia (VC) (pernottamento).
2° giorno – Fig. C) Varallo Sesia (VC), Trivero e Val Sessera (BI), Valle Mosso (BI), Curino-San Bononio (BI), Borgomanero (NO), Varallo Sesia (VC) (pernottamento).
3° giorno – Figg. D, E) Varallo Sesia (VC), Finero (VB). Al termine dell'escursione si può raggiungere il centro di Santa Maria Maggiore (Val Vigezzo, VB), dove si può facilmente raggiungere l'Aeroporto di Milano Malpensa o la Stazione Ferroviaria di Milano Rogoredo, in auto, bus o treno.

General info

Duration: 4 days (Day of arrival of participants + 3 days of field trip).
Field trip program (Figs. B, C, D, E).
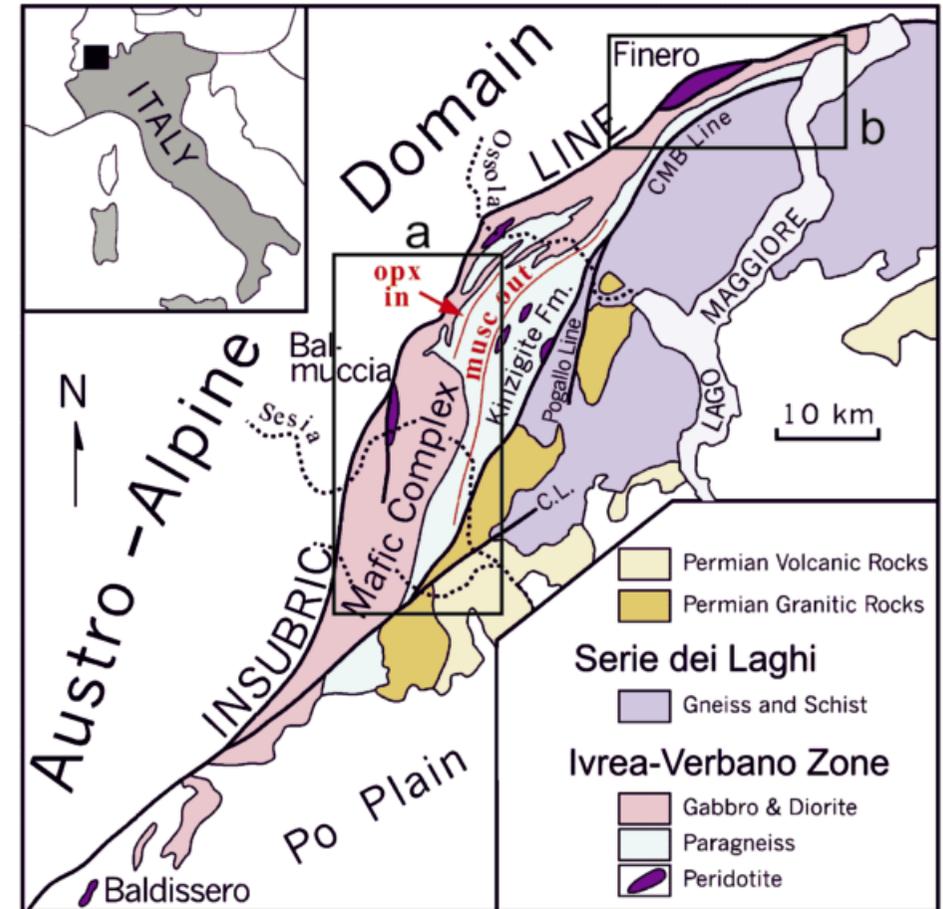
Fig. A – Mappa schematica della Zona Ivrea-Verbano, da Zingg (1983) e modificata secondo Sinigoi et al. (2010); **a)** area tipo-Sesia, **b)** area tipo-Finero. *Sketch map in the vicinity of the Ivrea-Verbano Zone, based on Zingg (1983) and modified after Sinigoi et al. (2010); **a)** Sesia area, **b)** Finero area.*

Fig. B – Posizione geografica di Varallo Sesia (VC) e itinerario automobilistico dall'Aeroporto di Milano Malpensa o dalla Stazione Ferroviaria di Milano Rogoredo all'hotel (giorno di arrivo dei partecipanti).
Geographic Location of Varallo Sesia (VC) and car itinerary from Milano Malpensa Airport or Milano Rogoredo Railway Station to the hotel (day of arrival of the participants).
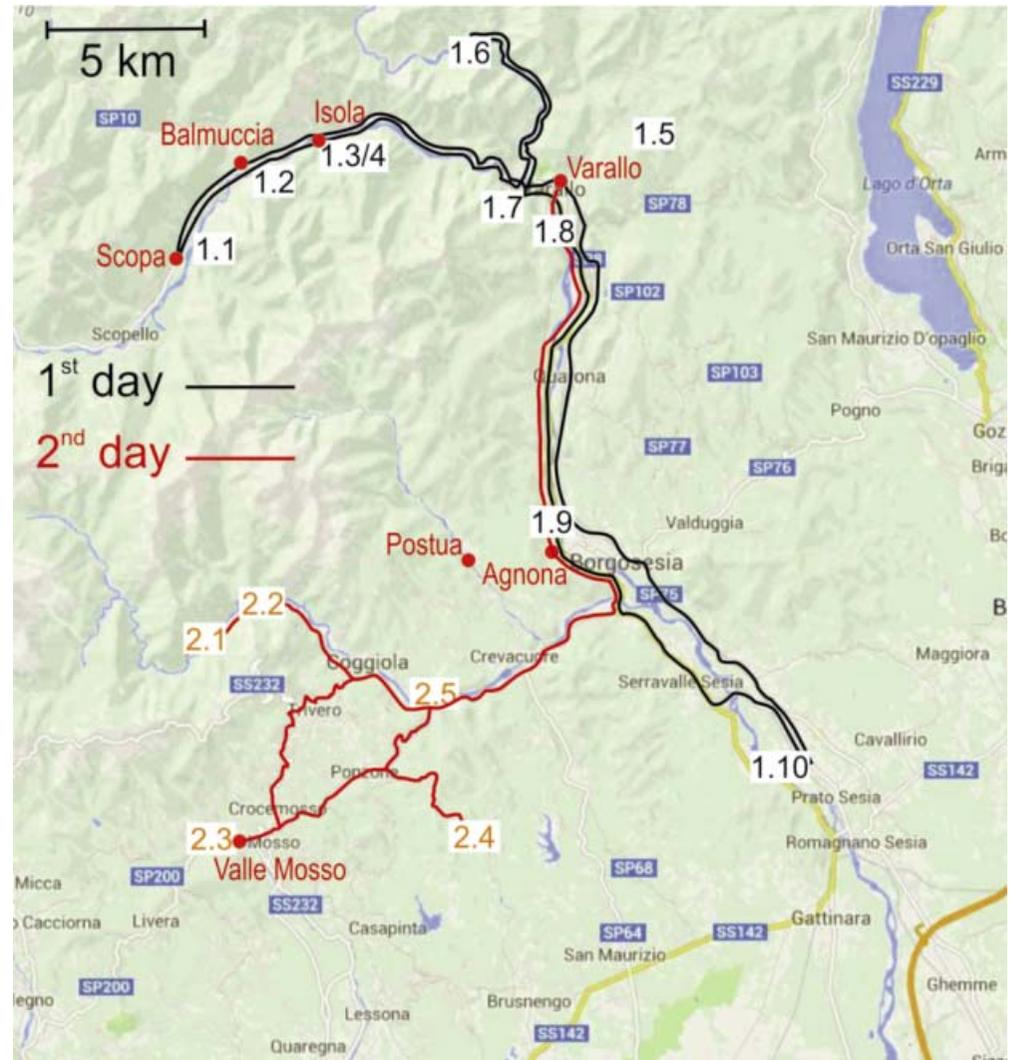
Fig. C – Itinerari del 1° (in nero) e 2° giorno (in rosso) con l'ubicazione degli Stop.
Itinerary of the 1st (black) and 2nd (red) day, along with the Stop positions.

Day of arrival – Fig. B) It is recommended to stay in Varallo Sesia. A list of hotels in Varallo Sesia is available at the following website: www.comune.varallo.vc.it

Varallo Sesia is accessible by car or train, both from Milano Malpensa Airport or Milano Rogoredo Railway Station.

1st day – Fig. C) Varallo Sesia (VC), Scopa (VC), Balmuccia (VC), Isola (VC), Varallo Sesia (VC), Agnona (VC), Postua (VC), Prato Sesia (VC), Varallo Sesia (VC) (night accomodation).

2nd day – Fig. C) Varallo Sesia (VC), Trivero e Val Sessera (BI), Valle Mosso (BI), Curino-San Bononio (BI), Borgomanero (NO), Varallo Sesia (VC) (night accomodation).

3rd day – Figs. D, E) Varallo Sesia (VC), Finero (VB). At the end of the excursion you can reach the center of Santa Maria Maggiore (Val Vigezzo, VB), where you can easily reach the Milano Malpensa Airport or the Milano Rogoredo Railway Station, by car, bus or train.

Fig. D - Itinerari del 3° giorno: Varallo–Finero.
Itinerary of the 3rd day: Varallo-Finero.
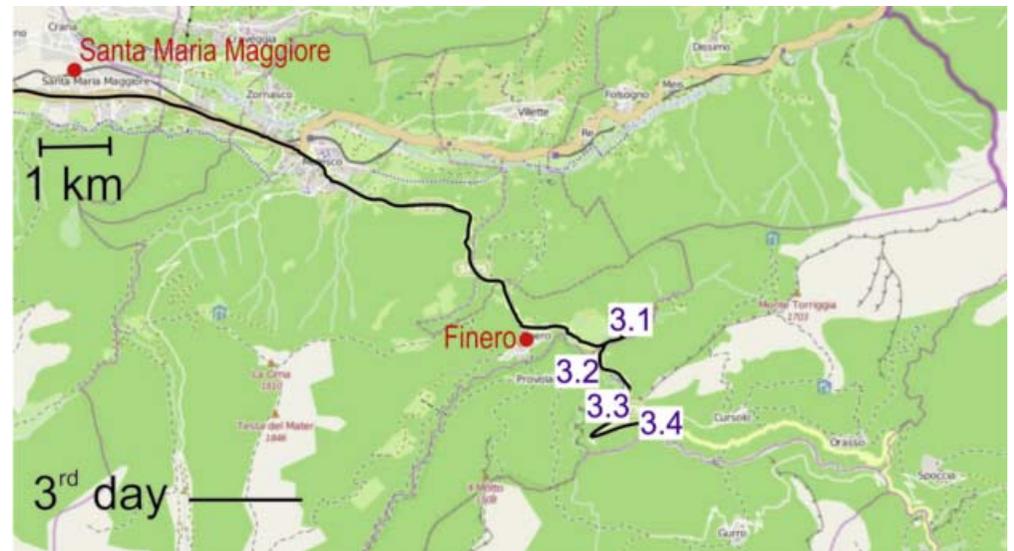
Fig. E – Itinerari del 3° giorno: escursione nell'area di Finero con l'ubicazione degli Stop.
Itinerary of the 3rd day: field trip in the Finero area, along with the position of the Stops.

Riassunto

La sezione di crosta profonda della Zona Ivrea-Verbano (ZIV, Alpi occidentali, Fig. A) ha ricevuto grande attenzione nel corso degli ultimi tre decenni come uno dei migliori esempi di "magmatic underplating" continentale. Recenti indagini, comprendenti dati strutturali, petrochimici e geocronologici, hanno evidenziato la presenza di una "ZIV tipo-Sesia" (cioè la ZIV centrale) e una "ZIV tipo-Finero" (cioè la ZIV settentrionale), che hanno subito diverse evoluzioni magmatiche e tettoniche.

Nella zona tipo-Sesia (riquadro a in Fig. A), l'enorme plutone gabbroico, conosciuto come complesso basico (che raggiunge spessori > 8 km), si è intruso durante il Permiano nelle rocce più profonde della crosta, che comprendono paragneiss in facies da anfibolitica a granulitica e corpi intercalati di peridotiti di mantello, mentre erano ancora residenti nella crosta profonda. Il contesto magmatico di questa enorme intrusione è rimasto poco chiaro fino a quando Quick et al. (2009) hanno dimostrato che la messa in posto del complesso basico era coeva a un vulcanismo prevalentemente acido, comprendente estesi depositi di caldera, e con la crescita di plutoni acidi nella crosta superiore dell'adiacente "Serie dei Laghi". Il sistema magmatico del Sesia costituisce un'esposizione senza precedenti del sistema di alimentazione di una caldera dalla superficie ad una profondità di circa 25 km (Quick et al., 2009). In questo quadro, il complesso basico registra i processi che avvengono nella crosta profonda sotto la caldera.

L'inizio dell'attività vulcanica è strettamente correlata con il culmine della crescita della parte superiore del complesso basico, quando l'intrusione basica interessò livelli crostali fertili e la crosta fu riscaldata in modo pervasivo. Nella crosta superiore, l'attività eruttiva è stata dominata da fusi ibridi ricchi in silice, prodotti da anatessi nella crosta profonda, ma costituiti anche da quantità significative di componenti di mantello. Durante il ciclo dell'attività vulcanica, il complesso basico è cresciuto da una camera magmatica relativamente piccola ma continuamente alimentata secondo un processo di tipo "gabbro glacier".

L'escursione attraverserà l'intero sistema igneo, a partire dagli affioramenti più profondi del complesso basico fino a raggiungere gli affioramenti spettacolari di megabreccia all'interno della caldera.

La zona tipo-Finero (riquadro b in Fig. A) è caratterizzata dalla presenza dell'unico esempio al mondo di un corpo di mantello pervasivamente metasomatizzato costituito da rocce ultramafiche contenenti flogopite (cioè harzburgiti, duniti e pirosseniti in facies a spinello). Queste litologie sono stati prodotte da diversi episodi di

migrazione, da pervasiva a canalizzata, per flusso poroso di fusi idrati arricchiti in K, LILE e Mg contenenti grande quantità di componenti crostali. L'unità di mantello è circondata da un'intrusione stratiforme femica-ultrafemica, il complesso basico di Finero, costituita da orneblenditi a granato, peridotiti ad anfibolo di cumulo, gabbri e dioriti ad anfibolo, che mostra affinità geochimica da tholeiitica a transizionale.

Recenti datazioni U-Pb su zirconi indicano un'età di intrusione medio-triassica per il complesso basico di Finero, che può così rappresentare la controparte di crosta profonda del vulcanismo Triassico Medio e Superiore presente nelle Alpi Meridionali. In ogni caso, il complesso basico di Finero non può essere più considerato come parte del complesso basico Permiano affiorante nell'area della Val Sesia. Diversamente, l'età U-Pb di zirconi rinvenuti in orizzonti cromititici massicci del corpo di peridotite di mantello appartengono al Giurassico Inferiore. Questa marcata differenza di età suggerisce che il complesso basico di Finero e il corpo di mantello associato hanno subito una diversa evoluzione geodinamica fino al Giurassico Inferiore, in quanto sono stati tettonicamente giustapposti durante l'apertura della neo-Tetide giurassica oppure più recentemente. Il contesto geodinamico legato all'intrusione del complesso basico di Finero, le sorgenti, l'età e l'ambiente geodinamico del metasomatismo del corpo di peridotite di mantello e l'età della messa in posto di quest'ultimo a contatto con le rocce crostali sono alcuni dei temi che verranno trattati nella guida.

Questa escursione intende così illustrare la ZIV tipo-Sesia come una sequenza completa di una sezione crostale dal mantello a un supervulcano e mostrare le diverse caratteristiche petrografiche, geochimiche e geocronologiche fra la ZIV tipo-Sesia e la ZIV tipo-Finero alla luce dei risultati delle ultime ricerche.

Parole chiave: *Zona Ivrea-Verbano, sistema magmatico del Sesia, supervulcano, Finero, complesso basico, peridotite di mantello.*

information

Igneous evolutions across the Ivrea crustal section: the Permian Sesia Magmatic System and the Triassic Finero intrusion and mantle

M. Mazzucchelli - J. E. Quick - S. Sinigoi - A. Zanetti - T. Giovanardi

10

information

Abstract

The famous deep crustal section of the Ivrea-Verbano Zone (IVZ, western Alps, Fig. A) has received enormous attention over the last three decades as one of the best examples of continental "magmatic underplating". Recent investigations, comprising structural, petrochemical and geochronological data, point to the occurrence of a "Sesia-type IVZ" (i.e. central IVZ) and a "Finero-type IVZ" (i.e. northern IVZ), which underwent different magmatic and tectonic evolution. In the Sesia area (box a in Fig. A), the Permian gabbroic pluton known as the mafic complex (reaching thicknesses > 8 km) intruded the deepest rocks of the crustal section, comprising amphibolite to granulite-facies paragneiss and interlayered mantle peridotite bodies, while they were resident in the deep crust. The broader magmatic context of this voluminous intrusion remained unclear until Quick et al. (2009) demonstrated that the emplacement of the mafic complex was coeval to the activity of a mainly silicic volcanic field, including extensive caldera deposits, and to the growth of silicic plutons in the upper crust of the adjacent "Serie dei Laghi". The Sesia magmatic system constitutes an exposure of the plumbing system of a caldera from the surface to a depth of about 25 km (Quick et al., 2009). In this framework, the mafic complex records processes occurring in the deep crust beneath the caldera.

The onset of volcanic activity correlates strictly with the climax of the growth of the upper mafic complex, when the mafic intrusion invaded fertile crustal levels and the crust was pervasively heated. In the upper crust, igneous activity was dominated by hybrid silicic melts produced by anatexis in the deep crust, but including significant amounts of mantle component. During the life of the volcanic activity, the mafic complex grew from a relatively small but continuously fed magma chamber according to the "gabbro glacier" process. The excursion will transect the entire igneous system, starting from the deepest exposures of the mafic complex up to reach the outcrops of megabreccia within the caldera fill.

The Finero area (box b in Fig. A) is characterized by the occurrence of a pervasively-metasomatised mantle unit made by phlogopite-bearing ultramafic rocks (i.e. spinel-facies harzburgites, dunites and pyroxenites). These rock types were produced by several episodes of pervasive-to-channeled porous flow migration of K-LILE-Mg-enriched hydrous melts containing large amount of crustal components. The mantle unit is surrounded by a layered mafic-ultramafic intrusion, i.e. the Finero mafic complex, comprising garnet hornblendites, cumulus amphibole peridotites, amphibole gabbros and diorites, with tholeiitic to transitional geochemical affinity.

Recent U-Pb zircon data point to a Middle-Triassic intrusion age for the Finero mafic complex, which may thus represent the deep-crustal counterparts of the Middle-Upper Triassic volcanism widespread throughout the Southern Alps. In any case, the Finero mafic complex can no longer be considered as part of the Permian mafic complex exposed in the Sesia area. Instead, U-Pb ages of zircons from massive chromitites of the mantle unit are Lower Jurassic. The marked age span of the Finero mafic complex and the associated mantle unit suggests that they experienced different evolutions until Lower Jurassic, and were subsequently tectonically juxtaposed during the opening of the Jurassic Neo-Tethys or later. The geodynamic setting related to the intrusion of the Finero mafic complex, the sources, the age and geodynamic environment of the metasomatism of the mantle unit and the age of the emplacement of the latter in contact with the crustal rocks are some of the issues that will be discussed in this guide.

This excursion aims to illustrate the Sesia-type IVZ as a complete sequence of a section from the mantle to a supervolcano and show the different geochronological, petrographic and geochemical characteristics between the Sesia-type and the Finero-type IVZ in the light of the results of latest research.

Key words: *Ivrea-Verbano Zone, Sesia magmatic system, supervolcano, Finero, mafic complex, mantle peridotite.*

11

information

1 - Geologic framework

The Sesia magmatic system includes coeval and genetically related intrusive and volcanic rocks within the IVZ and "Serie dei Laghi", two lithostratigraphic units in the Alps of northwestern Italy that have been historically studied as separate entities (Fig. 1). The IVZ comprises plutonic and high-temperature, high-pressure rocks (Mehnert, 1975; Fountain, 1976) that are juxtaposed against the basement units of the Austro-Alpine Domain along the Insubric Line (Schmid et al., 1987) and bounded to the southeast by amphibolite-facies metamorphic rocks and granites of the "Serie dei Laghi" (Boriani et al., 1990b).

The boundary between the IVZ and "Serie dei Laghi" is defined locally by to a high-temperature mylonite mapped as the Cossato-Mergozzo-Brissago Line (Boriani & Sacchi, 1973; Zingg, 1983; Handy, 1987; Boriani et al., 1990a), but within the Sesia Valley, a tectonic boundary is not evident (Quick et. al, 2003). Most investigators agree that the IVZ together with the "Serie dei Laghi" are the deep- and the middle- to upper-crustal components, respectively, of a section through the pre-Alpine crust of northwest Italy (e.g. Fountain, 1976; Handy & Zingg, 1991; Henk et al., 1997; Rutter et al., 1999).

Gravity and seismic reflection data suggest that the IVZ dips steeply to the southeast near the surface but flattens into a subhorizontal orientation at a depth of 20 to 30 km beneath the Po Plain (Nicolas et al., 1990; also see Berckhemer, 1968). The emplacement of the IVZ rocks into the upper crust resulted from the combined effects of vertical uplift due to Mesozoic crustal thinning and subsequent lithospheric wedging related to Alpine collision (Schmid et al., 1987; Nicolas et al., 1990).

Rocks of the IVZ have been grouped historically in terms of two major units, the Kinzigite formation and the basic formation (also referred to as the mafic formation). The Kinzigite formation comprises amphibolite- to granulite-facies paragneiss that formed from protoliths dominated by pelitic sedimentary rocks and wackes, but also included limestone and mafic volcanic rocks (Zingg, 1983; Sills & Tarney, 1984; Wedepohl et al., 1989). Amphibolite-facies assemblages dominate in the southeastern IVZ, and granulite-facies assemblages are volumetrically more significant in the northwest. The basic formation is subdivided into the voluminous mafic complex and lenses of mantle peridotite.

The mafic complex (Rivalenti et al., 1975, 1981, 1984) is a large composite body of mostly gabbroic plutonic rocks and subordinate amounts of dioritic, tonalitic, charnockitic and cumulus ultramafic rocks. These rocks are recrystallised to different degrees, and are interleaved with and underlie the Kinzigite formation in terms of pre-Alpine orientations.

The southern IVZ and the southern "Serie dei Laghi" were impacted by the same early Permian magmatic event. SHRIMP U-Pb zircon ages for volcanic rocks south-east of the Cremosina line and for the spatially-related granite bodies of the Roccapietra-Valle Mosso pluton, which intrude the "Serie dei Laghi", demonstrated that volcanic and plutonic activity overlapped in time with crystallisation and cooling of the mafic complex in the southern IVZ (Quick et al., 2009), and that peak magmatic activity was confined to approximately 10 m.y. from 288 to 278 Ma. Quick et al. (2009) also demonstrated that the volcanic field is largely occupied by caldera fill tuffs and megabreccia, concluding that volcanic and middle- to deep-crustal plutonic rocks collectively constitute an exposure of the magmatic plumbing system to a depth of 25 km beneath a caldera with a minimum diameter of 13 kilometers. The association of these rocks in space and time points to a cause-and-effect link between intrusion of mantle-derived basalt in the deep crust, and large-scale, silicic volcanism.

Historically, the mafic complex was considered as a single mafic body extending from Baldissero to the Finero (Fig. 1). However, recent SHRIMP U-Pb zircon ages demonstrated that, whereas the central mafic complex crystallised at the Permo-Carboniferous boundary (Peressini et al., 2007), gabbro constituting the northern mafic complex, in the Finero area, is Triassic, and can no longer be regarded as part of the same igneous body (Zanetti et al., 2013, 2014).

2 - The mantle peridotites

An extended review on the geological, petrological and geochemical characteristics of the Ivrea-Verbano mantle peridotites is reported in Rivalenti & Mazzucchelli (2000). Here, a summary of the main features of the mantle slices is presented.
The largest and best known Ivrea-Verbano peridotites are, from south to north, the Baldissero, Balmuccia and Finero massifs (Fig. 1).

These bodies are aligned at the northwestern margin of the basic complex, i.e. in the lowest stratigraphic units of the IVZ. These are not the only bodies of the region. Tens of minor peridotites, recognized as lithospheric mantle material, occur at various stratigraphic levels throughout the IVZ and are less studied either because of their small dimensions or because of difficult access (Lensch, 1968, 1971; Marchesi et al., 1992; Mazzucchelli et al., 1992a; Barbieri, 1996). Some of these bodies occur, like the major ones, in the lower units of the basic complex (e.g., the peridotite lenses occurring north and south of the Balmuccia massif in Vallone di Meula and Val Mala, respectively, the Premosello lens in Val d'Ossola, several other unnamed lenses in northern Ivrea-Verbano, Fig. 2a). Other minor peridotites occur in Val Strona and Val d'Ossola
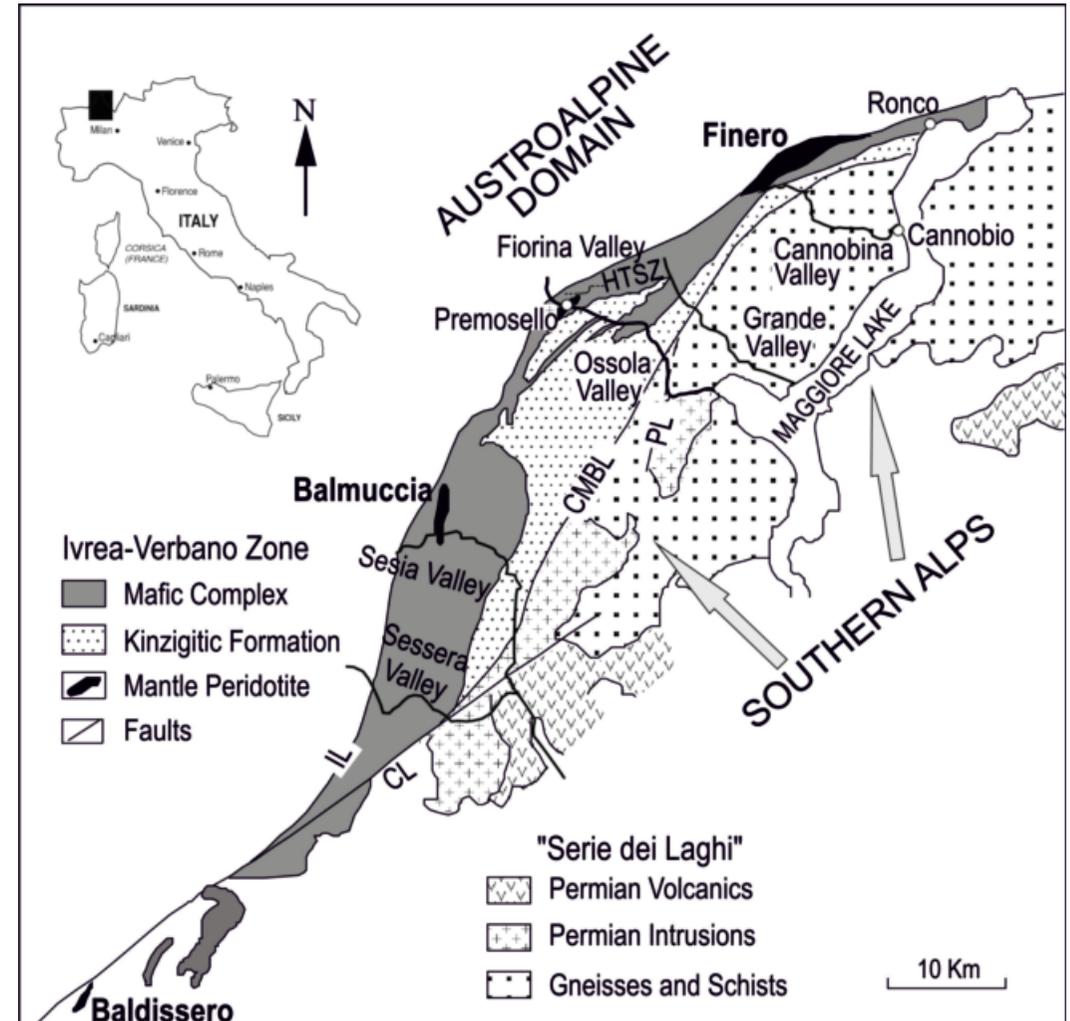

Fig. 1 - Sketch map of the Ivrea-Verbano zone.
CL = Cremosina line; IL = Insubric line; CMBL = Cossato-Mergozzo-Brissago line; PL = Pogallo line; HTSZ = high-temperature shear zone. From Zanetti et al. (2013), modified.

within the metasedimentary rocks of the Kinzigite formation, in the high temperature shear zone marking the transition from granulite to amphibolite facies (Alpe Francesca, Alpe Crotta, Alpe Piumero, and various unnamed lenses, Fig. 2a). Further peridotites occur in Val Strona (Alpe Morello, Fig. 2a), and probably elsewhere, at the Ivrea-Verbano top, in the shear zone at the contact between the Ivrea-Verbano and the "Serie dei Laghi" formations (Pogallo line; Boriani & Sacchi, 1973). In the northern Ivrea-Verbano part (Val Grande region, Fig. 2b) several peridotite lenses occur which have characteristics similar to those of the major, better known, Finero massif.
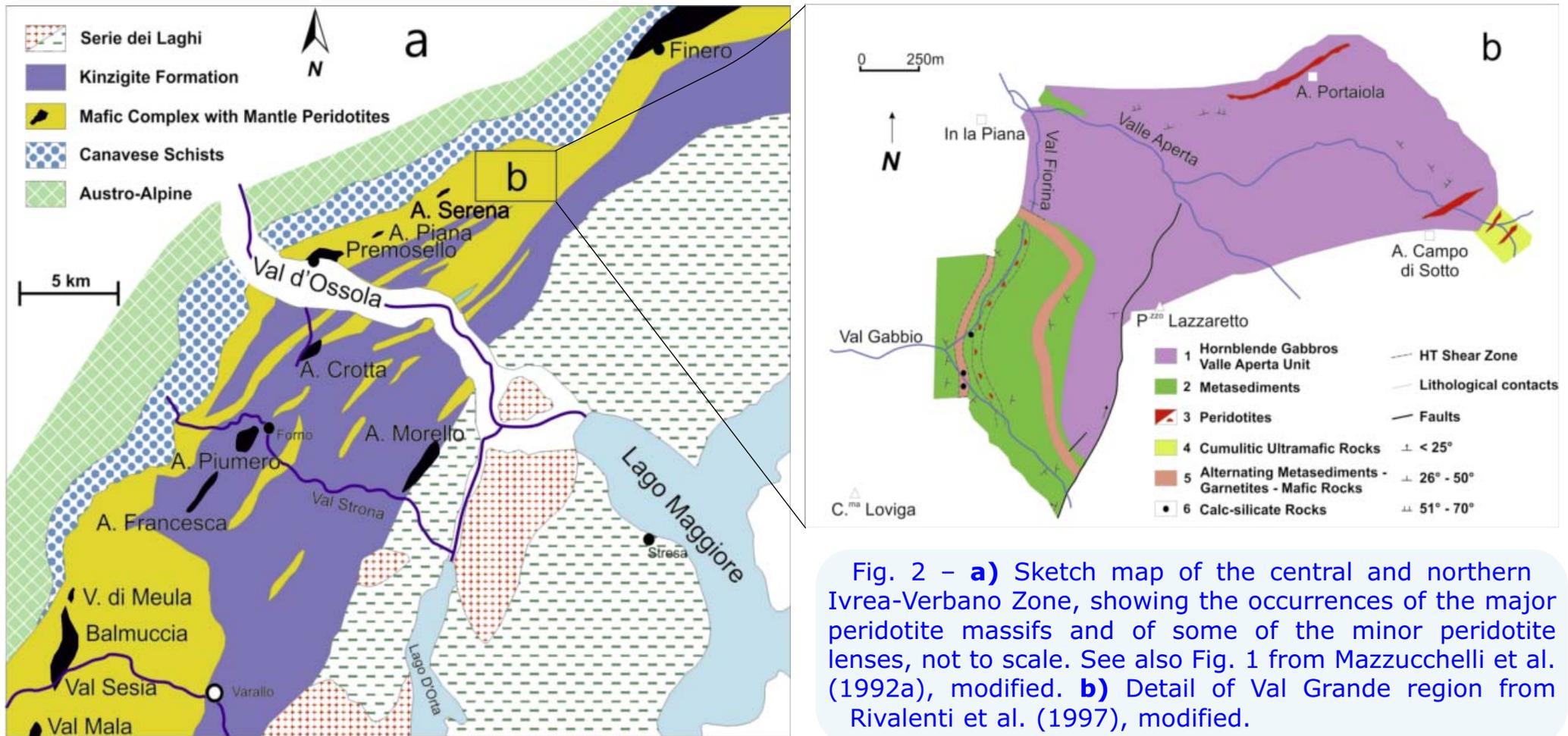
Fig. 2 – **a)** Sketch map of the central and northern Ivrea-Verbano Zone, showing the occurrences of the major peridotite massifs and of some of the minor peridotite lenses, not to scale. See also Fig. 1 from Mazzucchelli et al. (1992a), modified. **b)** Detail of Val Grande region from Rivalenti et al. (1997), modified.

The constant association of the Ivrea-Verbano mantle peridotites with high-T shear zones indicates that none of them, including the major massifs, was emplaced into the crust by mantle diapirism (Shervais, 1979). Consequently, the IVZ does not represent an in situ mantle-crust transition (Quick et al., 1995). This hypothesis was proposed by Mehnert (1975) and Fountain (1976) based on the geophysical evidence that mantle rises from a depth of about 20 km under the Po plane to within a few kilometers from the surface beneath the IVZ. The presence of igneous contacts with the igneous rocks of the mafic complex (e.g. in Val Sesia) cannot be interpreted as an exposed Moho, but merely indicate that peridotite emplacement predates the mafic intrusions. The relationships of the peridotites with the metamorphic volcano-sedimentary sequence are less clear. Taking into account their constant association with high-T shear zones, interpreted to be extensional (Brodie & Rutter, 1987; Brodie et al., 1992; Rutter et al., 1993), peridotites might have been emplaced at the onset of this regime. Alternatively, they may be a component of an accretionary wedge of a probably Ordovician subduction zone (Quick et al., 1995). However, interpretation rests largely understanding of the geodynamic history and processes which affected the volcano-sedimentary sequence, which are far from being known in sufficient detail. Whatever the mechanism of emplacement of the mantle lenses, their systematic differences suggest they represent samples of different lithospheric mantle segments and/or lithosphere from different geodynamic environments.

For a review of the field relations and petrography of both major and minor peridotite bodies see Rivalenti & Mazzucchelli (2000). During the excursion we will not visit outcrops of the Baldissero body. An updated study on the characteristics of this massif was recently published (Mazzucchelli et al., 2010). Here the age and geochemistry of the mantle peridotites and some diorite dykes are discussed within the frame of the Paleozoic-Mesozoic evolution of the Southern Alps.

3 - The Balmuccia dunites

Tabular dunite bodies occurring in ophiolites are interpreted to be the result of the reaction between the ambient mantle peridotite and melts flowing in high-porosity channels (Bodinier, 1988; Kelemen & Dick, 1995; Suhr, 1999; Morgan & Liang, 2005). In the mantle system the olivine primary field expands at the expense of pyroxenes at decreasing pressure (O'Hara, 1968; Stolper, 1980). Therefore, dunites are the expected result of the reaction between melts infiltrating mantle levels shallower than those of the melt source (Kelemen et al., 1997; Morgan & Liang, 2005). This is the reason why most ophiolitic dunites occur at relatively shallow (plagioclase-facies) mantle levels. The ophiolitic dunites are generally equilibrated with Mid-Ocean-Ridge-Basalts (MORB) consistent with their being conduits for MORB magma transport (Kelemen et al., 1995, 1997; Piccardo et al., 2007). Other dunites, however, exhibit geochemical features consistent with magma types other than MORB (Kelemen et al., 1997, p. 293), such as alkali basalts, possibly related to ocean island basalts (OIB), or highly refractory boninitic melts, possibly representative of subduction-related magmas (e.g. the highly refractory dunites in the Bay of Islands ophiolite; Suhr et al., 2003).

Fig. 3 – Geology of the Balmuccia area, from Quick et al. (2003), modified.
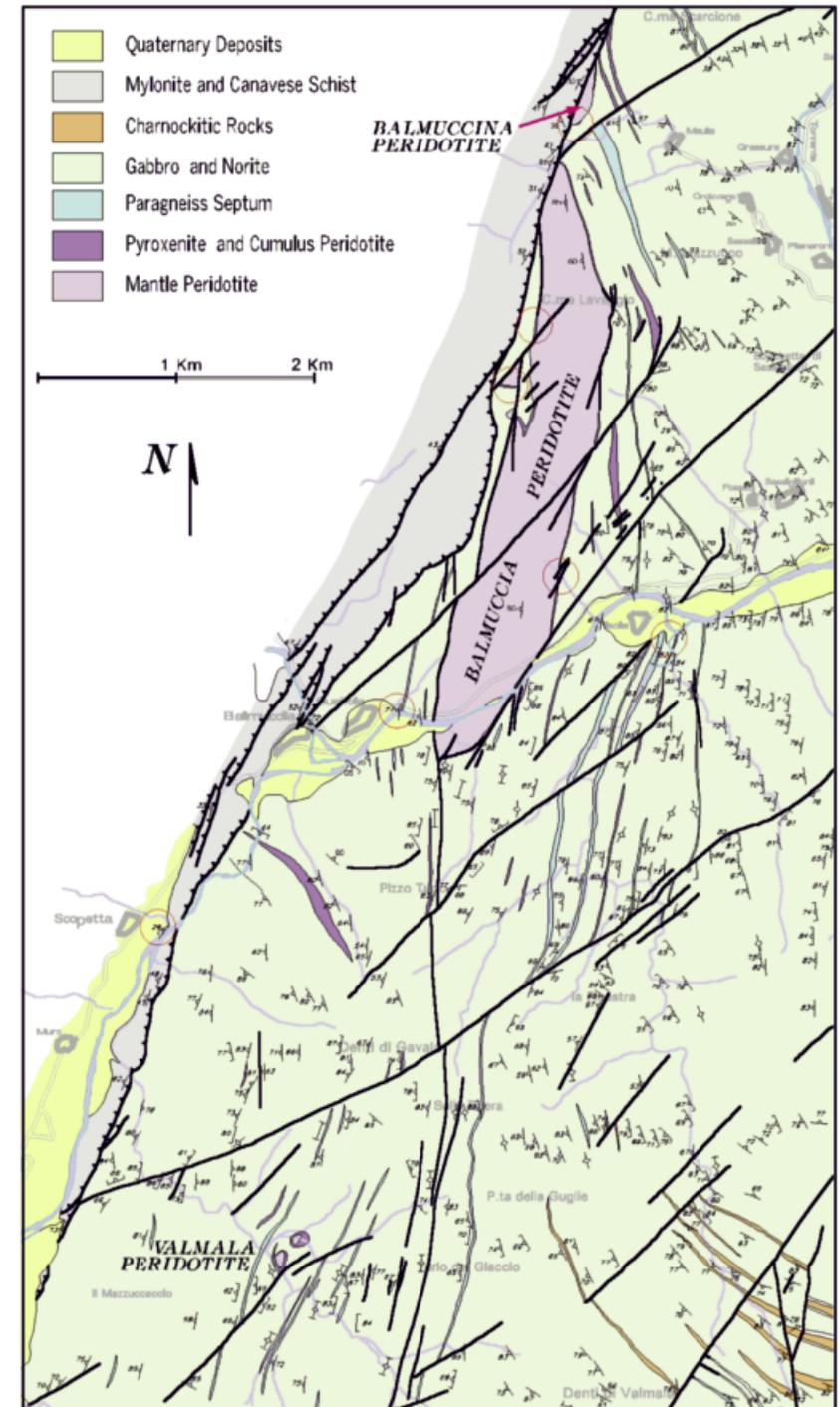
The occurrence of dunites in the spinel-facies mantle massif of Balmuccia presents an opportunity to investigate the mineralogical and petrochemical processes governing the dunite formation at relatively high-P conditions (i.e. spinel-facies conditions).
Three types of dunites are recognised in the Balmuccia massif (Fig. 3):

1) Reactive dunites at the contact with websteritic dykes (Rivalenti et al., 1995; Mukasa & Shervais 1999). These dunites never exceed 40 cm in thickness and are systematically in contact with the websterite dykes (Fig. 4). On the basis of the field relationships, petrology and modelling, these dunites are interpreted as originated by pyroxene-dissolving reactions caused by melt infiltration into the wall-rock from the dyke conduit. The peridotite-dyke transitions described by Rivalenti et al. (1995) and Rivalenti & Mazzucchelli (2000) refer mainly to this outcrop.

Fig. 4 – Reactive dunite at the contact with websteritic dykes.

2) "Anhydrous" dunites, 10 cm to 40-50 m thick, characterised by the presence of discontinuous layers of Cr-rich spinel (Figs. 5, 6). Mazzucchelli et al. (2009) proposed that these dunites were generated in a part of the mantle veined by early Cr-diopside websterites by a three-stage process involving partial melting of pyroxenite, infiltration of the pyroxenite-derived melt into the depleted lherzolite and its consequent open-system partial melting and focused flow of the resultant partial melts leading to the production of reactive dunite channels through both peridotite and pyroxenite. The proposed mechanism allows dunite formation to occur well within the spinel stability field, and therefore at greater depth than ophiolitic dunites, which generally formed within the plagioclase stability field. The aggregated model melts extracted from the segments where dunite forms are high-Mg alkali basalts resembling, after olivine fractionation, the compositions of enriched-type MORB from slow- and ultraslow-spreading ocean ridges.

Fig. 5 – The "anhydrous" dunite outcrop investigated by Mazzucchelli et al. (2009).

3) "Hydrous" dunite lenses 15-20 m thick and up to 60 m long (Fig. 7b) containing gabbroic pods and dykes rich in amphibole, plagioclase, phlogopite and rutile (Fig. 7a). Studies of these dunites are currently in progress. The "hydrous" dunites are mainly located at the western margin of the Balmuccia body in the northwesternmost edge of the Balmuccia quarry located at the north side of the Varallo Sesia – Balmuccia road. The gabbroic pods and veins are centimeters to decimeters thick,
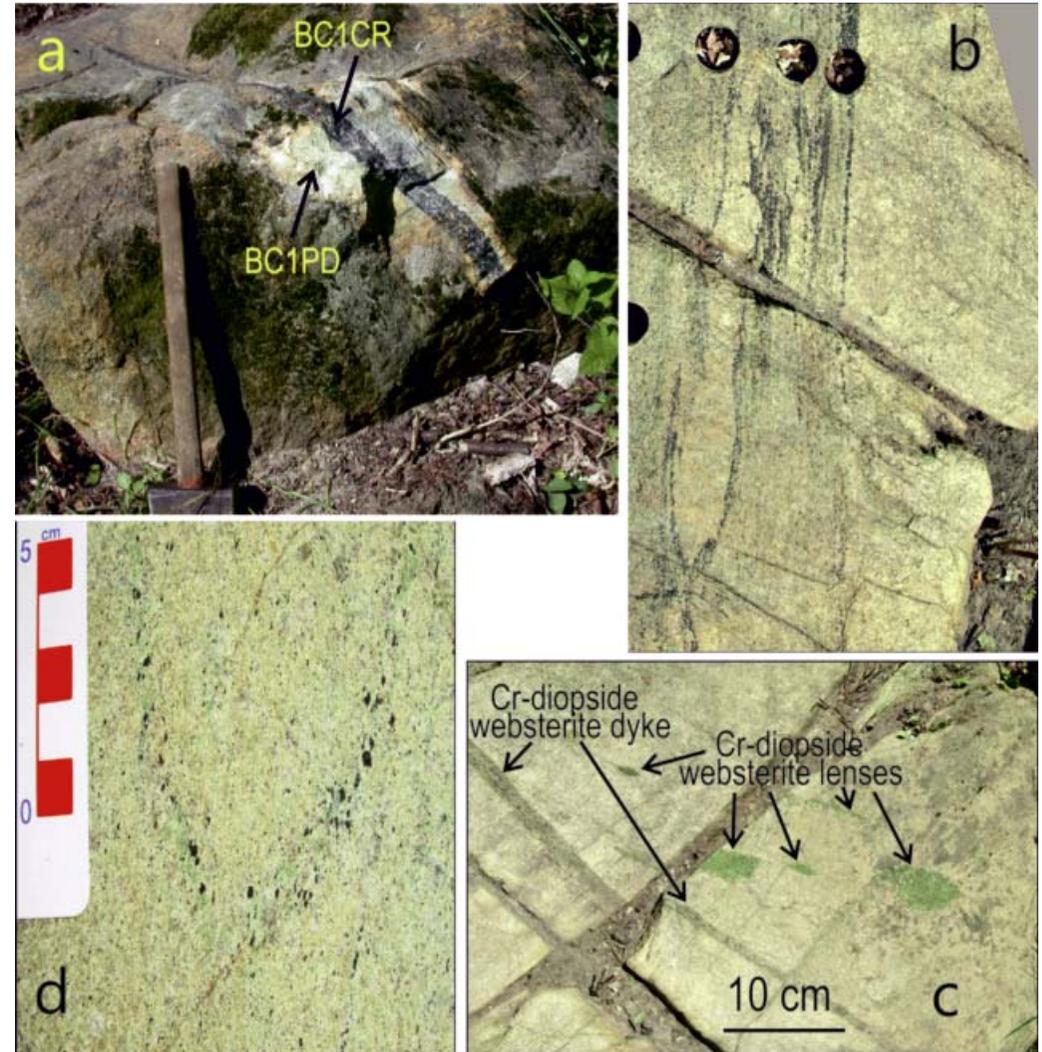
Fig. 6 – a) Massive spinel layer (head of the hammer is 15 cm long); b) flow structures in the spinel layer (diameter of the drill holes is 2.5 cm); c) spinel-rich dunite containing Cr-diopside websterite lenses (note the Cr-diopside websterite dyke at the left); d) ghost Cr-diopside websterite dyke, in which clinopyroxene is partially replaced by spinel and olivine. From Mazzucchelli et al. (2009), modified.

Igneous evolutions across the Ivrea crustal section: the Permian Sesia Magmatic System and the Triassic Finero intrusion and mantle

M. Mazzucchelli - J. E. Quick - S. Sinigoi - A. Zanetti - T. Giovanardi
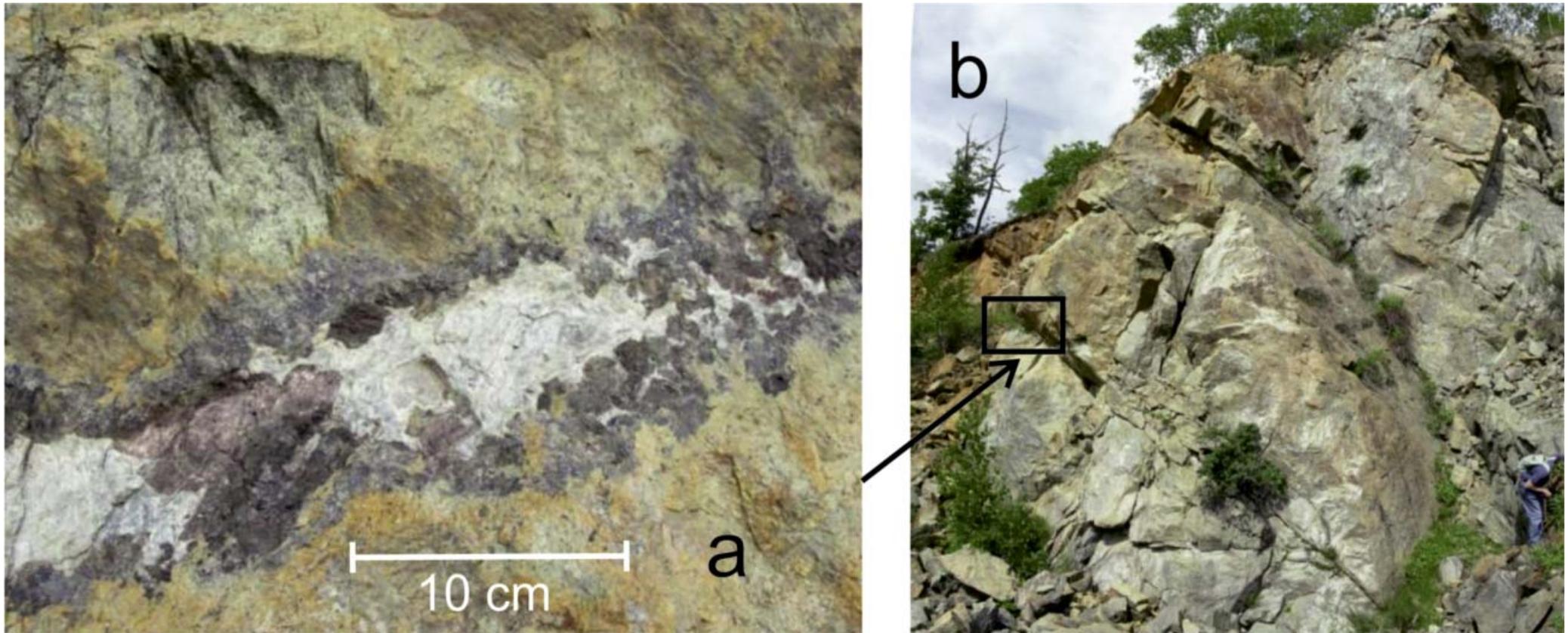
Fig. 7 – **a)** Coarse grain gabbroic dyke rich in amphibole, plagioclase, phlogopite and rutile; **b)** "hydrous" dunite outcrop.

coarse grained (3-5 cm) and cut dykes of the Cr-diopside and Al-augite suites. Preliminary petrographic investigations suggest that melt escaped from the gabbroic pods and/or dykes into the surrounding dunite. This resulted in reaction zones (dm-thick) characterised by segregation of newly-formed minerals, basically amphibole and clinopyroxene. However, at approximately 3-8 cm from the dunite-gabbroic pod/dyke contact, the early recrystallisation is systematically characterised by the formation of mm-large grains with a tight intergrowth of clinopyroxene and amphibole lamellae (Figs. 8, 9 and 10).

In these sectors, amphibole and clinopyroxene crystallised in the interstices as relatively late products of the melt-peridotite interaction. Petrographic study shows that amphibole sometimes overgrows grains with clinopyroxene-amphibole intergrowths (Tarantino et al., 2012). The latter show the outermost rim without amphibole lamellae and formed by pure clinopyroxene, likely as a result of chemical reequilibration (Fig. 8).
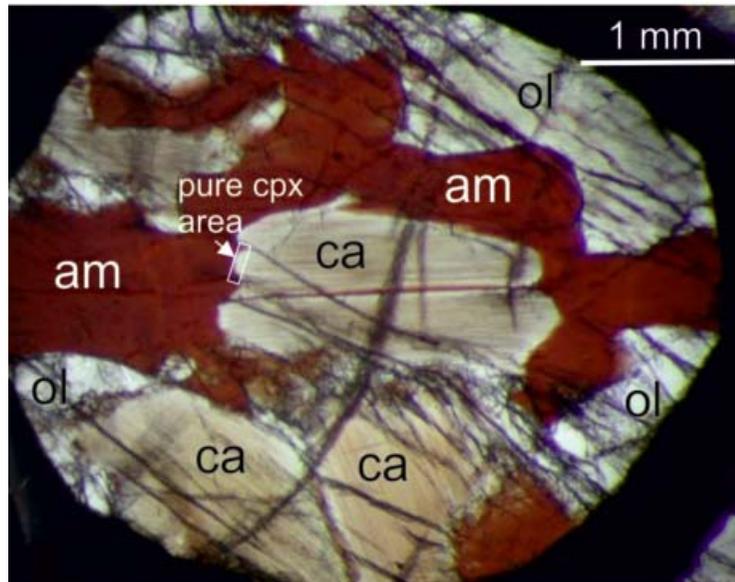
Fig. 8. Petrographic details of a "hydrous" dunite from Balmuccia massif showing pockets related to melt infiltration. These are characterised by early crystallisation of mm-long grains with tight clinopyroxene-amphibole intergrowth (ca). Amphibole (am) and clinopyroxene (cpx) crystallise as late minerals, and the former locally overgrows the grains with amphibole-clinopyroxene lamellae. ol = olivine, sp = spinel. All the microphotos with ppl.

21

excursion notes
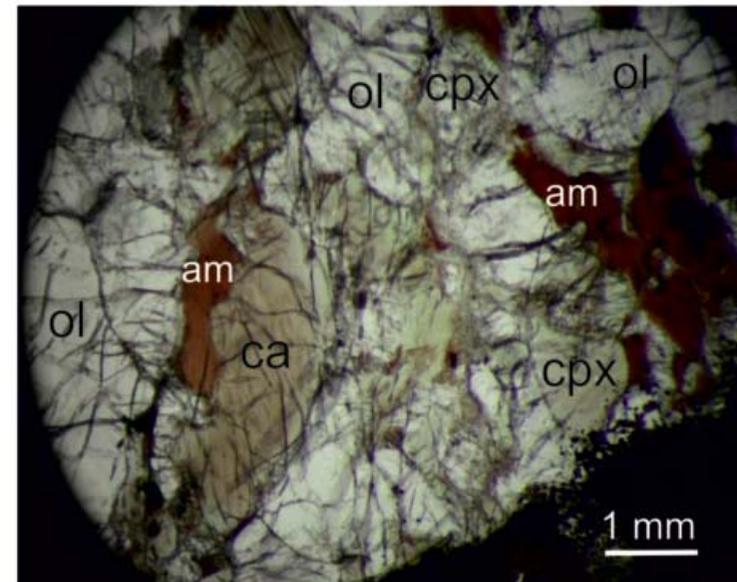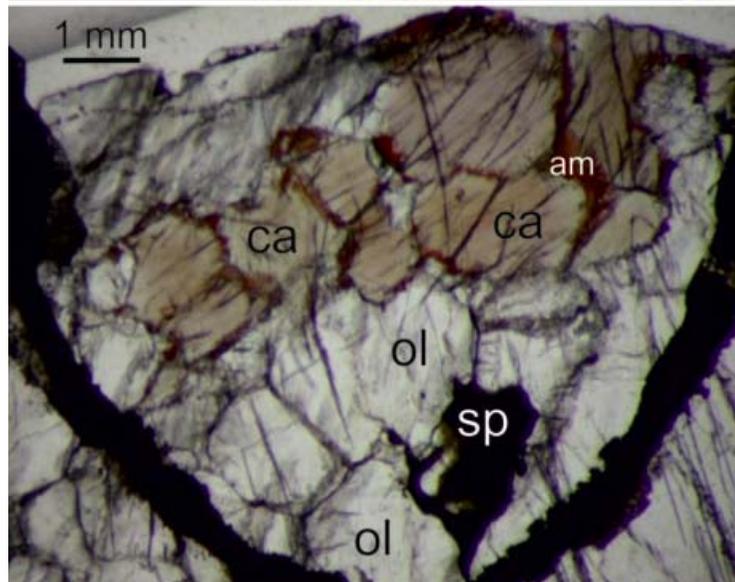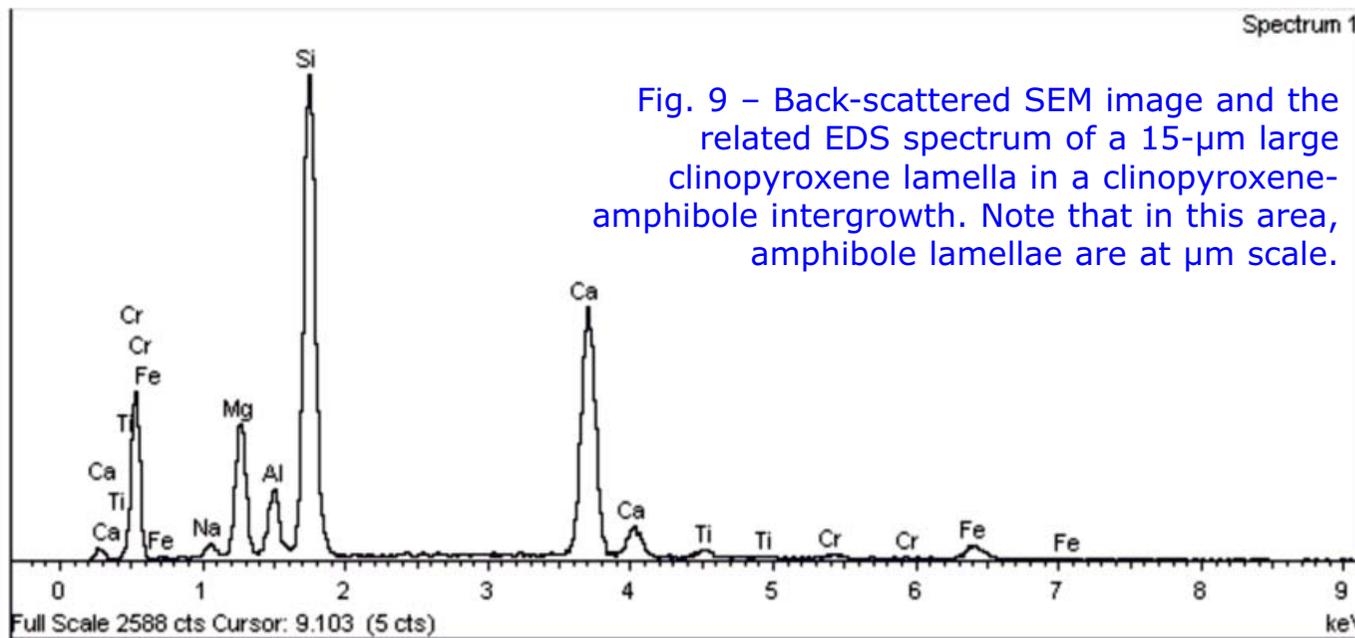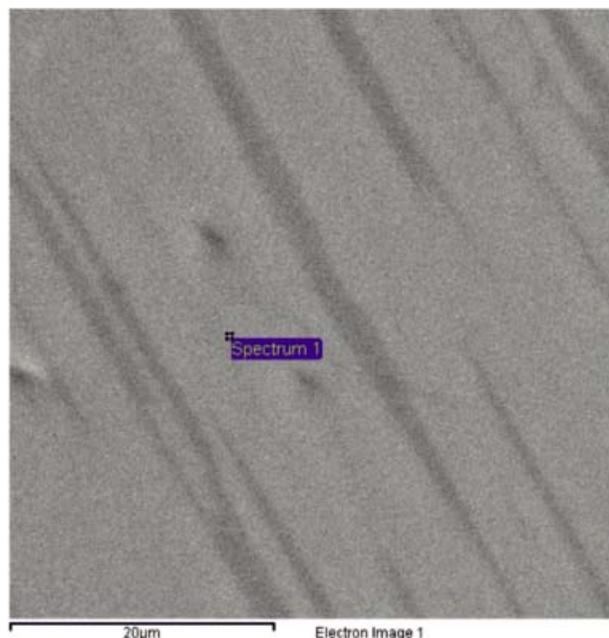
Fig. 9 – Back-scattered SEM image and the related EDS spectrum of a 15-μm large clinopyroxene lamella in a clinopyroxene-amphibole intergrowth. Note that in this area, amphibole lamellae are at μm scale.
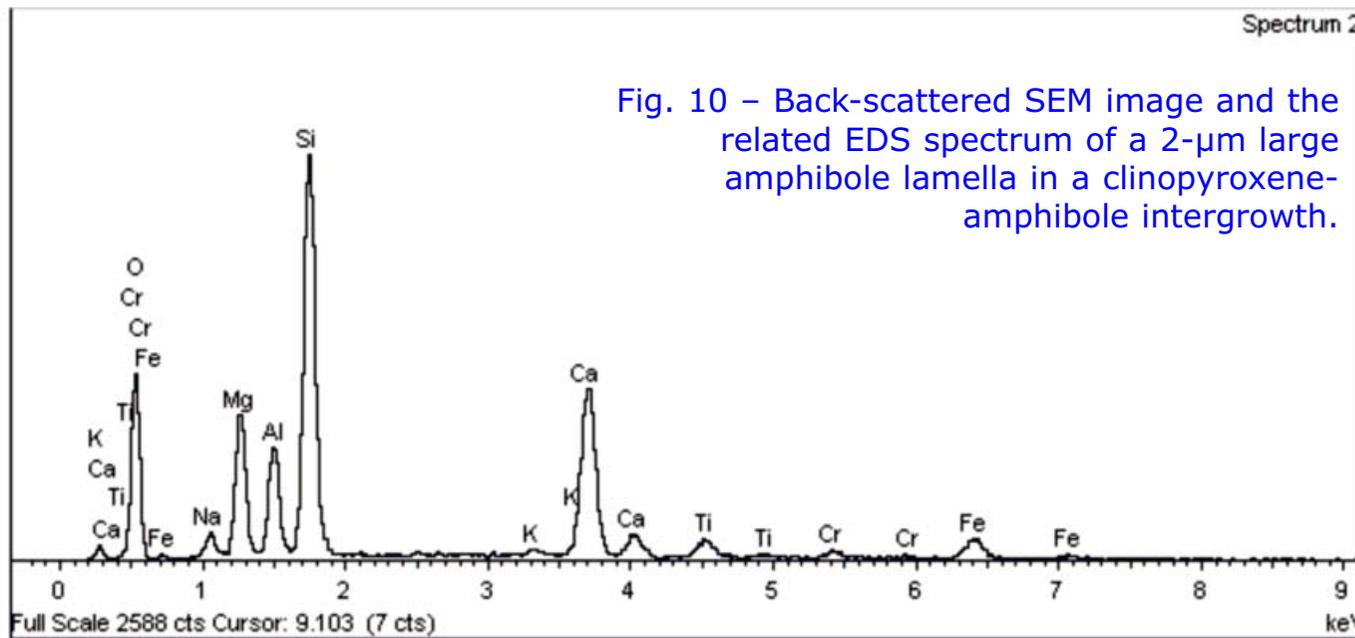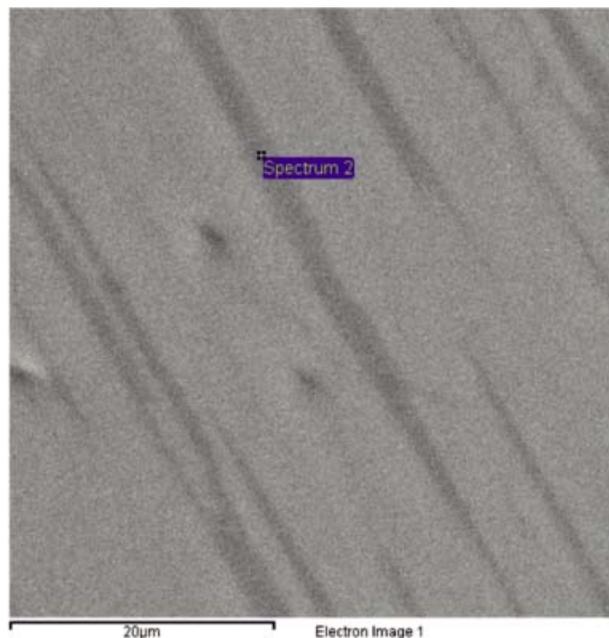
Fig. 10 – Back-scattered SEM image and the related EDS spectrum of a 2-μm large amphibole lamella in a clinopyroxene-amphibole intergrowth.

In the following diagrams (Figs. 11 - 20) the main geochemical characteristics of whole rocks and mineral phases of the three types of dunites, associated peridotites and dykes are shown.

Legend:
- ● "Anhydrous" Dunites + Pd
- ■ Chromitites
- ▲ "Anhydrous" Cr-Di Webst.
- ● "Hydrous" Dunites + Pd
- ▲ "Hydrous" Cr-Di Webst.
- ● Dunites + Pd 1995
- ▲ Cr-Di Webst. 1995
- ▲ Al-Aug Webst. 1995
- ◆ Al-Aug Gabbros 1995
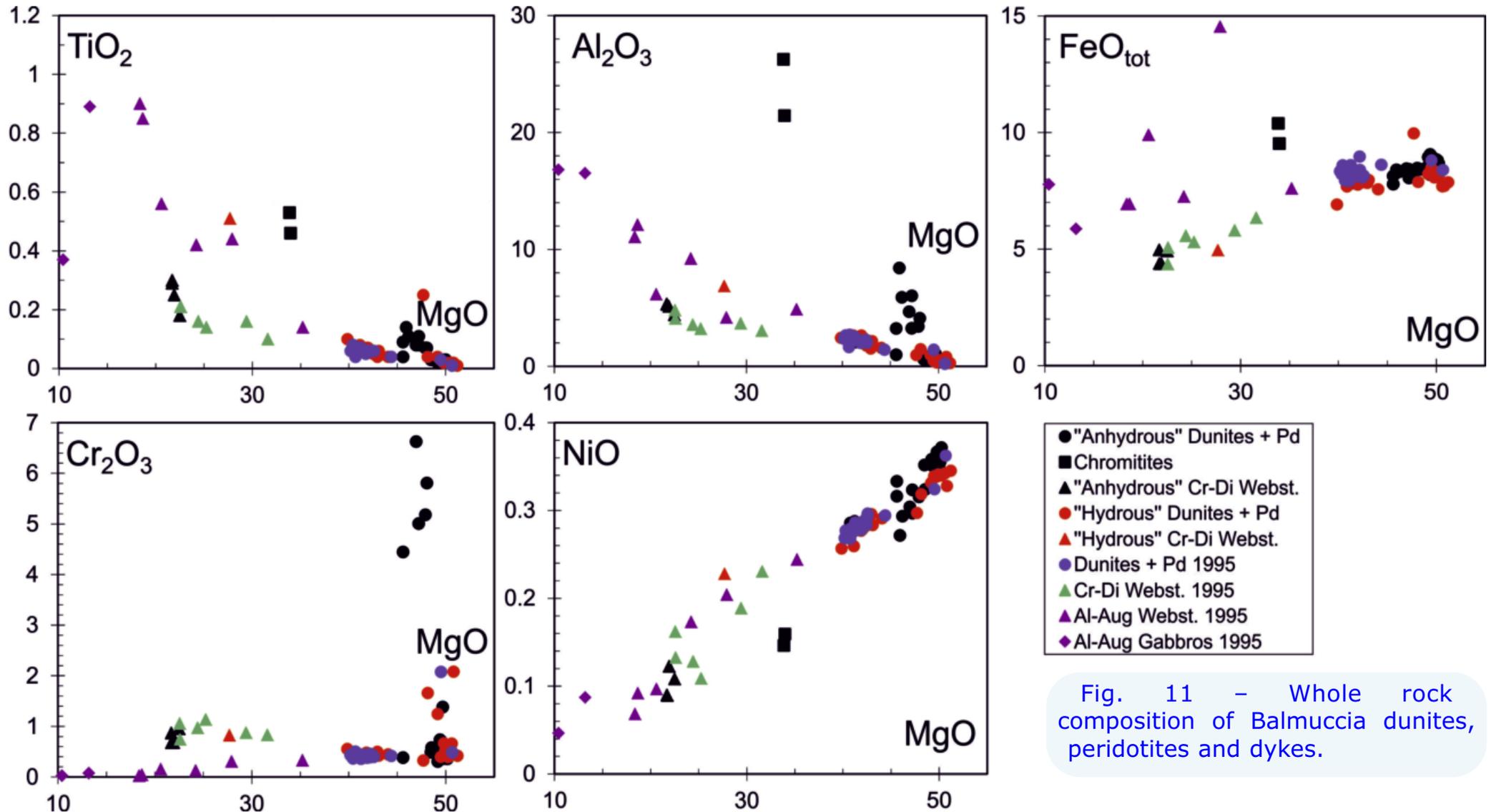
Fig. 11 – Whole rock composition of Balmuccia dunites, peridotites and dykes.
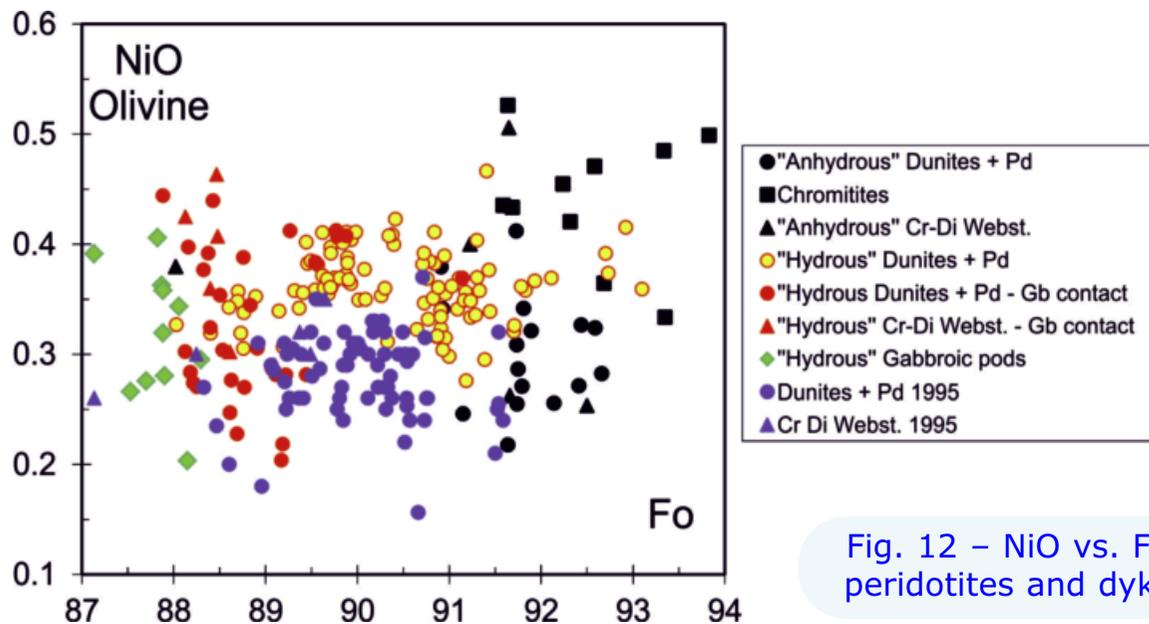
Fig. 12 – NiO vs. Fo content in olivine of Balmuccia dunites, peridotites and dykes.
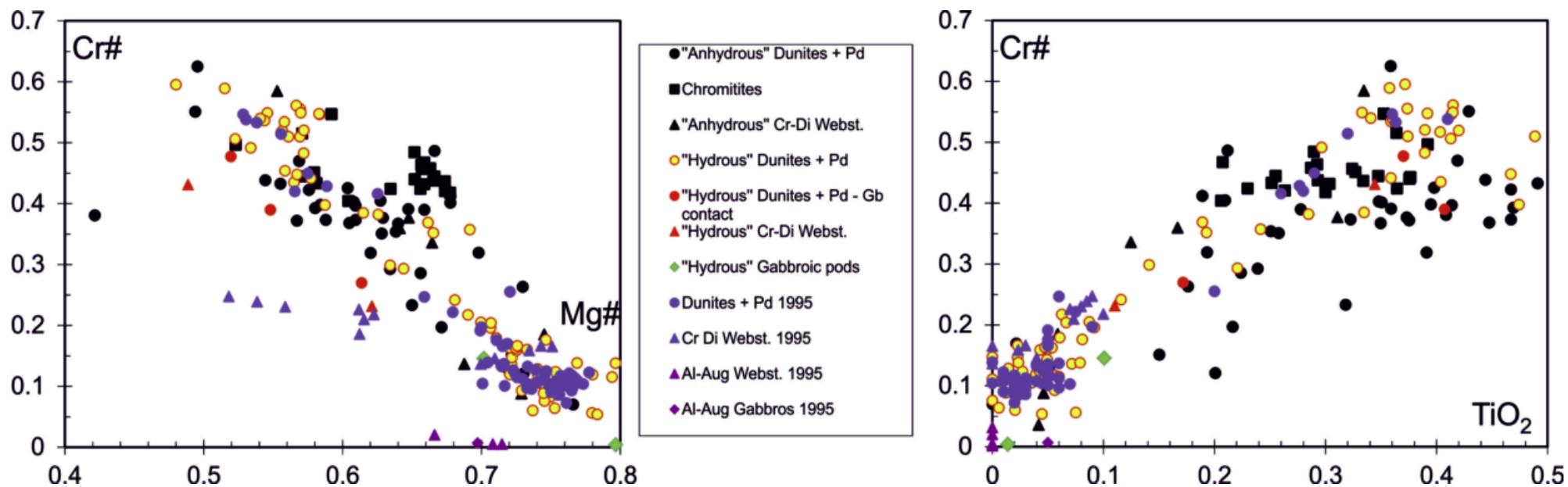
Fig. 13 – Spinel composition of Balmuccia dunites, peridotites and dykes.
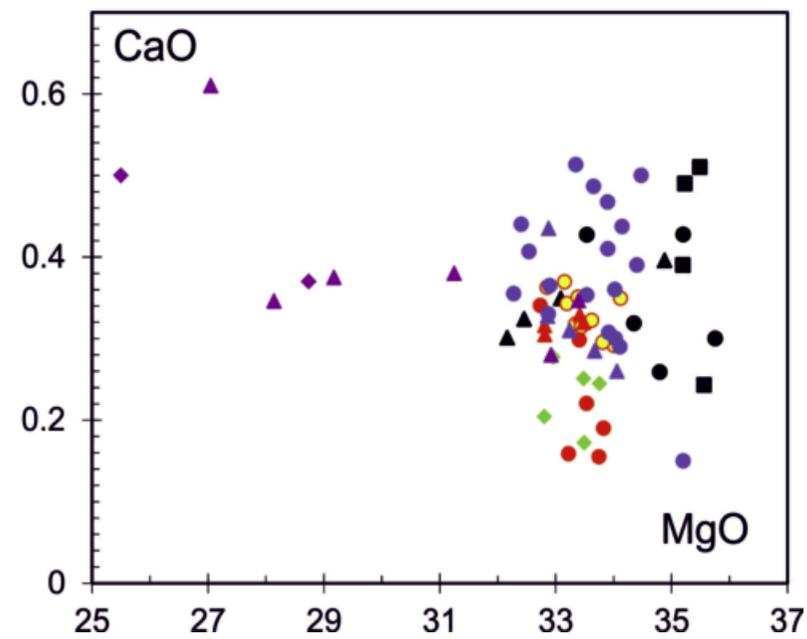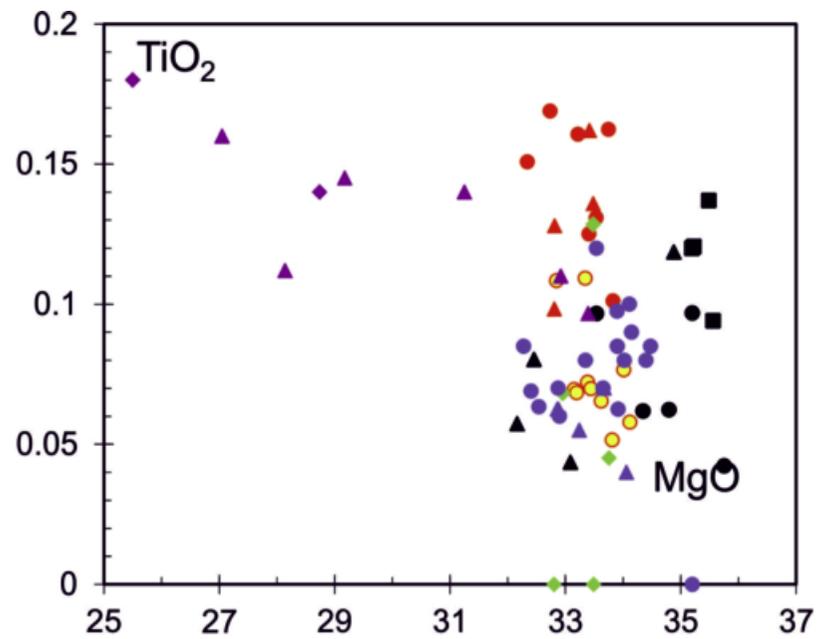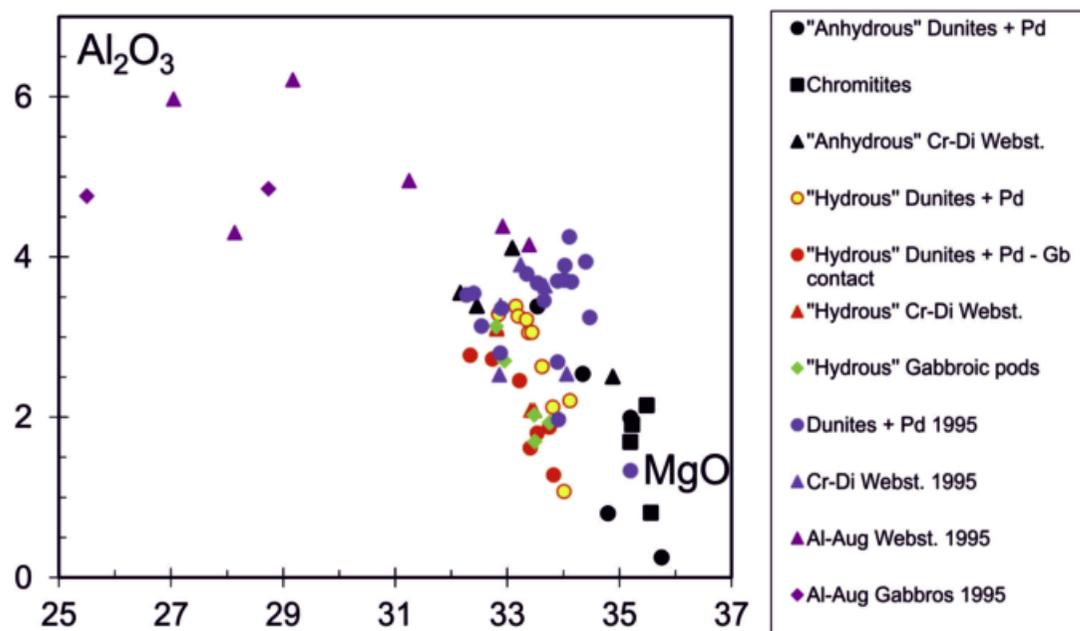
Fig. 14 – Orthopyroxene composition of Balmuccia dunites, peridotites and dykes.

26

excursion notes
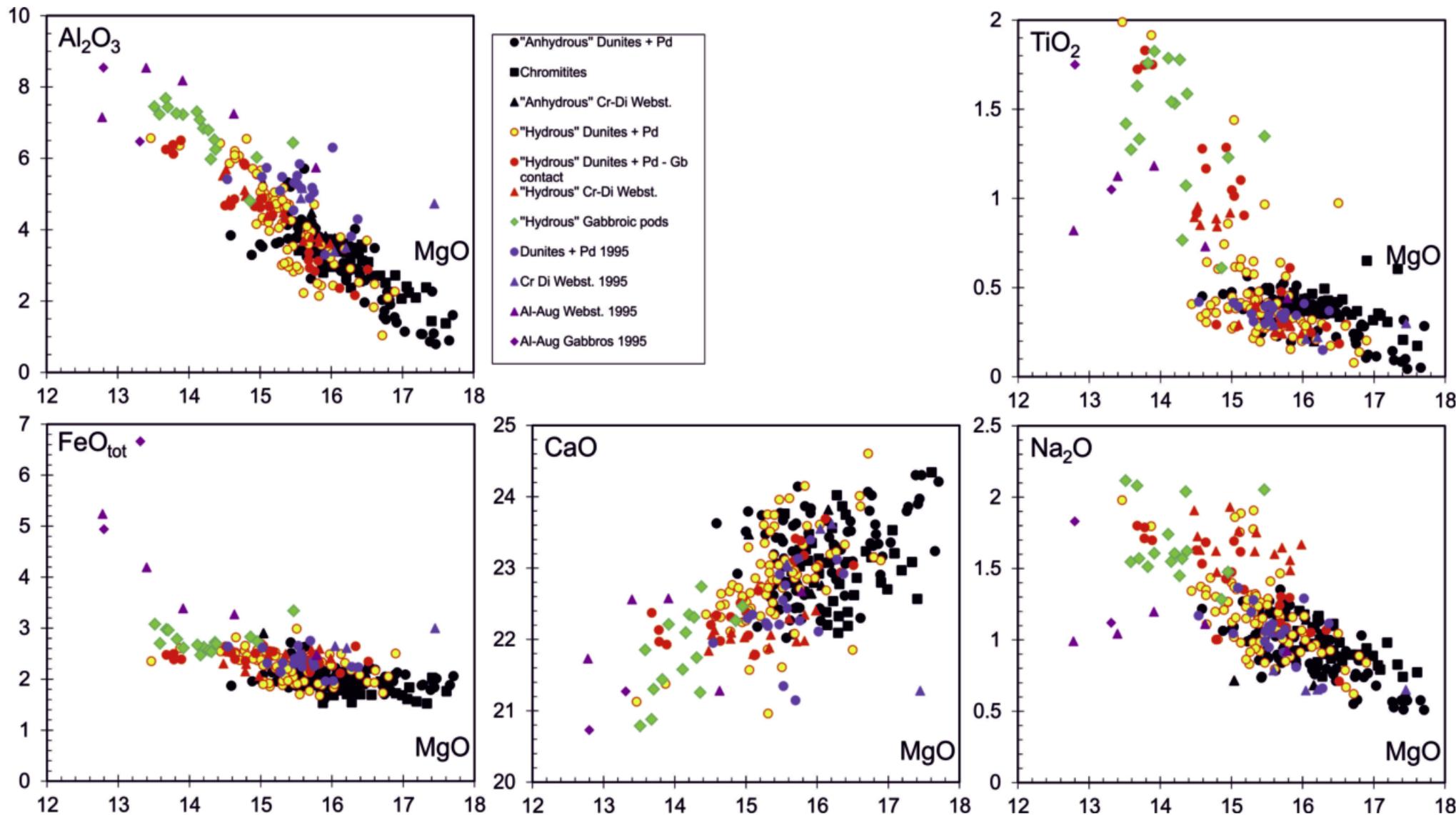
Fig. 15 – Clinopyroxene composition of Balmuccia dunites, peridotites and dykes.

Legend:
- ● "Anhydrous" Dunites + Pd
- ■ Chromitites
- ▲ "Anhydrous" Cr-Di Webst.
- ○ "Hydrous" Dunites + Pd
- ● "Hydrous" Dunites + Pd - Gb contact
- ▲ "Hydrous" Cr-Di Webst.
- ◆ "Hydrous" Gabbroic pods
- ● Dunites + Pd 1995
- ▲ Cr Di Webst. 1995
- ▲ Al-Aug Webst. 1995
- ◆ Al-Aug Gabbros 1995
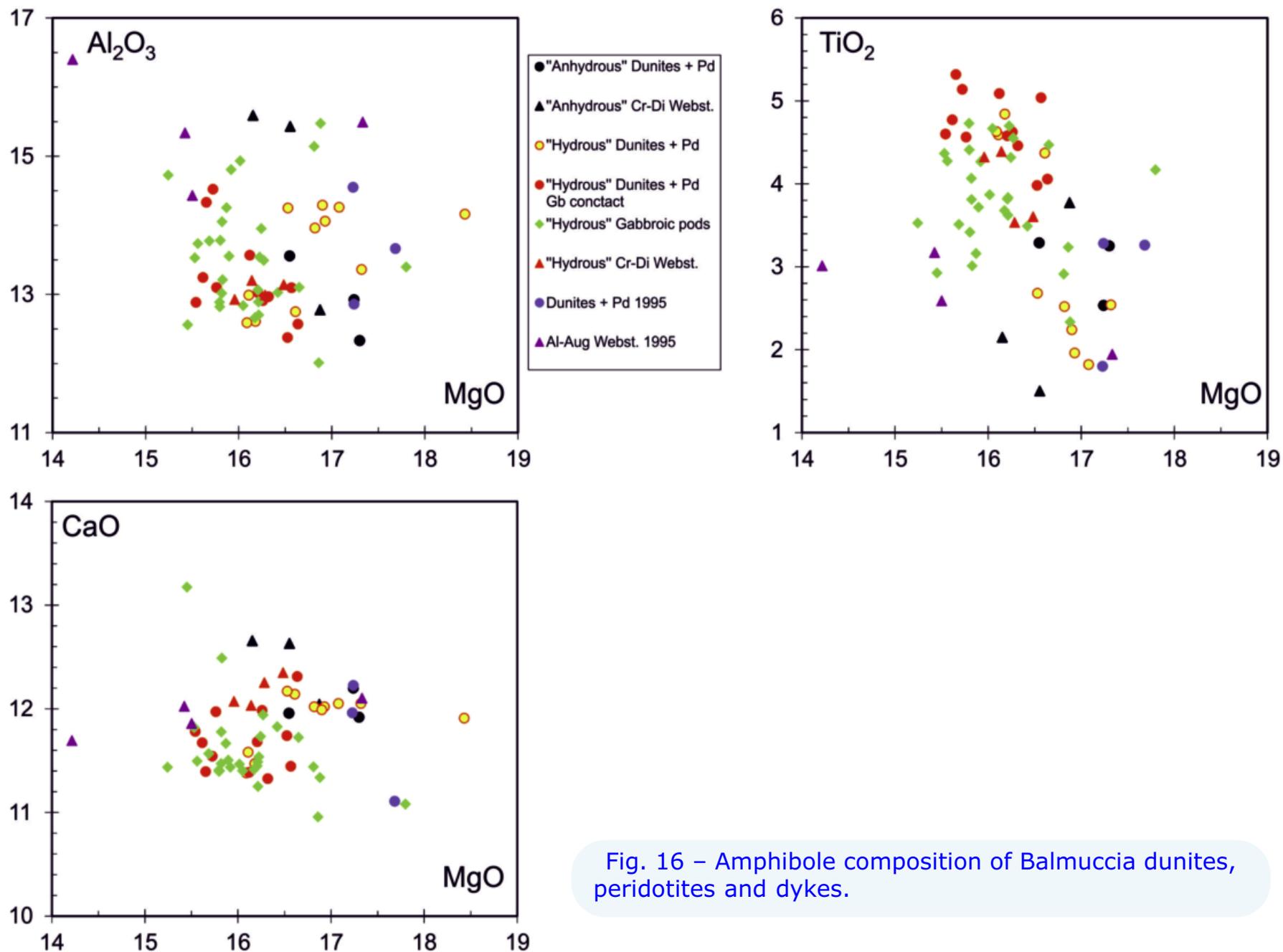
Fig. 16 – Amphibole composition of Balmuccia dunites, peridotites and dykes.

28

excursion notes
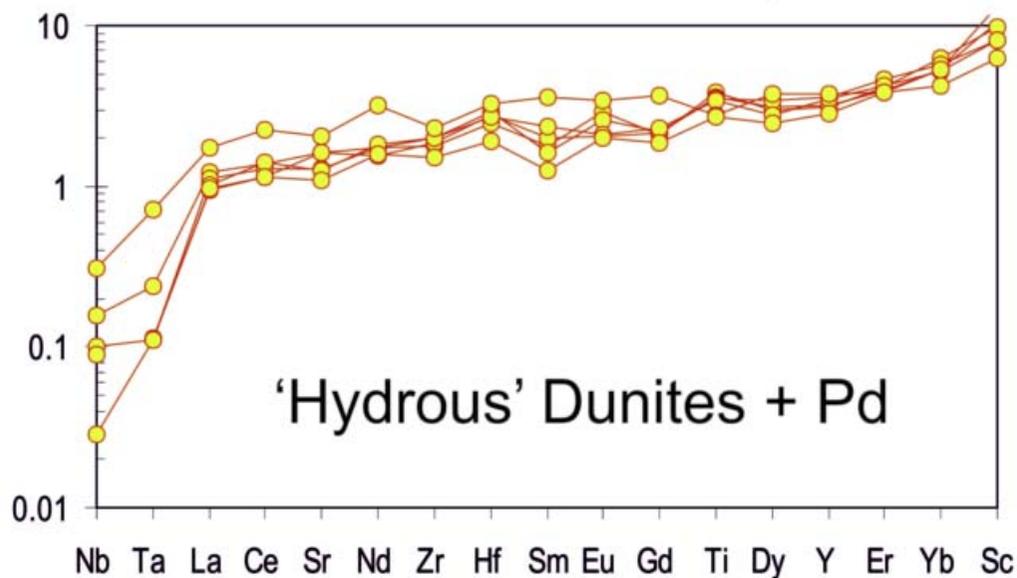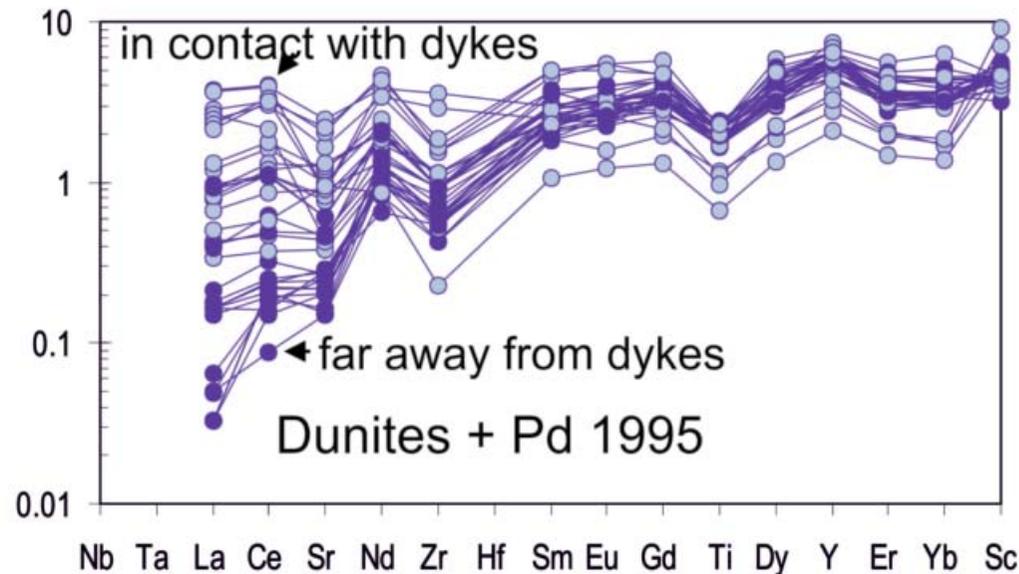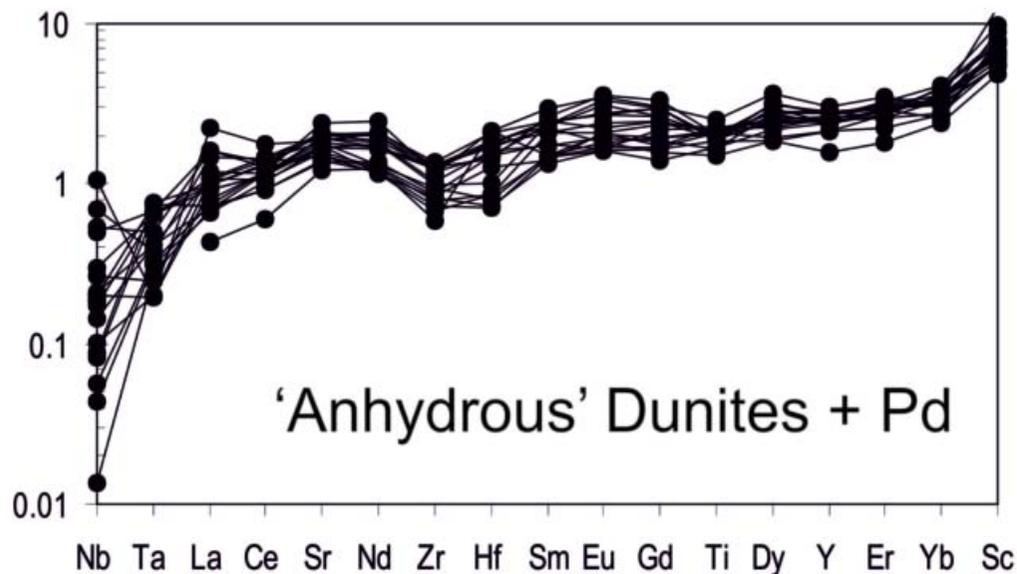
Fig. 17 – Extended trace element spidergram (normalised to PM, Hofmann, 1988) of clinopyroxene Balmuccia dunites and peridotites (Pd).
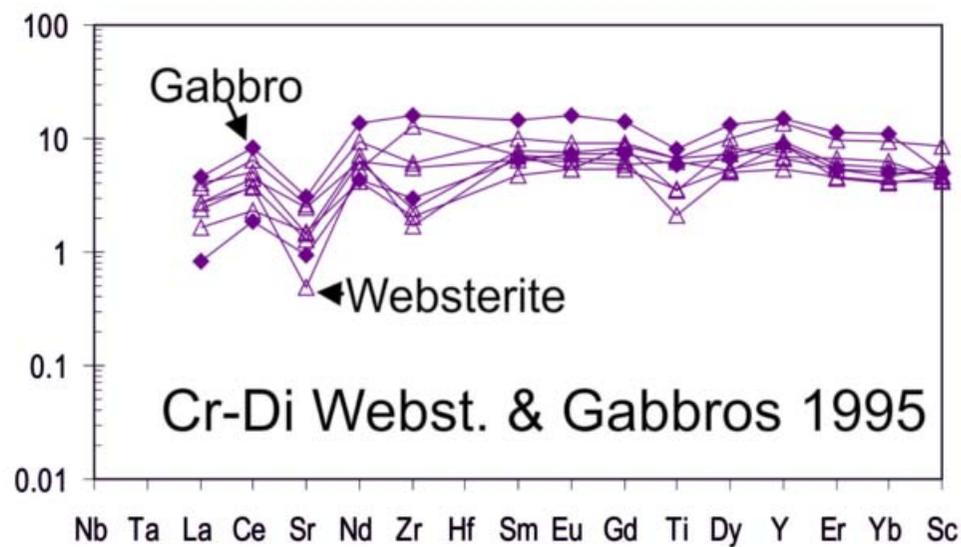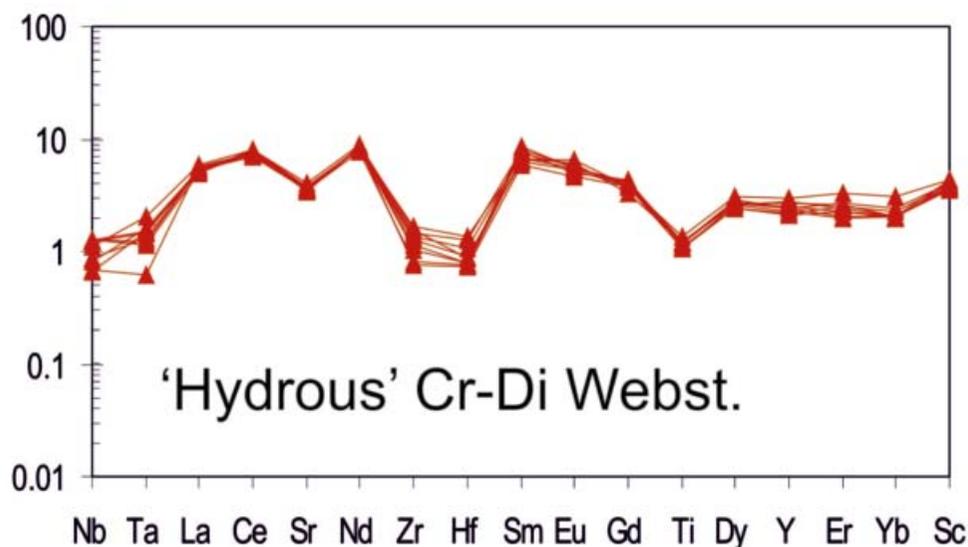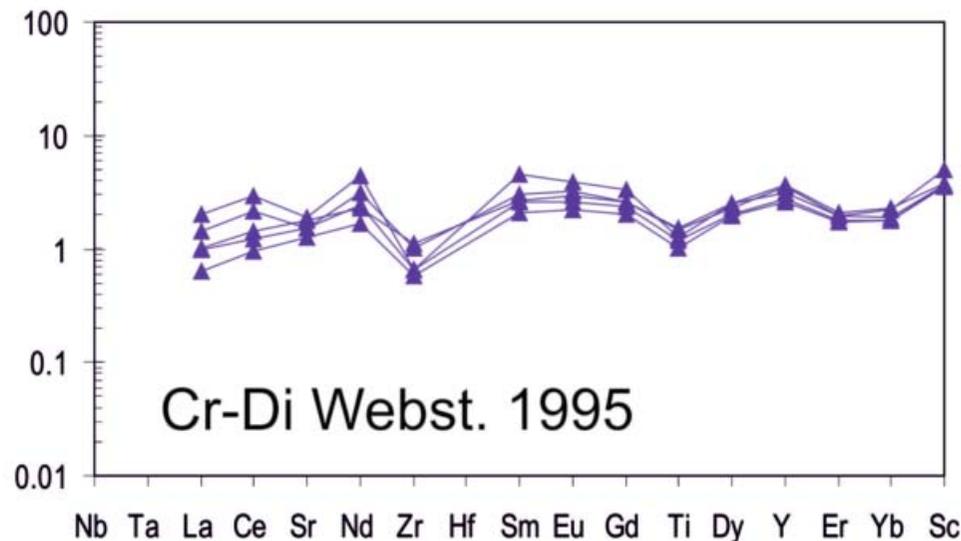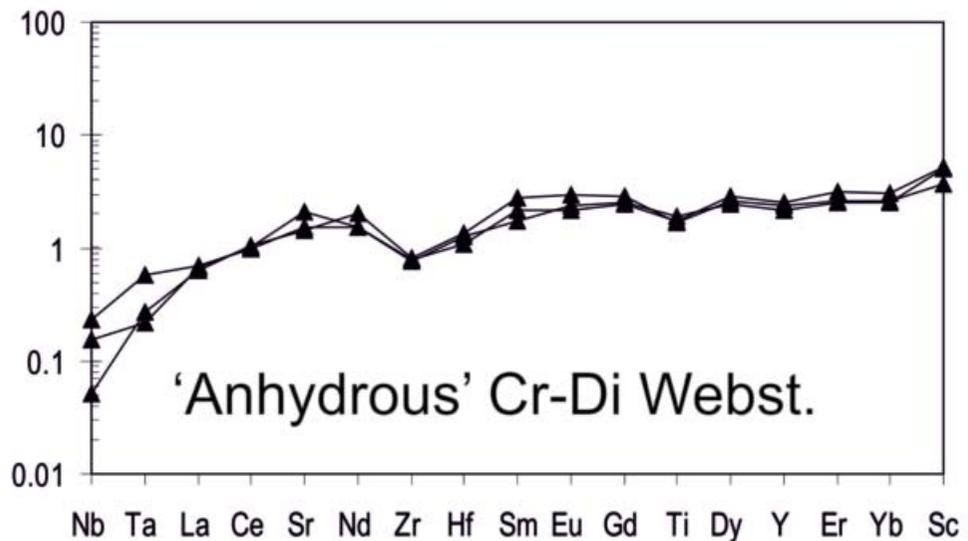
Fig. 18 – Extended trace element spidergram (normalised to PM, Hofmann, 1988) of clinopyroxene Balmuccia dykes.
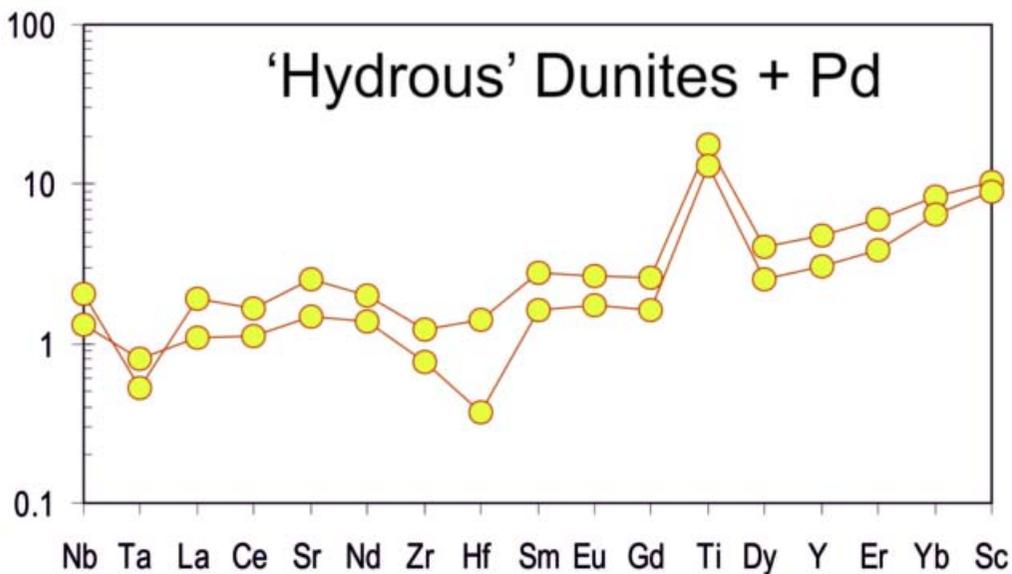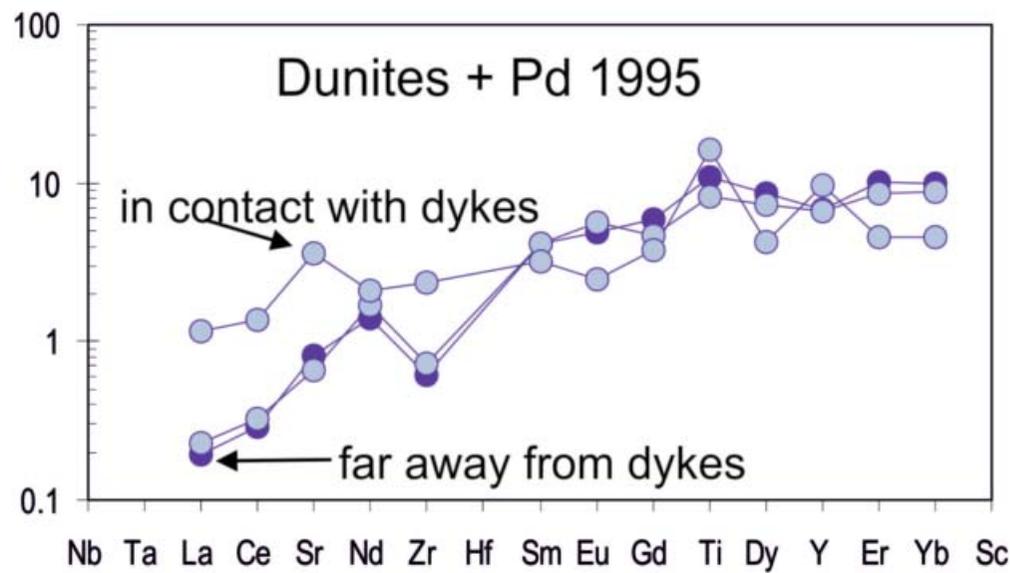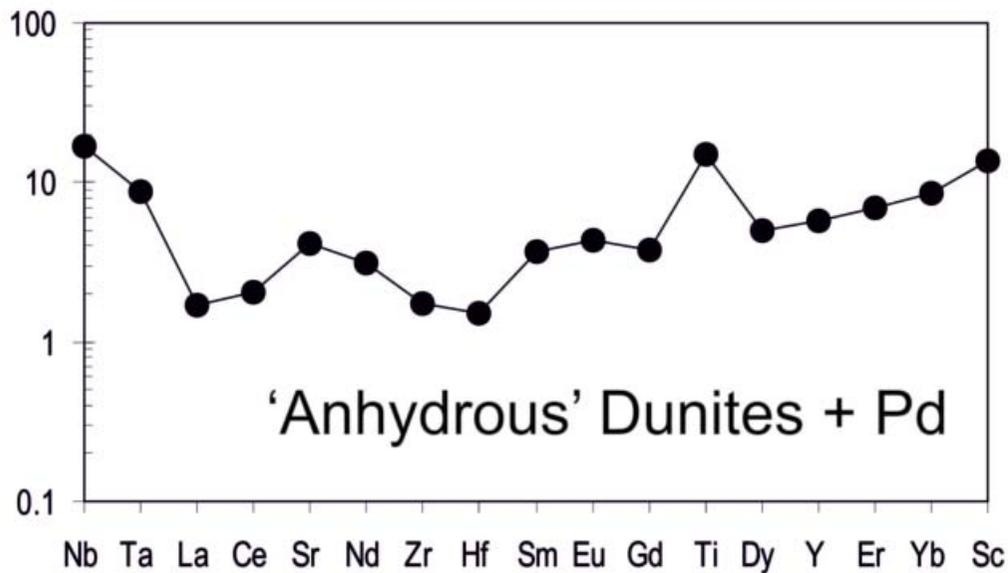
Fig. 19 – Extended trace element spidergram (normalised to PM, Hofmann, 1988) of amphibole Balmuccia dunites and peridotites (Pd).
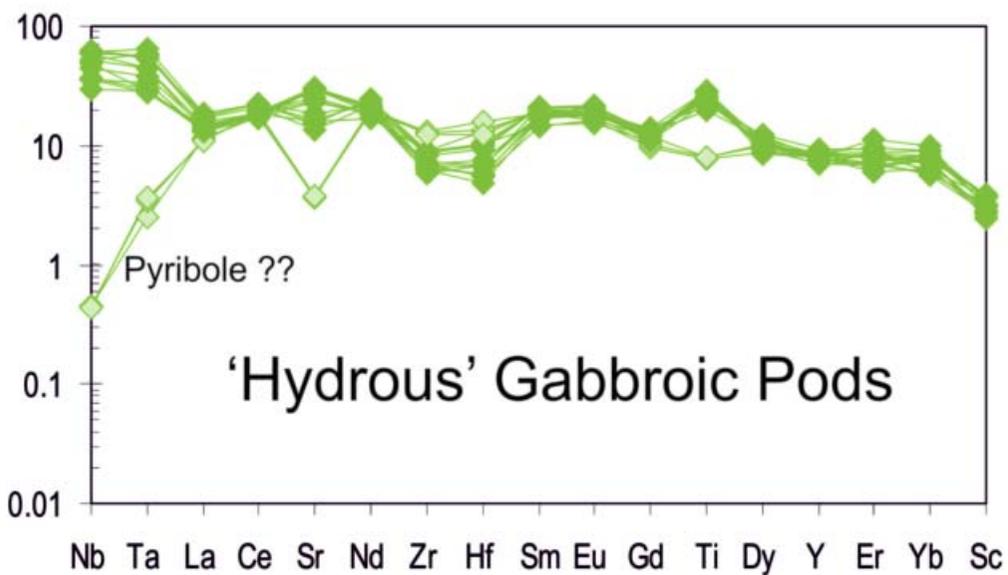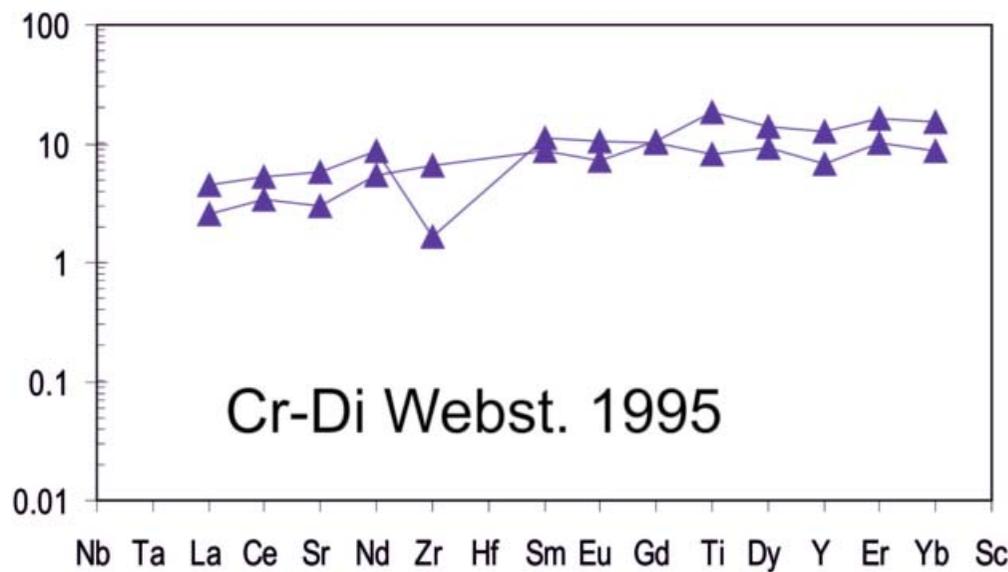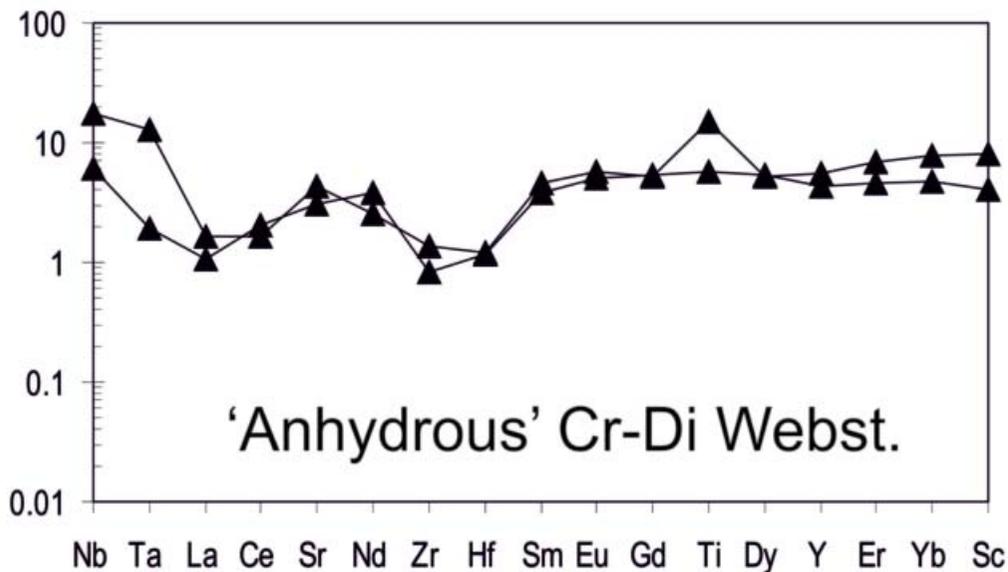
Fig. 20 – Extended trace element spidergram (normalised to PM, Hofmann, 1988) of amphibole Balmuccia dykes.

4 - The Sesia magmatic system

4.1 - The mafic complex

The gross, internal structure of the mafic complex (Fig. 21) is dominated by an arcuate structure focused on the village of Varallo and defined by layering, foliation and mappable units (Quick et al., 1994, 2003). Granitic and dioritic bodies do not crosscut the gabbro. Instead, their concordance with foliation and banding is remarkable, and crosscutting relationships are limited to faults, scarce dikes, and late-stage melt segregations. Paragneiss septa derived from the Kinzigite formation and granitic to dioritic bodies are traceable for kilometers around this arcuate structure without major breaks although they are increasingly attenuated with depth in the complex. In fact, disruption of the internal structure of the mafic complex is remarkably minor considering that the complex has been exhumed from a depth of >15 km and tilted about 90°. Most faults displace mappable units and (or) the roof of the mafic complex less than 100 m.

Isobars in the complex cut across the arcuate structure and parallel the contact with the Kinzigite formation south of the Sesia River (Demarchi et al., 1998). This indicates that the gross arcuate structure was established before equilibration pressures (Fig. 22) were locked in, and is, therefore, a pre-Alpine feature.
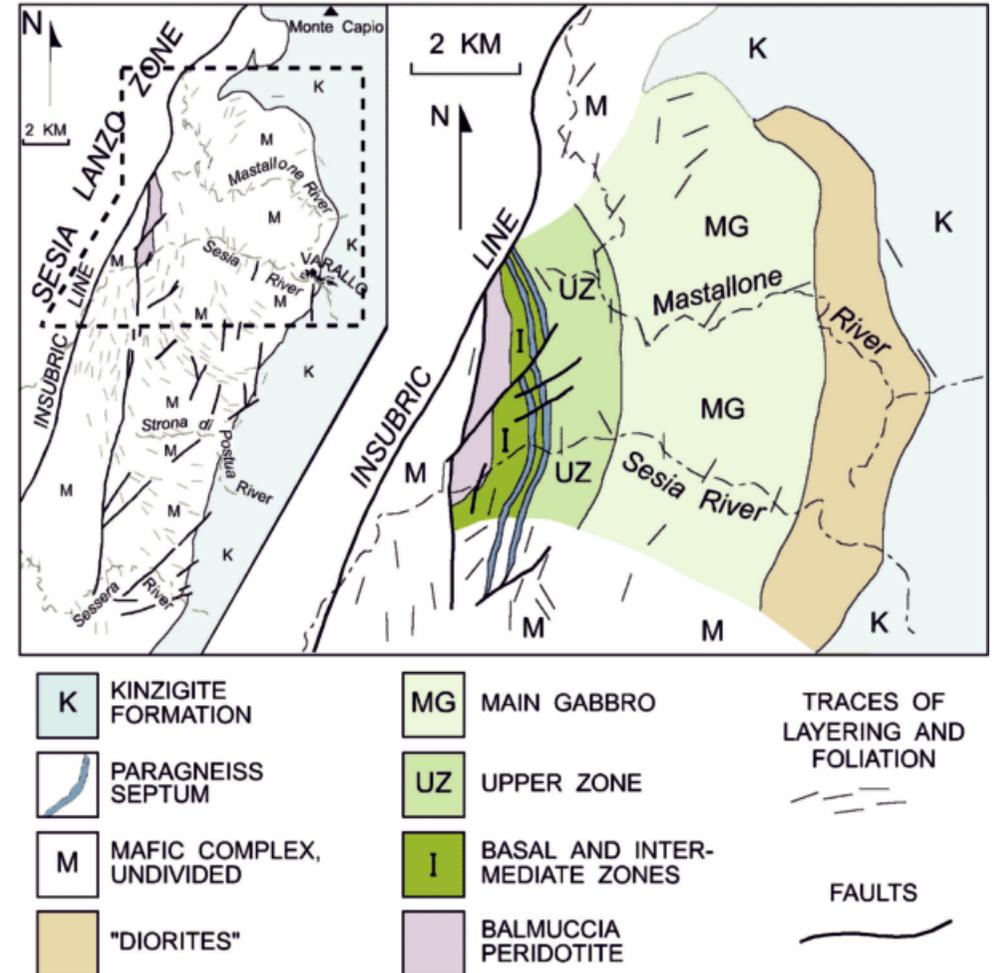
Fig. 21 – The mafic complex in the Sesia Valley, reporting the stratigraphy according to Rivalenti et al., 1975. In the inset, foliation patterns from Quick et al., 2003. Modified from Sinigoi et al., 2010.
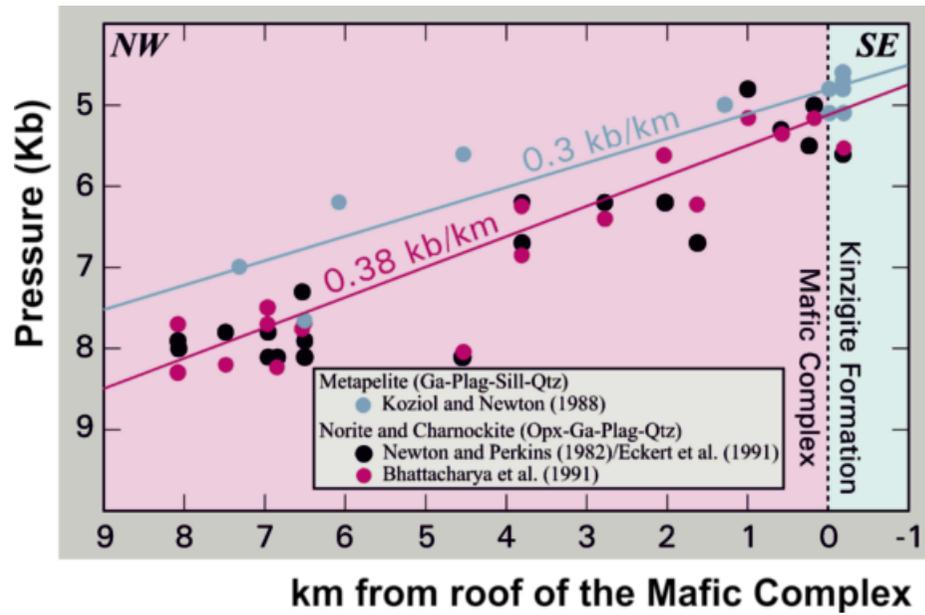
Fig. 22 – Equilibration pressure. From Demarchi et al., (1998), modified.

In terms of pre-Alpine orientations, the gross structure of the complex would have been a trough that was roofed and flanked on the north side by the Kinzigite formation. Synmagmatic deformation in the mafic complex was first described by Rivalenti et al. (1981), who interpreted intrafolial folds and high-temperature shears in terms of slumping of cumulates onto the floor on a large magma chamber. Quick et al. (1992a) observed that similar features are present in many places south of the Sesia Valley (Fig. 23), and suggested that these structures resulted from pervasive, large-scale deformation of crystal mush. Layer-parallel stretching is evidenced by boudinage and small stretching faults. Banding is locally deformed by tight to isoclinal folds with axial planes concordant with the regional foliation and fold axes parallel to the stretching lineation. Locally, undeformed,

33

excursion notes
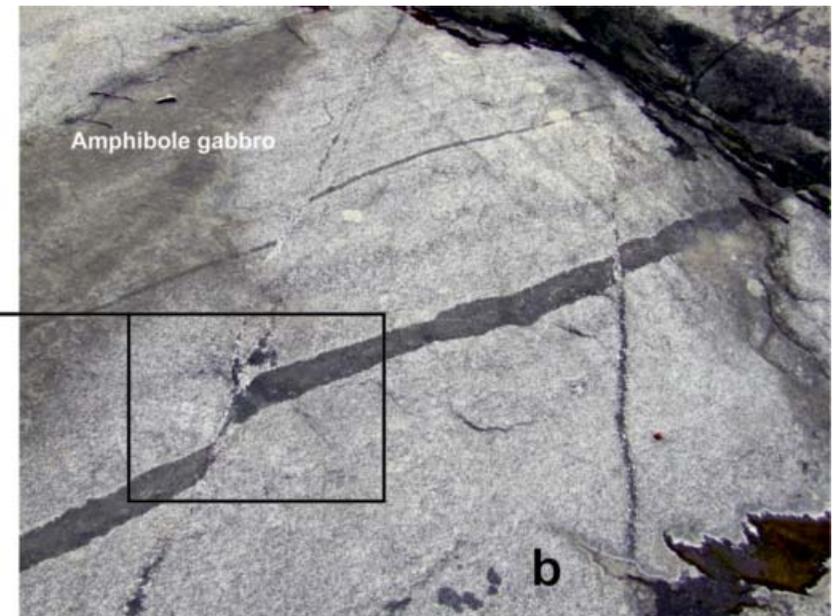
Fig. 23 – Hypersolidus faults (Stop 2.1 Sessera Valley).

poikilitic amphibole grew across the foliation indicating that a small amount of interstitial melt was present when the foliation formed. Many stretching faults are healed by thin, undeformed veins of leucogabbro, which crystallised from segregations of late-stage interstitial melts. Late stage melts segregated into undeformed patches that crosscut foliation and fill tension gashes and pressure shadows at the ends of boudins. Analogous relationships involving charnockitic anatectic melts occur in the paragneiss septa (Fig. 27).

A general increase in strain structurally downward in the complex is suggested by the following. Mappable units are increasingly attenuated with depth. Magmatic textures and structures are commonly well preserved near the top of the complex (Fig. 24) but, excluding small melt segregations, are absent at deep levels. Granoblastic textures and synmagmatic deformation are more abundant in the lower third of the complex.

Fig. 24 – Magma mingling (Stop 1.5, Aniceti, Mastallone Valley); **a)** overview along the Mastallone river; **b)** a detail where, in dioritic rocks, enclaves of fine-grained gabbro with plagioclase xenocrysts are highlighted.

4.2 - The gabbro-glacier model

The gross structure and the distribution of hypersolidus deformations are best explained by the gabbro-glacier model (Quick & Denlinger, 1992, 1993; Quick et al., 1992a, b). Quick et al. (1992a, 1994) noted that well studied analogs for the arcuate structure and synmagmatic deformation of the mafic complex are found in ophiolitic gabbro (for review, see: Nicolas, 1989, 1992; Quick & Denlinger, 1992, 1993). In addition, both the mafic complex and ophiolitic gabbro display similar strain gradients with increasing strain downward in the section. Numerical modeling (Quick & Denlinger, 1992, 1993; Phipps Morgan & Chen, 1993; Henstock et al., 1993) demonstrates that these characteristics can be produced by large-scale necking of a thick section of partially molten cumulates beneath a small magma chamber as the crust moves away from a spreading center. According to this model, a huge

volume of gabbroic crystal mush is created from a relatively small and continuously fed magma chamber, as crystallising cumulates are continuously transposed outwards and downwards from the chamber. Consistently, the best preserved igneous textures, like swarms of mafic enclaves mingled in diorite (Fig. 24), are close to the roof in the vicinity of Varallo, at the core of the arcuate structure, whereas most feeders are annealed and were largely transposed at low angle or parallel into the foliation.

4.3 - Paragneiss septa

Within the mafic complex are numerous layers of granulitic paragneisses, termed septa, comprising metapelites, wackes and minor calc-silicates. These layers are characterized by an extreme aspect ratio, and some may be followed along strike for kilometers although they are only a few meters thick. Compared to the amphibolite-facies roof rocks, they are richer in garnet and extremely depleted in micas. Feldspars are generally antiperthitic and sillimanite forms discrete crystals, rather than the fibrolite that is typical of the roof of the complex.

Measured density of these rocks varies from 2.9 to 3.4 g/cm^3, whereas roof rocks range from 2.7 to 2.9 g/cm^3. The increase in density of the septa correlates with decreasing SiO_2 and Rb abundance and increasing Al_2O_3 and FeO abundance, consistent with decrease of micas and increase of garnet in the restite as a result of larger extraction of anatectic granitic melt from the septa than from the roof rocks. Both measured densities of gabbro and computed densities of the parental gabbroic melt at 5 Kb are close to 3 g/cm^3, i.e. intermediate between the septa and roof rocks (Sinigoi et al., 1995).

The following mechanism was proposed by Sinigoi et al. (1995) to explain the density, field and geochemical data. A basaltic sill ponded in the lower crust at its level of neutral buoyancy (Ryan, 1993). Upward migration of anatectic melt from the roof rocks left behind an increasingly dense restite until the density of the restite exceeded that of the underlying mafic magma. Local weakening due to the coalescence of the upward migrating anatectic melts may have facilitated detachment of the roof rocks. These denser roof rocks were incorporated into the complex as new additions of mafic melt ponded over them. A septum was formed and the new roof began to melt as a new cycle of intrusion, melting and density change began. After having been incorporated in the growing mafic complex, the melting septa were transposed together within the crystallising gabbro glacier, so attaining their extreme aspect ratio and parallel fabric.

Most septa are grouped near the transition between the lower mafic complex, dominated by mafic, granoblastic amphibole gabbro, and the upper mafic complex, comprising gabbro, norite and diorite (Fig. 26). On the basis of this distribution of the septa, Sinigoi et al. (1996) introduced the term "paragneiss bearing belt", with the aim of defining a region where septa are more abundant.

In fact, septa flair upward into higher levels of the mafic complex, and their apparent concentration at deeper levels is interpreted to be a consequence of flow within the gabbro glacier.

Thus, the paragneiss bearing belt should not be interpreted as a well-defined layer with any temporal or stratigraphic significance. Furthermore, it should be noted that rare septa, too small to depict in Fig. 25, are present in both the upper and lower mafic complex. In several cases, septa diverging upwards in the mafic complex connect with foliated granitoid bodies, suggesting segregation of anatectic melts from melting paragneiss septa during the growth of the gabbro glacier.

36
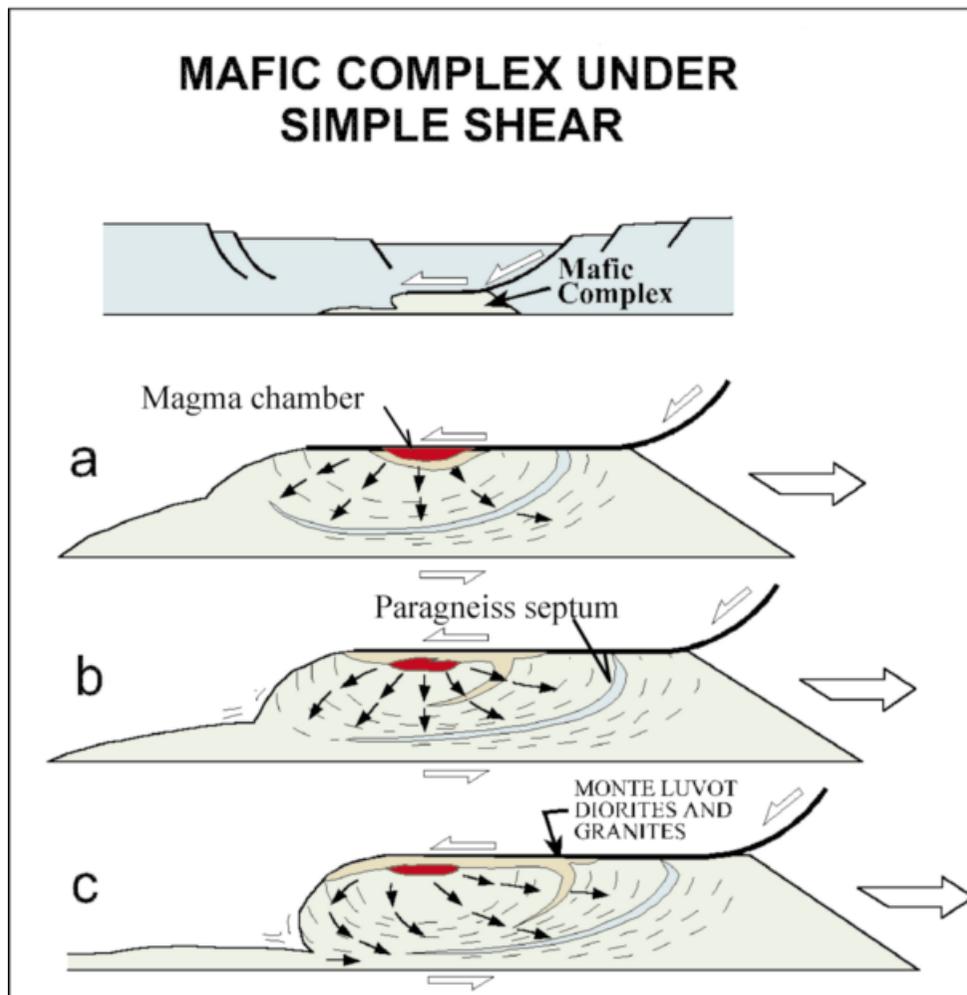
Fig. 25 – Schematic diagram summarizing the evolution of the mafic complex in the context of an extending crust under simple shear. Location of the mafic complex in the crust is followed by enlargements to show details of internal structure of the mafic complex. Red, magma chamber; green, cumulates, with variable amounts of interstitial melt; orange, dioritic and granitic rocks; blue, pre-underplating crustal rocks. Large, open arrows indicate direction of crustal movements. Small arrows in mafic complex indicate trajectories of cumulates and septa during ductile deformation. Foliation indicated by dashes (modified from Quick et al., 1994).

Fig. 26 – Geologic map of the mafic complex, simplified from Quick et al., 2003.
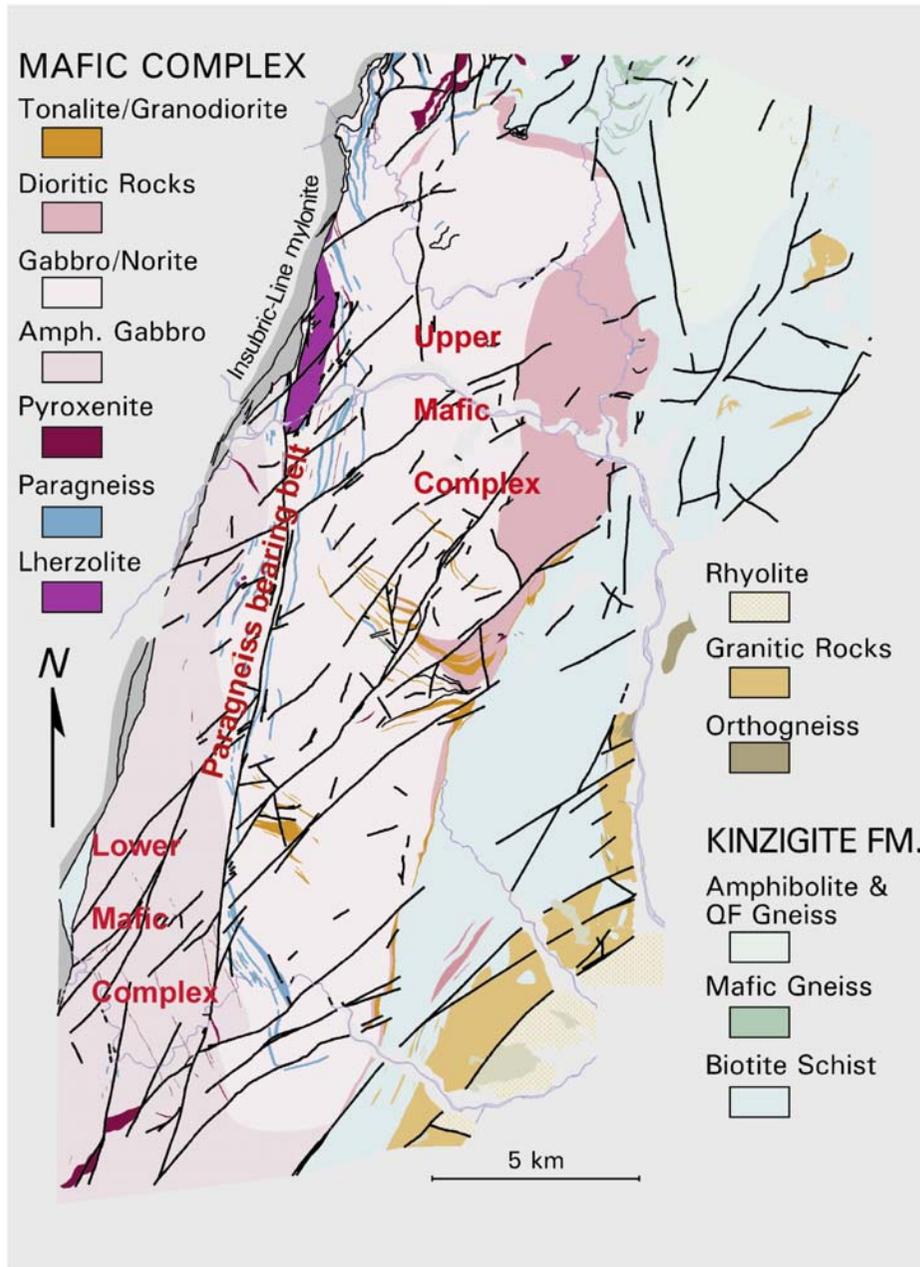
Fig. 27 – Paragneiss septum (Sessera Valley).

In the paragneiss bearing belt, septa are interleaved with mafic gabbros, a suite of rocks ranging from norite to charnockite and ultramafic cumulates. Among the latter, cumulus peridotites layers are up to 100 m thick east of the Balmuccia peridotite, in the area between Sesia and Mastallone Valleys (intermediate zone of the previous stratigraphic subdivision of Rivalenti et al., 1984; Fig. 21), but become attenuated to few meters to the south.

In the Sesia area, cumulus peridotite shows up to 2-cm-thick reaction rims of pyroxene + spinel at the contact with gabbro (Fig. 29a, b and c). These rims developed under high-T subsolidus conditions, possibly still in presence of interstitial melt, as evidenced by synmagmatic deformation structure in proximal gabbros, (Fig. 29d) and were previously interpreted as cooling growths over slump structures (Rivalenti et al., 1981). The cumulus peridotites in the Sesia area and associated gabbros are interleaved with paragneiss septa, and most-likely crystallised in sills rather than in a huge magma chamber.

Moreover, they show north-dipping lineations consistent with lineations of the gabbro (Fig. 29a and c). Collectively, these observations lead to the conclusion that these structures are better interpreted as sheath folds developed at very high temperature during stretching at the deep levels of the glacier. The reaction ol+plag = px+spinel is very sensitive to P and less sensitive to T (Presnall, 1976). The fact that these features developed beneath the core of the mafic body suggest they formed during the increase in pressure that affected these cumulates during stretching as they were transposed downward within the deforming gabbro glacier and buried beneath several kilometers of gabbro.
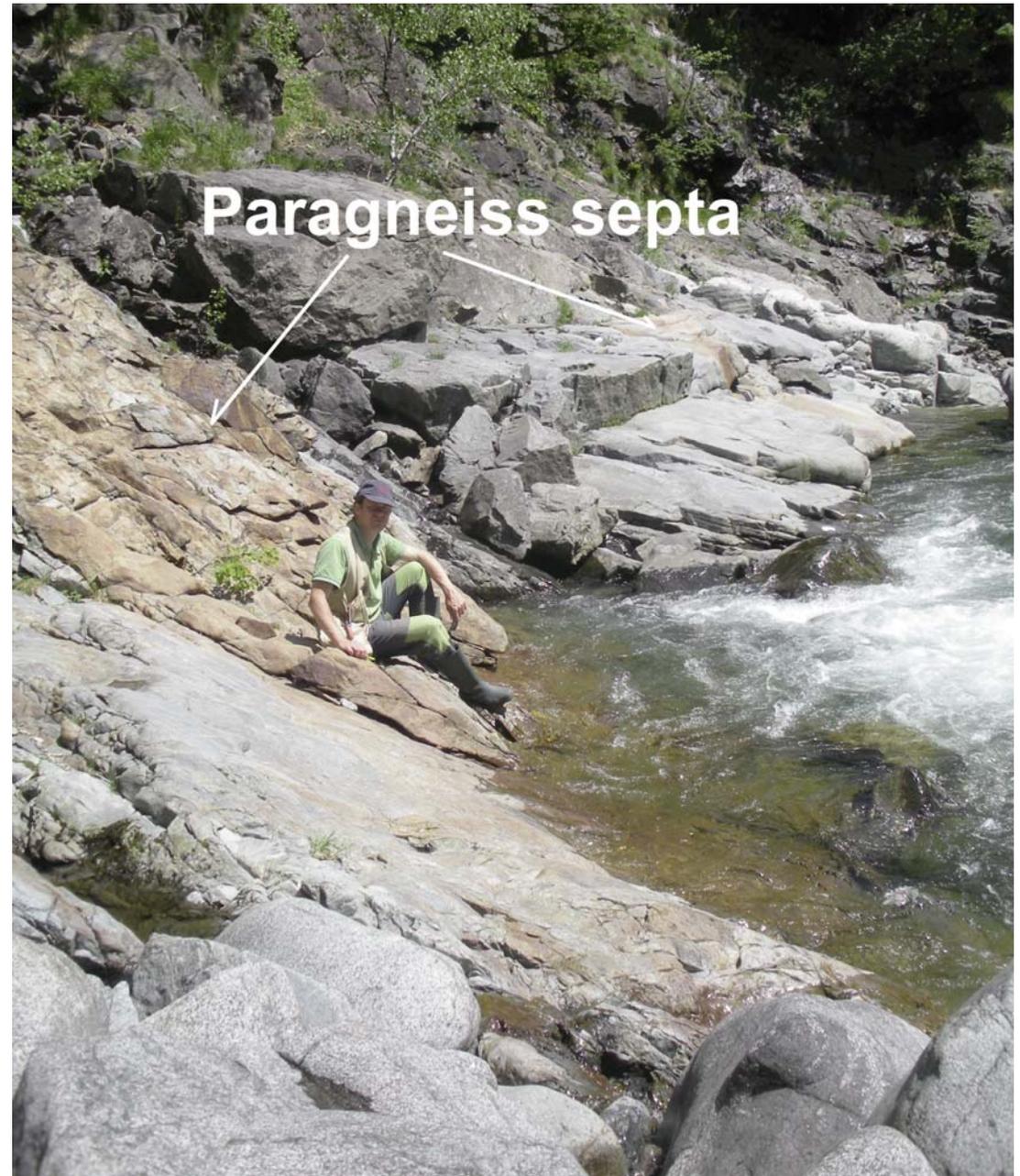
Fig. 28 – Paragneiss septa at deep levels, red because of the abundance of garnet.
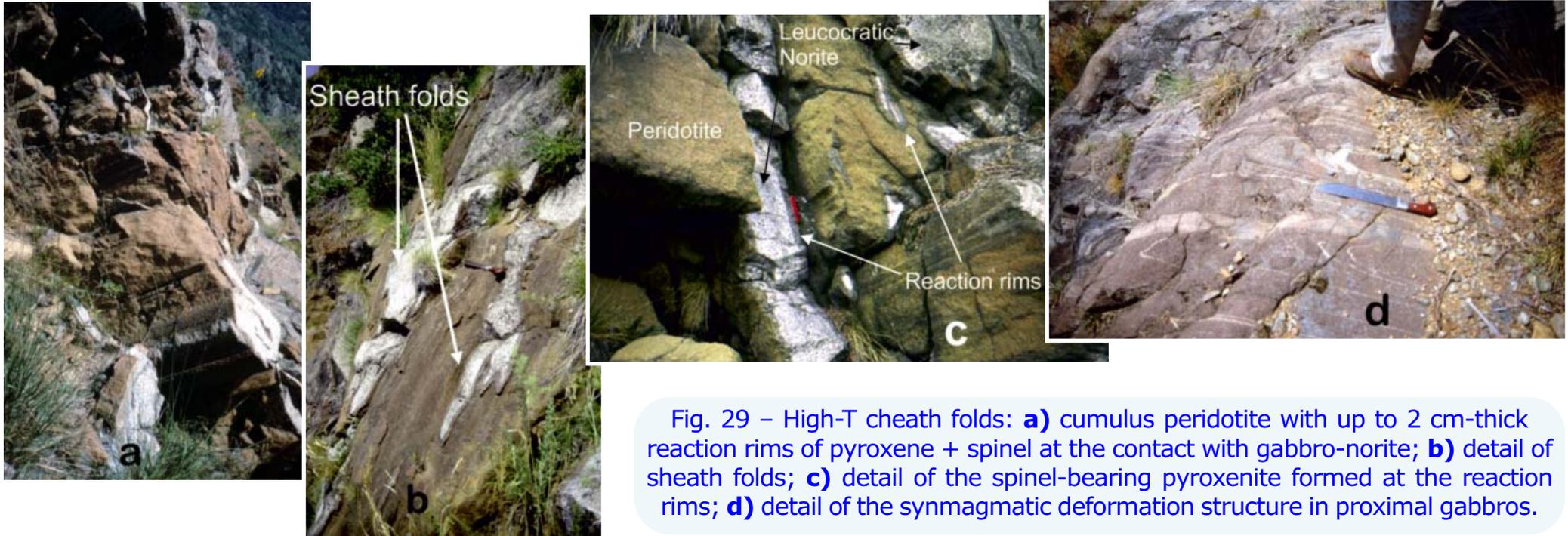
Fig. 29 – High-T cheath folds: **a)** cumulus peridotite with up to 2 cm-thick reaction rims of pyroxene + spinel at the contact with gabbro-norite; **b)** detail of sheath folds; **c)** detail of the spinel-bearing pyroxenite formed at the reaction rims; **d)** detail of the synmagmatic deformation structure in proximal gabbros.

4.4 - Geochemistry of the mafic complex

Voshage et al. (1990) first showed that igneous rocks within the paragneiss-bearing belt (their basal and intermediate zones) have Nd_i and Sr_i isotopic ratios that display considerable variation, in contrast to a relatively more homogeneous isotopic composition of the upper mafic complex (their "Main Gabbro" and "Diorites"). Within the paragneiss-bearing belt, Voshage et al. (1990) report a few gabbros with isotopic compositions compatible with uncontaminated, mantle-derived melts (Sr_i = 0.702 to 0.704, εNd = 6.2 to 7.2), and MORB-like, depleted REE patterns. Sinigoi et al. (1996) report an additional sample with these MORB-like characteristics within the paragneiss-bearing belt and close to the mantle peridotite.

Although some of these uncontaminated samples could be interpreted as older mafic granulites unrelated to the mafic complex, one sample, TS4 (Mayer et al., 2000) is an undeformed gabbroic dyke that intrudes the Balmuccia peridotite border zone, cross-cutting the intense spinel foliation and boudinaged Cr-diopside and Al-augite dykes and bands. This dyke clearly post-dates the emplacement of the mantle tectonite in the deep crust, and appears to have preserved its primary composition, with Sr_i=0.7021 (Voshage et al., 1988) and depleted REE patterns (Fig. 30) as

Igneous evolutions across the Ivrea crustal section: the Permian Sesia Magmatic System and the Triassic Finero intrusion and mantle

M. Mazzucchelli - J. E. Quick - S. Sinigoi - A. Zanetti - T. Giovanardi

40

excursion notes
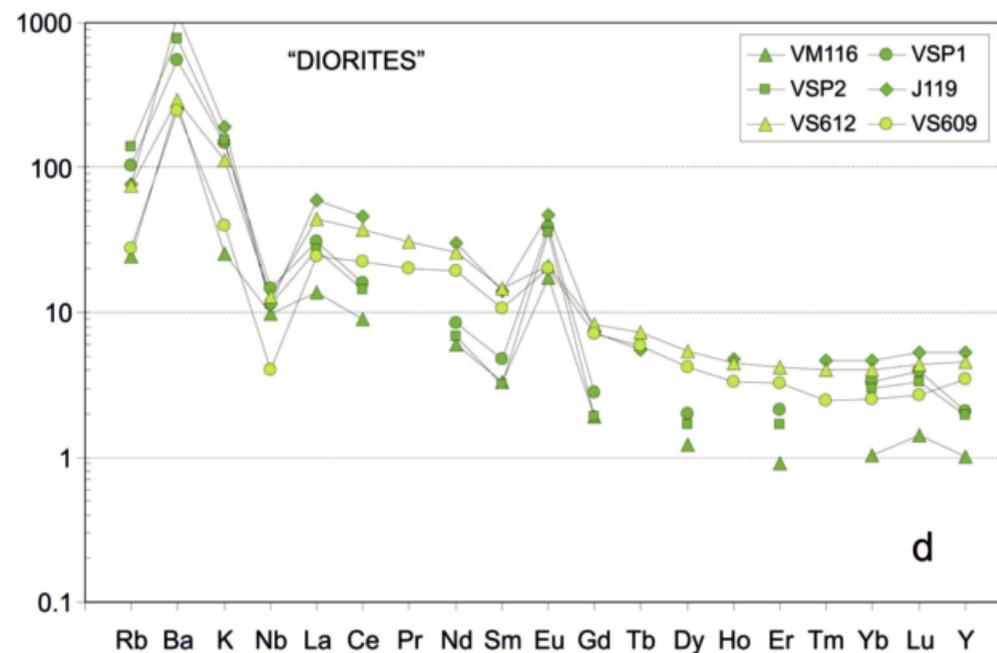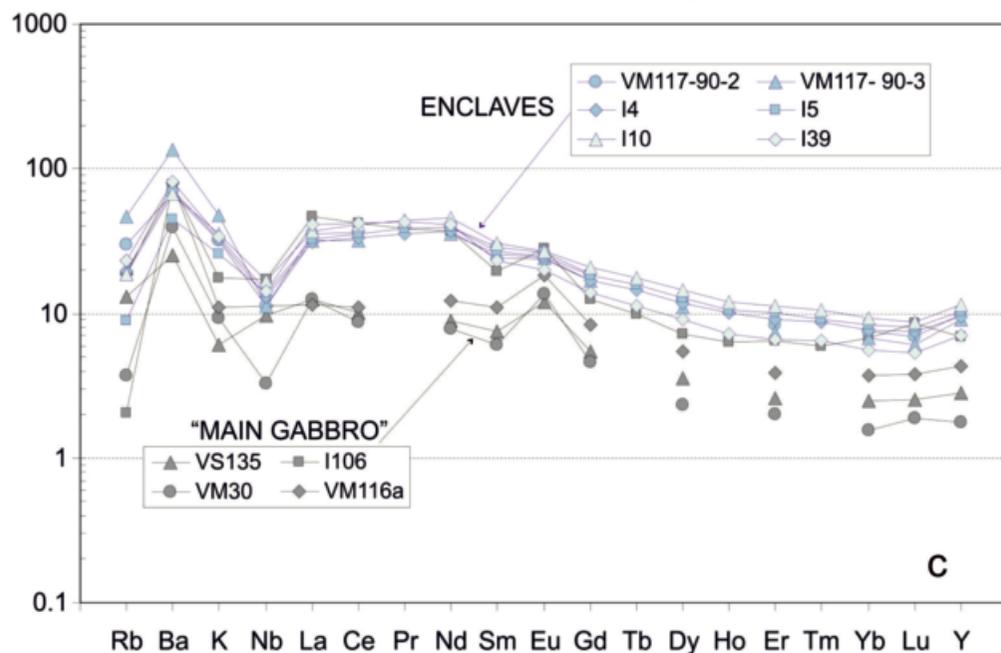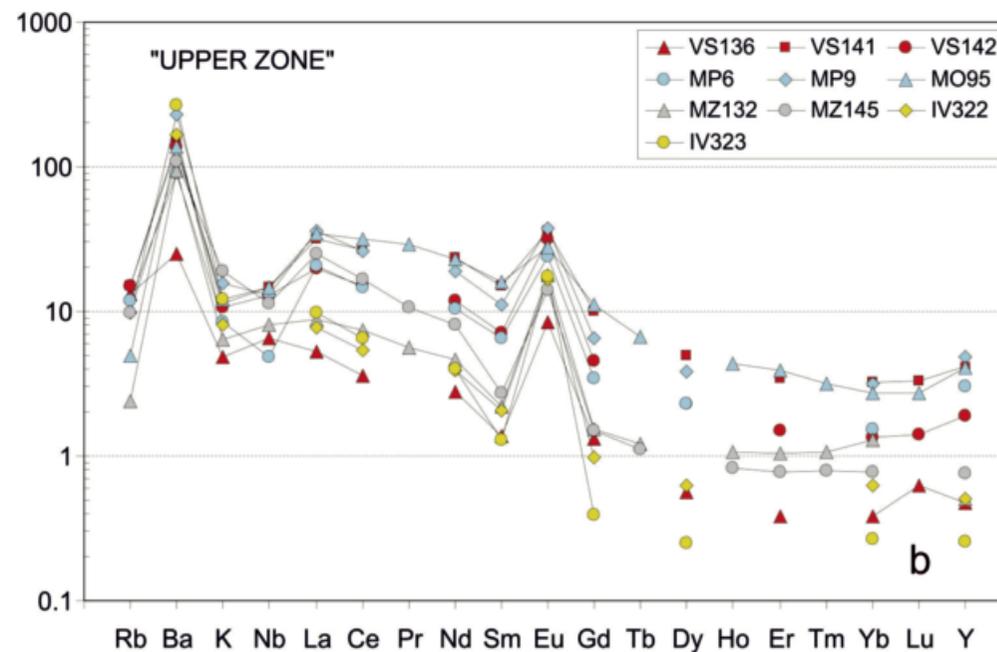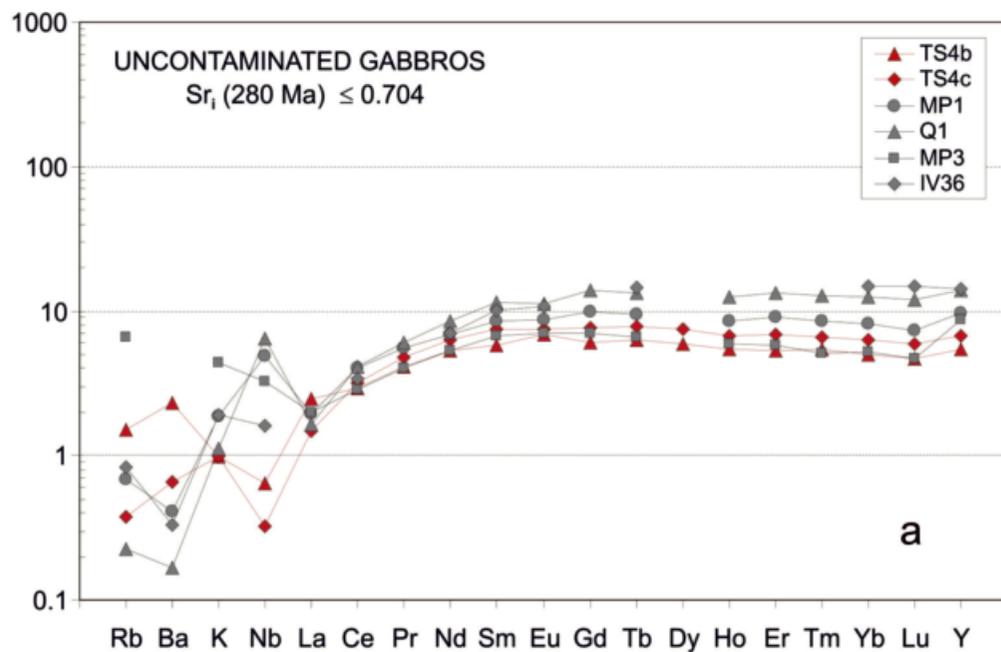
Fig. 30 – Extended spidergrams.

a consequence of intruding peridotite rather that isotopically evolved paragneiss. Dyke TS4 yelds an internal Sm-Nd isochron of 274 Ma (Mayer et al., 2000), consistent with slow cooling after emplacement of the entire mafic complex at about 288 ± 4 Ma (Peressini et al., 2007). Thus, its intrusion is bracketed within the emplacement of the mantle tectonite and the cooling of the mafic complex and, therefore, must be related to the main Permian event. These considerations support the interpretation of Voshage et al. (1990) that first mantle melts intruded the deep crust quenched too fast for their compositions to be influenced significantly by crustal contamination, and only after successive intrusions pushed temperatures of the country rocks above their solidi were intruding mantle melts contaminated by isotopically evolved crust.

Excluding the few uncontaminated gabbros discussed above, the isotopic and trace-element compositions of most igneous rocks of the mafic complex indicate high degrees of crustal contamination. Voshage et al. (1990) showed that the εNd of the upper mafic complex (their upper zone, "Main Gabbro" and "Diorites" according to the stratigraphy of Rivalenti et al., 1984) was relatively uniform and concluded that these rocks had crystallised from a magma chamber that had achieved a thermal balance between magma input, anatexis, assimilation, and crystallisation. Sinigoi et al. (1994) extended the analysis to include Sr and O isotopic compositions and trace element abundances. Most of the mafic complex is characterized by Sr_i > 0.706, $\delta^{18}O$ > 7.5 enrichment in LREE and an enrichment in Ba relative to K and Rb (Figs. 31 and 32). The absence of these characteristics in rocks with Sr_i < 0.704 suggests that they reflect crustal contamination and that the contaminant was enriched in Ba relative to K and Rb. Mazzucchelli et al. (1992b, 1992c) found positive Eu anomalies in plagioclase, clinopyroxene and garnet at deep levels of the upper mafic complex (their upper zone), which they interpreted to indicate that the melt that crystallised these phases had acquired a positive Eu by crustal contamination. Ba and Eu anomalies are in general positively correlated, indicating contamination by a biotite- and feldspar- enriched source that was previously depleted in Rb and K by dehydration melting and separation of anatectic melt. Positive Ba and Eu anomalies are also characteristics of the charnockites present as dikes or bands in the paragneiss bearing belt, which are interpreted as anatectic melts delivered from the septa. Similar Eu-enriched charnockites are described in other parts of the IVZ (Schnetger, 1988) and in other granulite terranes (e.g., Pride & Muecke, 1982; Barbey et al., 1990; Harris et al., 1986). Sinigoi et al. (1995) concluded that the septa must have been stripped in K and Rb by fractional melting before being peeled off from the Kinzigite formation and incorporated into the mafic complex, according to the process driven by evolving density contrast previously described. Following incorporation of the septa by the mafic
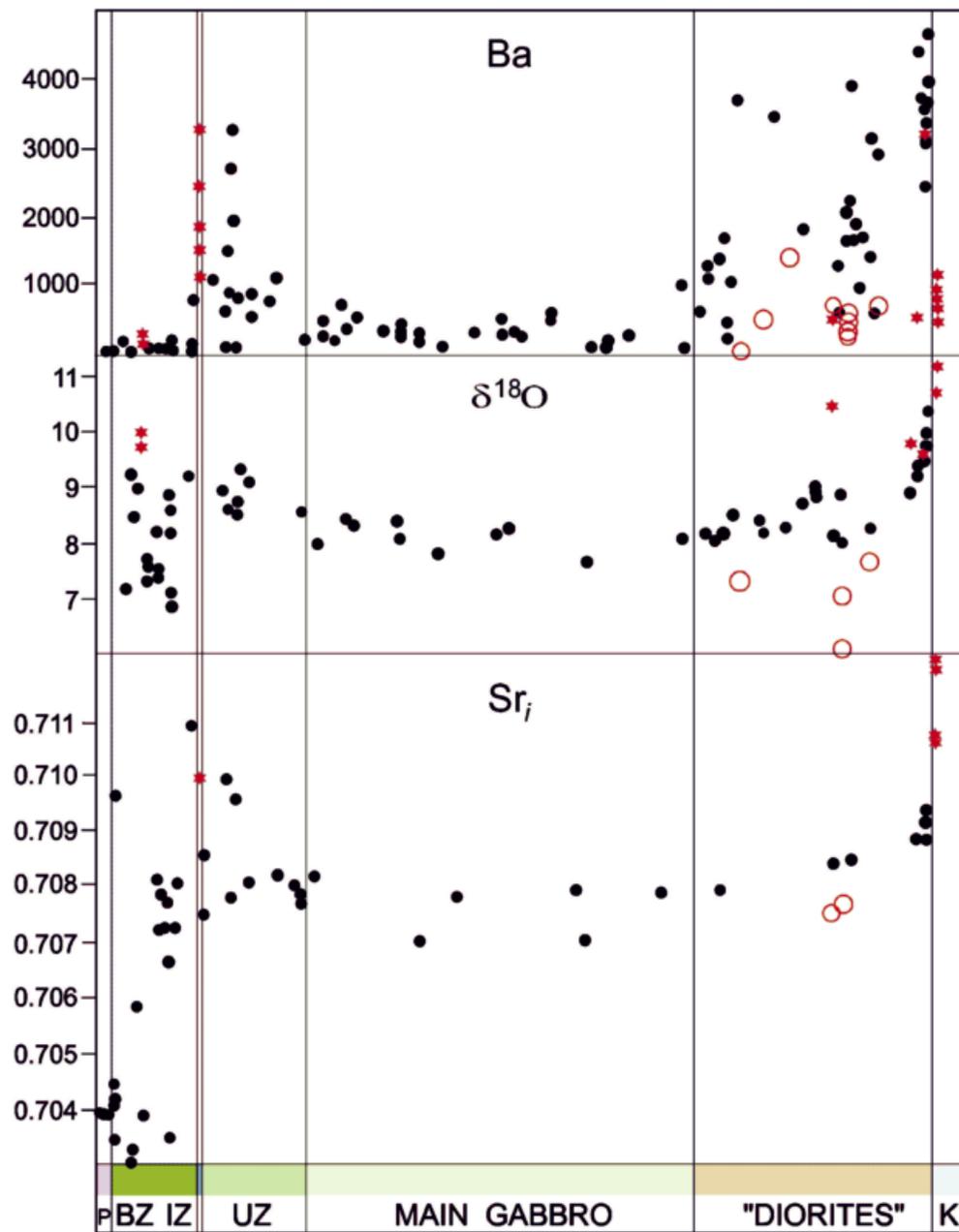
Fig. 31 – Ba, $\delta^{18}O$ and Sr_0 vs. stratigraphy (modified from Sinigoi et al., 1994).
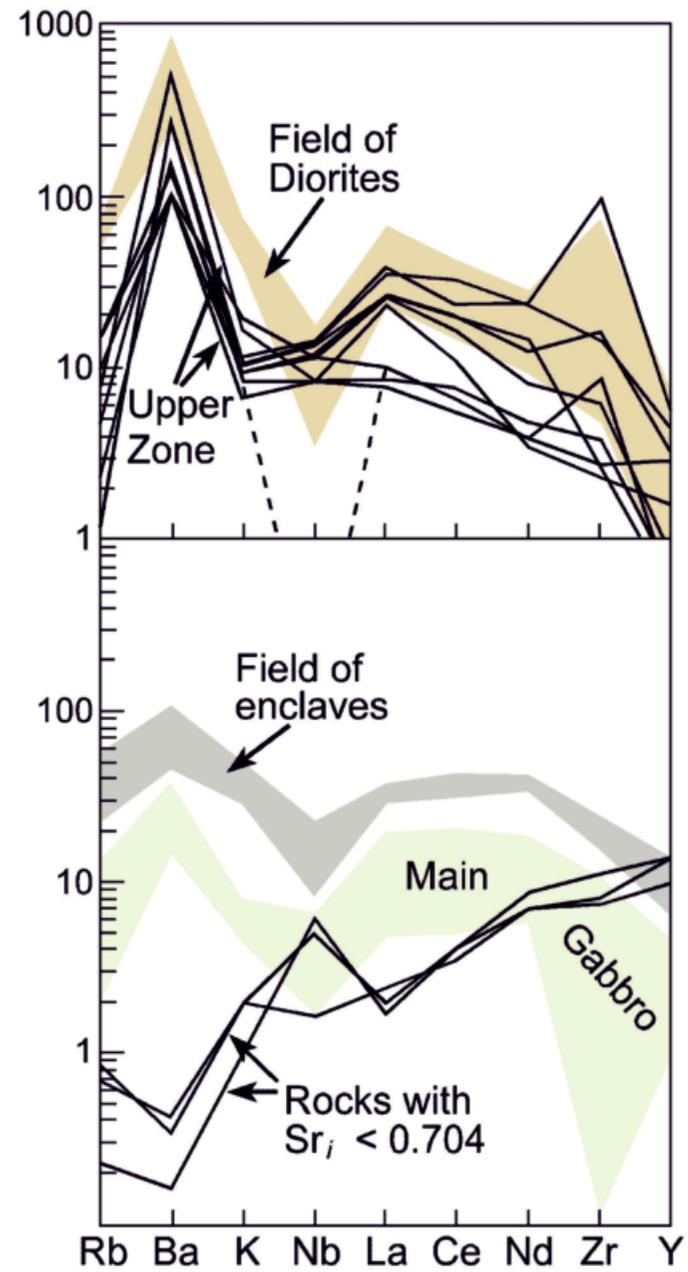
Fig. 32 – Normalized incompatible elements (modified from Sinigoi et al., 1994).

complex, advanced anatexis of residual biotite and especially K-feldspar, enriched in Ba and Eu, would provide the observed compositions. Ba and Eu are both compatible in K-feldspar, whereas only Eu is compatible only in plagioclase. In the mafic complex, the Ba and Eu anomalies are in general correlated positively, consistent with advanced melting of residual K-feldspar in the crustal source. A decoupling from this behavior may be caused by fractionation of plagioclase, with the result of increase Ba but decrease Eu to yeld a minor negative Eu anomaly, as observed in some norite from the paragneiss bearing belt (Fig. 33).

The highest Ba and Eu anomalies are found in cumulates above the paragneiss bearing belt, at the base of the upper mafic complex (upper zone of Rivalenti et al., 1984), an in the "Diorites", whereas they are minor in the "Main Gabbro" and in the mafic enclaves intruded in the "Diorites" (Figs. 34 and 35). This suggests that the "Diorites" are not differentiated melts (they should be lower in Eu, after fractionation of plagioclase-rich cumulates) but rather cumulates, as suggested also by the petrography (Fig. 34). If so, the "magma chamber" at the core of the arcuate structure of the gabbro glacier was actually a cumulitic crystal mush within which swarms of mafic enclaves intruded as irregular bodies.
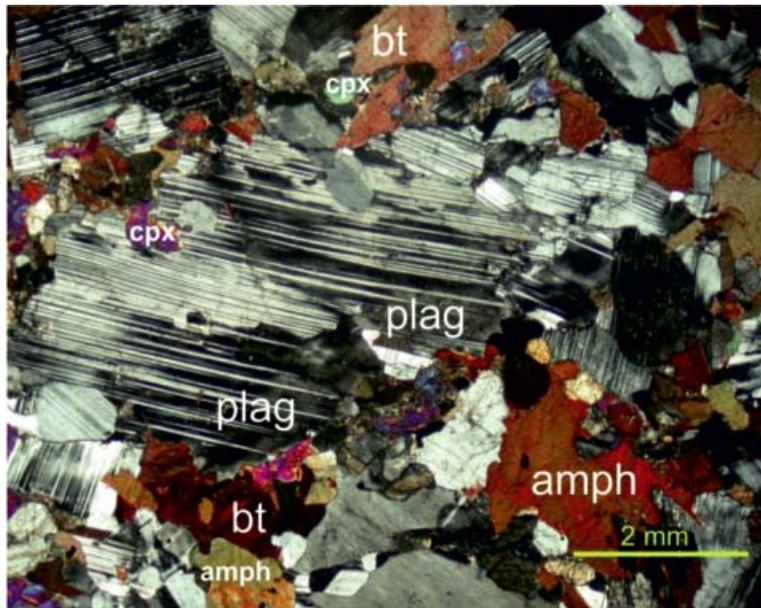
Fig. 33 – Ba* vs. Eu* showing a general positive correlation of Ba and Eu anomalies and the decoupling from this behavior, as observed in some gabbroic rocks from the paragneiss-bearing belt.

Fig. 34 – "Diorite" in thin section. amph = amphibole, bt = biotite, cpx = clinopyroxene, plag = plagioclase. After Sinigoi et al. (2010), modified.

44

Fig. 35 – Geologic map of the Sesia magmatic system with location of samples dated by Peressini et al. (2007) and Quick et al. (2009).

4.5 - Age of the Sesia magmatic system

Peressini et al. (2007) provided age determinations based on SHRIMP U-Pb analyses of zircons from 11 samples of the mafic complex. Five samples from the upper mafic complex range in age from 289 ± 3 to 286 ± 6 Ma, in agreement with a conventional U-Pb zircon age measured by Pin (1986), and three Pb-Pb evaporation ages measured by Garuti et al. (2001), and providing the best age estimate for the injection of mantle-derived melt into the deep crust to form the Upper mafic complex. Individual SHRIMP spot ages at deeper levels of the mafic complex range from > 310 to < 250 Ma, interpreted to reflect inheritance and continuous recrystallisation of zircons during a prolonged period of intrusion, slow cooling and deformation in the deep crust punctuated by repeated intrusive events.

Quick et al. (2009) determined SHRIMP U-Pb ages on zircons from granites intruded in both the IVZ and "Serie dei Laghi" above the mafic complex, and from volcanic rocks exposed in Val Sesia across the Cremosina line. As described by Quick et al. (2009), the exposed volcanic field is dominated by caldera fill tuffs and megabreccia, the distribution of which indicate a caldera > 13 Km across. The oldest

single-age for the volcanic rocks is of 288 ± 2 Ma, determined on zircons from andesitic basalt sample, R6. This age matches, within errors, that of a granodiorite collected at deep levels in the Roccapietra granite and that of the upper mafic complex determined by Peressini et al. (2007).

Zircons from samples of the predominant rhyolitic tuffs provided bi-modal ages, with a cluster of zircons at about 289 ± 3 Ma which were interpreted as "antecrysts" produced in early phases of related magmatism (e.g. Charlier et al., 2004; Bryan et al., 2008) and younger zircon ages spreading towards 282 Ma. The youngest ages of 278 ± 5 or 275 ± 4 were measured for the upper Valle Mosso aplitic granite, which constitutes the highest part of the Valle Mosso body and intrudes the volcanic rocks. An intermediate age of 282 Ma is reported by Schaltegger & Brack (2007) on the Montorfano granite, 12 km north of Fig. 35. A palinspastic restoration of the Alpine effects, considering the displacement of Alpine faults and the differential tilting, places the caldera and the Roccapietra-Valle Mosso pluton above the mafic complex (Fig. 36).

These data indicate that, in the Sesia Valley, bimodal volcanism and incremental growth of granitic plutons occurred within about 5 to 10 million years, during a time interval similar to early Permian volcanic activity elsewhere in the Alps (Schaltegger & Brack, 2007; Marocchi et al., 2008) and well within the time frame for volcanic activity in silicic large igneous provinces (e.g. Bryan et al., 2008) and the growth of zoned granitic plutons (Coleman et al., 2004). The coincidence of ages in the upper mafic complex indicates that onset of bimodal volcanism and granitic plutonism was most likely triggered by intrusion of mantle-derived mafic melt in the deep crust.
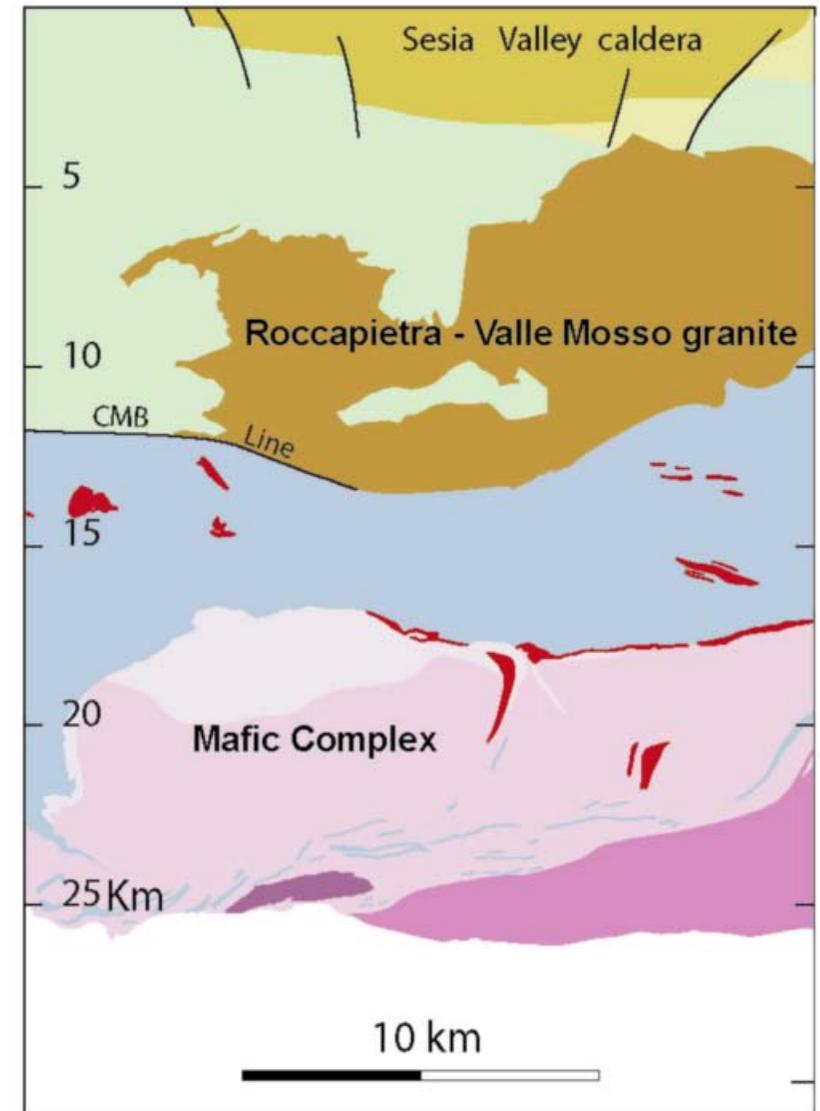
Fig. 36 – Palinspastic restoration of the Sesia magmatic system, modified from Quick et al. (2009).

Igneous evolutions across the Ivrea crustal section: the Permian Sesia Magmatic System and the Triassic Finero intrusion and mantle

M. Mazzucchelli - J. E. Quick - S. Sinigoi - A. Zanetti - T. Giovanardi

4.6 - The Sesia magmatic system – Conclusion

The Sesia magmatic system constitutes and unprecedented exposure of a plumbing system of a caldera exposed with good continuity from the surface to a depth of about 25 Km (Quick et al., 2009). In this framework, the mafic complex represents processes that affected the deep crust beneath the caldera. The onset of volcanic activity correlates strictly with the climax of the growth of the upper mafic complex, when the crust was pervasively heated. Igneous activity may have continued for as much 10 million years. In the middle to upper crust, this activity was dominated by silicic melts produced by anatexis in the deep crust, but included a minor amount of mantle component.

During the life of volcanic activity, the mafic complex was a huge, hot crystal mush body of slowly sinking cumulates, within which the magma chamber was limited to small bodies at the core of the arcuate structure, where injections of fresh, although still contaminated, mafic melt were mingled with dioritic cumulates. All available evidence indicates that large, predominantly molten magma chambers were not involved and that the magmatic plumbing system beneath the active volcanic field was composed of crystal mush bodies consistent with inferences from geophysical data (Guidarelli et al., 2006).

excursion notes

5 - The Finero-type Ivrea-Verbano Zone

The Finero sequence is located in the north-eastern part of the IVZ. It outcrops as a lens 11 km long and 3 km wide, covering an area embracing Val Vigezzo-Centovalli and Val Cannobina. It is separated from the Balmuccia sequence and the central part of IVZ by a High Temperature Shear Zone (HTSZ) situated approximately inside the National Natural Park of Val Grande (Fig. 37).

The Finero sequence shows a pseudo-antiform structure with mantle rocks at the core and a layered pluton (the Finero mafic complex) on the flanks. The sequence is bordered by the Insubric line to the N-NW and the Kinzigite formation to the S-SE. The origin of the pseudo-antiform structure is still debated. It is interpreted either as an antiform structure produced by tectonic movements during the Alpine orogeny or a drag fold created by the activation of the Insubric line.
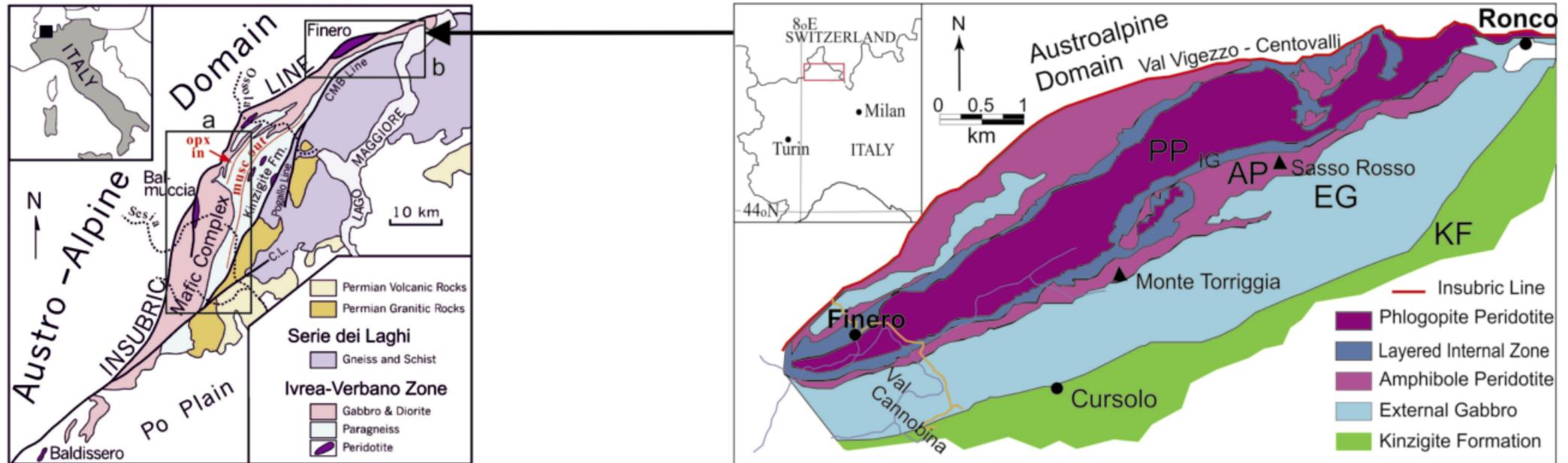
Fig. 37 – The Finero sequence.

The Finero sequence was divided by Cawthorn (1975) into three crustal units and one mantle unit. Crustal units forming the mafic complex have been successively renamed by Siena & Coltorti (1989) as follows: 1) Layered Internal Zone (LIZ); 2) Amphibole Peridotite (Amph-Pd); 3) External Gabbro (EG). The mantle sequence is identified as Phlogopite-Peridotite (Ph-Pd) unit.

As a whole, the association of mantle-crustal rocks cropping out in the Finero area is similar to that exposed in the Sesia Valley (central IVZ), where the Balmuccia mantle peridotite is surrounded by a mafic-ultramafic intrusive sequence (Quick et al., 1995). Nevertheless, the possibility that the mantle and crustal rocks of the Finero area might be unrelated to those of the central IVZ is suggested by differences in the ages of crystallisation/recrystallisation, as well as for many other structural, mineralogical and petrochemical features. The followings (e.g. Lu et al., 1997a,b; Mazzucchelli & Barbieri, 1997; Rivalenti & Mazzucchelli, 2000; Mazzucchelli et al., 2010) are the most striking:

Fig. 38 – Gabbro horneblendites in the layered internal zone.

i) the Finero mafic complex is dominated by garnet hornblendites (Fig. 38) and amphibole peridotites (Fig. 39; Cawthorn, 1975; Siena & Coltorti, 1989), which do not occur in the mafic complex of the Val Sesia;

Fig. 39 – Amphibole peridotites.

ii) the intrusive rocks of the Finero mafic complex are characterised by a trace element and isotopic signature (Figs. 40 and 41) consistent with a derivation from depleted to slightly enriched mantle sources (Lu et al., 1997a, b). Conversely, the gabbros in central IVZ (excluding only 5 samples documented by Voshage et al., 1990; Mazzucchelli et al., 1992b, c; Rivalenti et al., 1995; Mayer et al., 2000), have compositions enriched in LREE and radiogenic isotopes. These latter features require an addition of about 30% of crustal component (Voshage et al., 1987, 1990; Sinigoi et al., 2011);
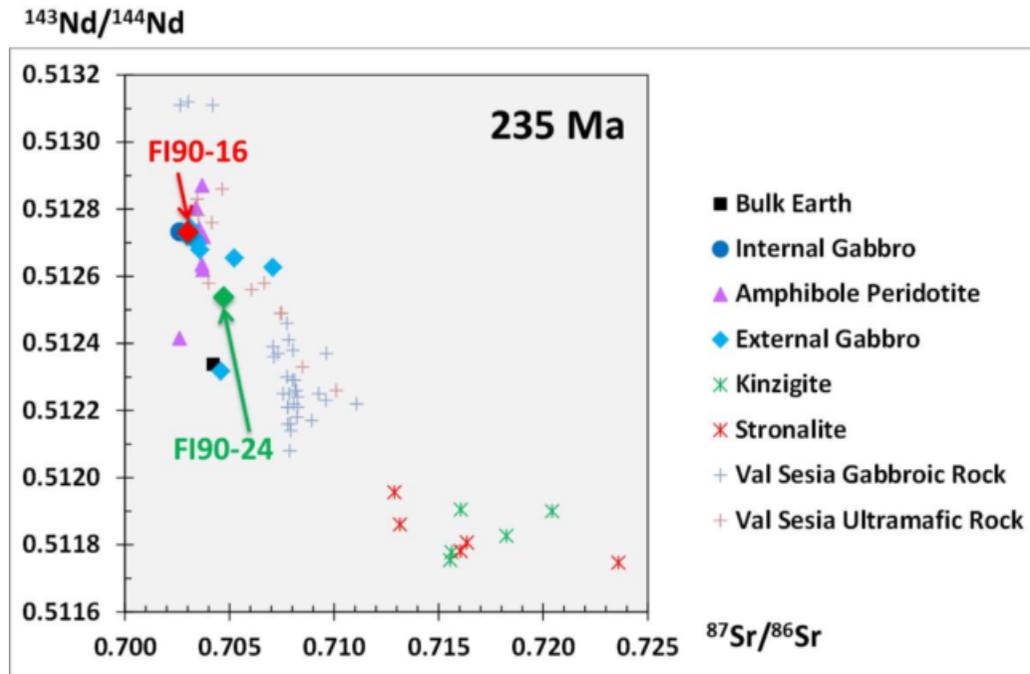
Fig. 40 – $^{143}Nd/^{144}Nd$ vs $^{87}Sr/^{86}Sr$ isotopic ratios recalculated at 235 Ma for whole rock of the Finero mafic complex, Val Sesia gabbroic and ultramafic rocks the Val Sesia area (central Ivrea-Verbano zone) and the metapelitic rocks of the Kinzigite formation.
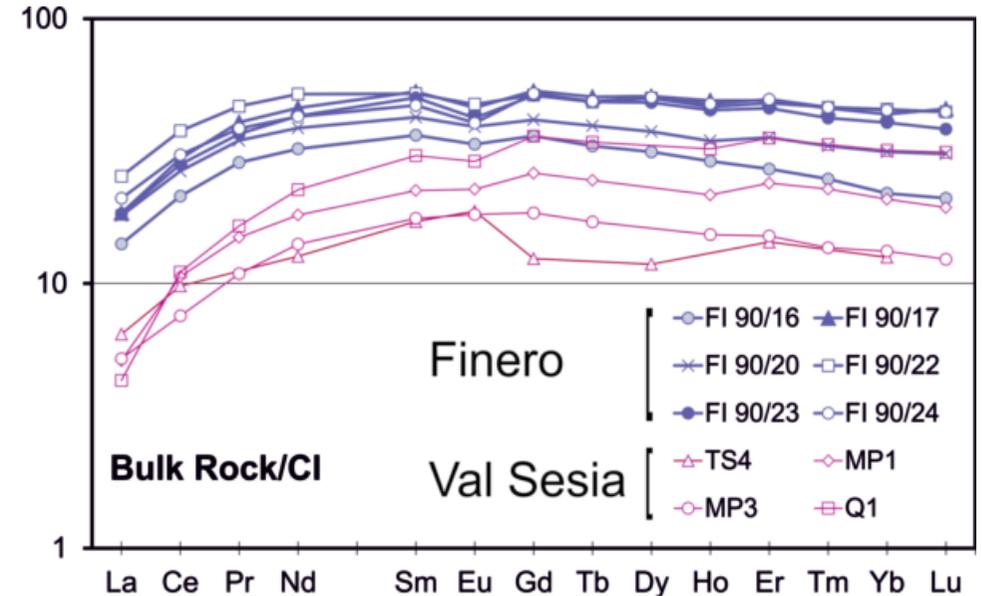
Fig. 41 – Bulk rock REE patterns of samples from the external gabbros unit of the Finero mafic complex, and the most primitive gabbroic melts documented in the Val Sesia.

49

iii) the Finero mafic complex presently outcrops as a layered pluton, which experienced three stages of deformation at granulite-facies conditions (Steck & Tièche, 1976). During its ascent towards the surface, it was tightly folded, along with the associated mantle unit, to form a major antiformal structure (Lensch, 1968; Steck & Tièche, 1976). Finally, it was significantly affected by large degrees of greenschist facies deformation,

possibly of Alpine age (Steck & Tièche, 1976). In contrast, the mafic complex in the Sesia Valley area shows a complex pattern of structures related to syn-magmatic to high-T deformation and recrystallisation established in the lower crust during Lower Permian (Figs. 23, 24 and 29). Coexistence of syn-magmatic and high-T subsolidus deformation structures indicate that the complex grew incrementally as large crystal mush bodies, which were continuously stretched while fed by pulses of fresh magma (Quick et al., 1995, 2009). Syn-magmatic recrystallisation during this deformation resulted in textures and structures which, although appearing metamorphic, are not ascribable to post-magmatic metamorphic event(s), but are instead characteristic of the growth process in huge and deep mafic intrusions, such as for instance the Niquelândia (Brazil) complexes (Correia et al., 2012). The associated Balmuccia peridotite displays thin, pseudotachylite-type fault systems and ductile extensional shear zones, which are interpreted as related to Variscan to Jurassic structural episodes (Handy & Stunitz, 2002; Souquière & Fabbri, 2009);

iv) the Finero mantle peridotite mostly consists of a pervasively-metasomatised spinel harzburgite (Fig. 42; containing abundant phlogopite and amphibole, and sometimes minor carbonates and apatite) in association with phlogopite-amphibole-bearing pyroxenites (Fig. 43; Hartmann & Wedepohl, 1993; Zanetti et al., 1999; Seitz & Woodland, 2000; Grieco et al., 2001; Matsumoto et al., 2005; Raffone et al., 2005, 2006; Morishita et al., 2003, 2008). Conversely, the mantle peridotite bodies in the central and southern IVZ, (e.g. Balmuccia and Baldissero) are devoid of metasomatic effects or, at most, weakly metasomatised (Rivalenti et al., 1995; Rivalenti & Mazzucchelli, 2000; Mazzucchelli et al., 2010);

Fig. 42 – Phlogopite and amphibole rich veins in dunite of the Finero mantle peridotite.

Fig. 43 – Phlogopite-amphibole bearing websterite ("celhodurite" of Zanetti et al., 1999).

v) field evidence shows that in the Finero area: a) the contact between peridotite and the mafic complex is always tectonic, being characterised by a dm-thick mylonitic band (Fig. 44); b) the intrusive bodies cutting the mantle peridotite are strongly LILE-enriched, thus resulting compositionally distinct from the mafic complex rocks that show tholeiitic to transitional affinity (Siena & Coltorti, 1989; Lu et al., 1997a, b; Zanetti et al., 1999; Stähle et al., 2001; Raffone et al., 2006; Morishita et al., 2008). Instead, in central IVZ the mantle peridotite bodies were tectonically emplaced at various levels in the Kinzigite formation before the Permian igneous event, possibly during the Variscan orogeny (Marchesi et al., 1992; Quick et al., 1995). For instance, they display: a) primary magmatic contact with intrusive rocks of the mafic complex (Fig. 45); b) intrusion of gabbroic dykes from the mafic complex; c) septa of paragneiss in granulite facies placed all around the peridotite massif (Mazzucchelli et al., 1992a; Quick et al., 1995; Rivalenti et al., 1995; Mayer et al., 2000).

Zanetti et al. (2013, 2014) determined a U-Pb SHRIMP concordant age of 232±3 Ma for magmatic zircons from a diorite of the external gabbro unit (Fig. 46), which has been proposed to establish the timing of intrusion of the Finero mafic complex.

51
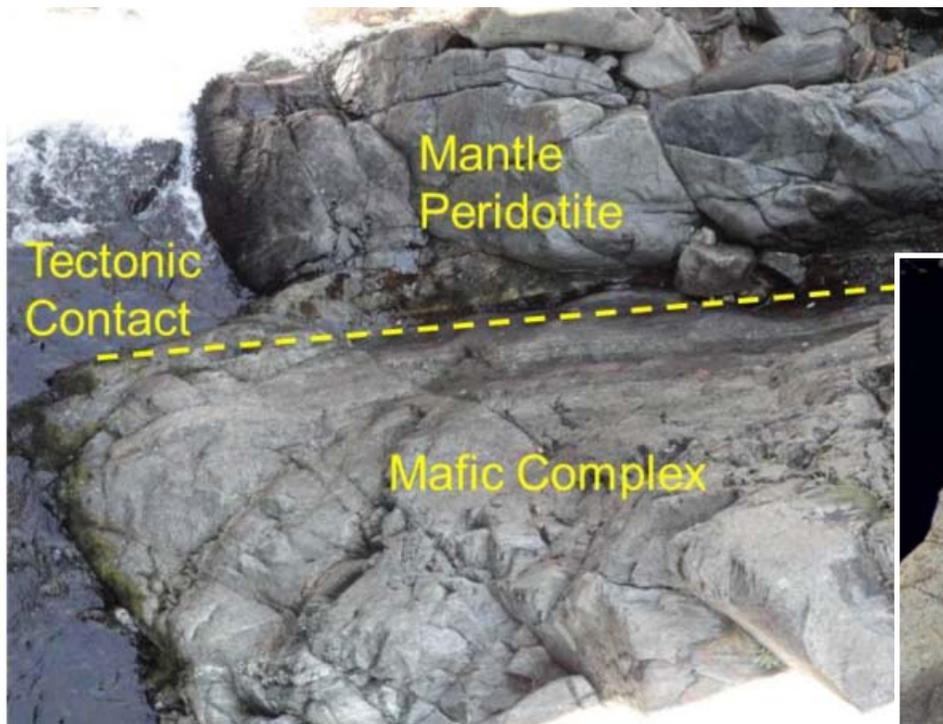
Fig. 44 – Tectonic contact between the Finero mantle peridotite and the rocks of the Layered Internal Zone of the Finero mafic complex.

Fig. 45 – Magmatic contact between the Balmuccia mantle peridotite and the websteritic rocks of the Val Sesia mafic complex.

Fig. 46 – **a)** Tera-Wasserburg plot of the U-Pb isotopic data of the zircons FI 90/16, split 16-C. Errors are shown as ellipses at the 1σ level. Ellipses are colour-coded for Th/U ratios. Numbers correspond to SHRIMP analytical spots located and labelled in (c).
b) Concordia age calculated on the basis of the U-Pb data for inner dark cores and oscillatory-zoned areas.
c) Cathodoluminescence images of the analysed zircons.
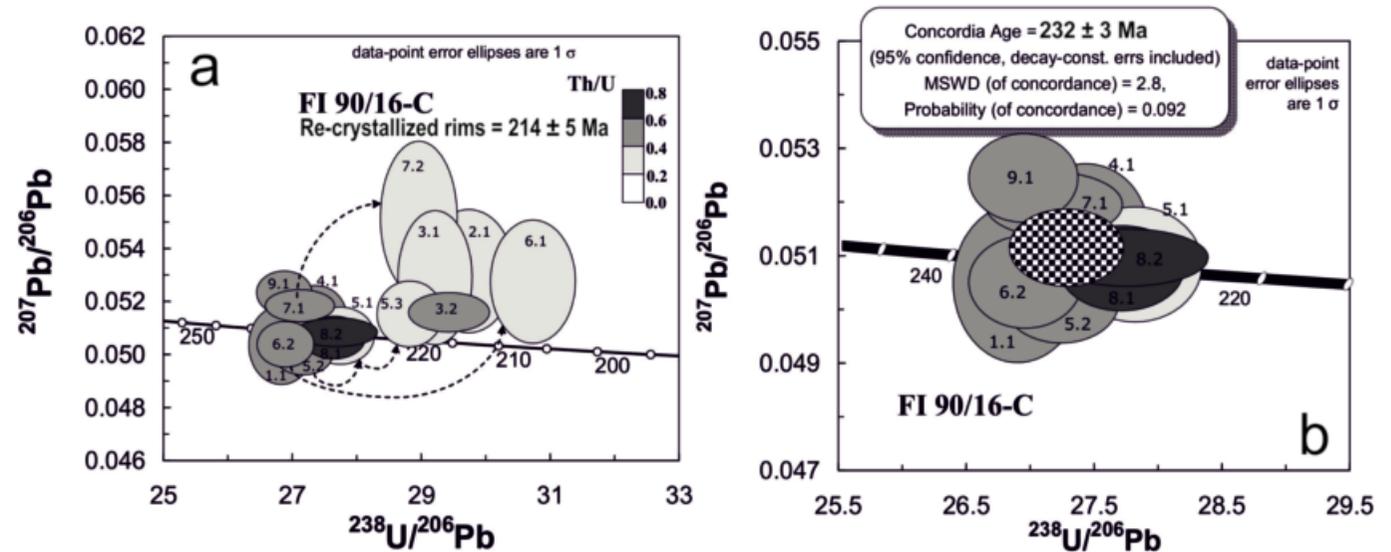
This evidence, as well as all the other structural, petrochemical and age features (Fig. 47) described above, confirms that the overall Finero area experienced a different geodynamic evolution with respect to the central IVZ, involving important tectono-magmatic Triassic events after the Upper Carboniferous-Lower Permian magmatic cycle. The boundary between the two different areas is still undetermined: however, some indications can be preliminarily obtained on the basis of the spatial distribution of the different types of peridotite. In particular, in Fiorina Valley, SW of the Finero complex, small lenses of phlogopite peridotite are aligned on strike with the main Finero peridotite lens (Marchesi et al., 1992; Barbieri, 1996; Rivalenti et al., 1997).

Conceivably, these are fragments of the same mantle sequence cropping out in the Finero antiform, stretched out along a shear-zone during or after the emplacement of the mantle sequence in contact with the crustal rocks. To the south, in the Ossola Valley, the small Premosello mantle peridotite body includes a phlogopite-free, fertile spinel lherzolite, which is surrounded by pegmatoidal pyroxenite, forming a lithologic sequence very similar to the outcrop in the Balmuccia area (Mazzucchelli et al., 1992a; Rivalenti & Mazzucchelli, 2000).
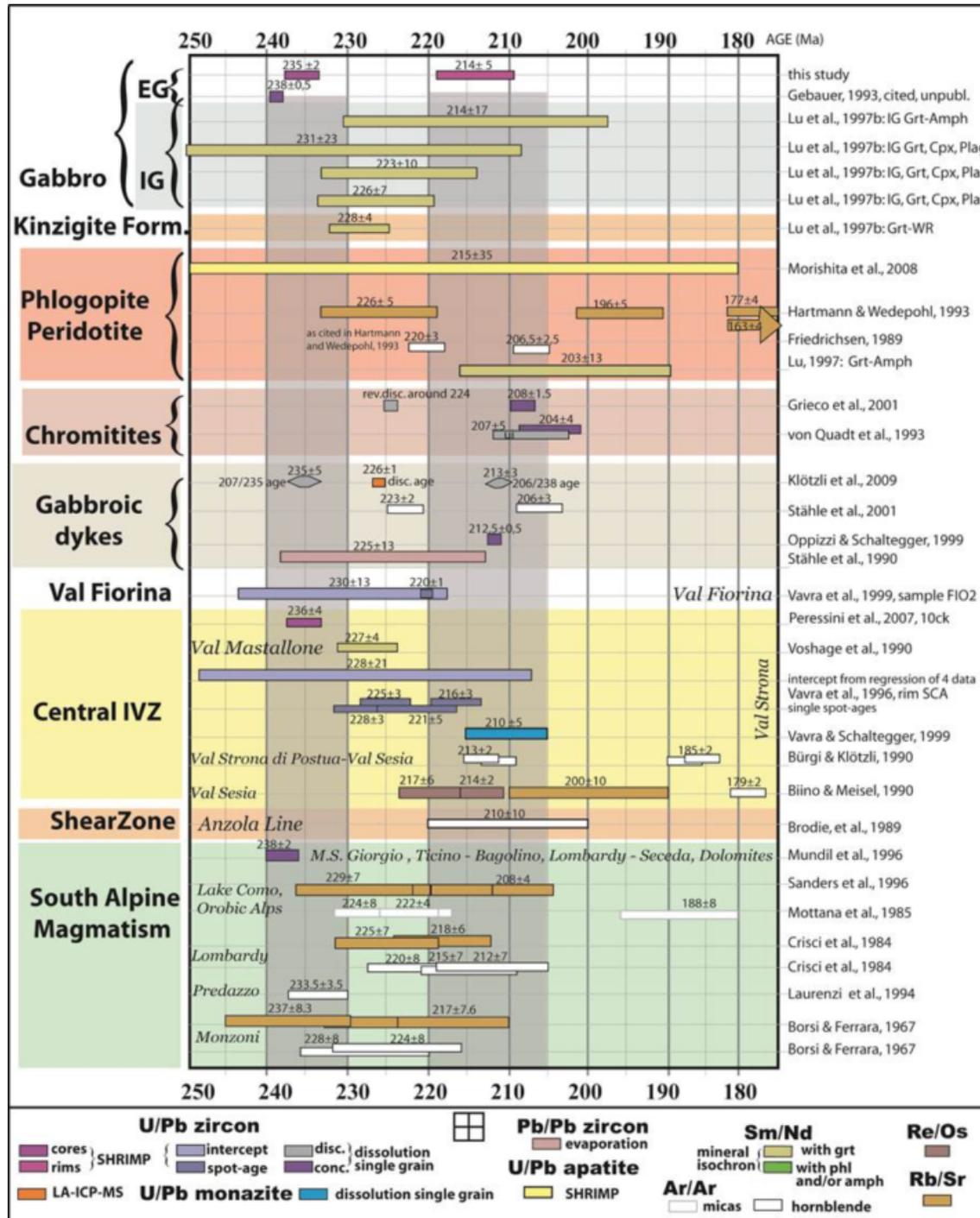
Fig. 47 – Summary of the published U-Pb (zircon and monazite), Sm-Nd (mineral isochons), Ar-Ar (hornblende) ages for the Finero mafic complex of the Ivrea-Verbano zone, and some selected, related shear zones.

Additionally the Finero mafic complex contains large amounts of cumulitic garnet hornblendites and amphibole peridotites (Cawthorn, 1975; Siena & Coltorti, 1989), which do not occur in the mafic complex of the other IVZ sectors. Thus, on the basis of the distribution of phlogopite-free and phlogopite-bearing mantle lenses, as well as of garnet hornblendites and amphibole peridotites in the mafic complexes, we suggest that a transition from a "Finero-type IVZ" (i.e. northern IVZ) and a "Sesia Valley-type IVZ" (i.e. central IVZ) likely exists somewhere between the Fiorina Valley and the Premosello mantle body. Owing to the lack of a detailed mapping, the boundary cannot be precisely located, although we infer that it may coincide with a high-T shear zone running SW-NE north of Premosello (Fig. 48; i.e. the Anzola - Grande Valley shear zone: Brodie et al., 1989; Rutter et al., 2007). It is thus concluded that the entire geological setting of the area should be
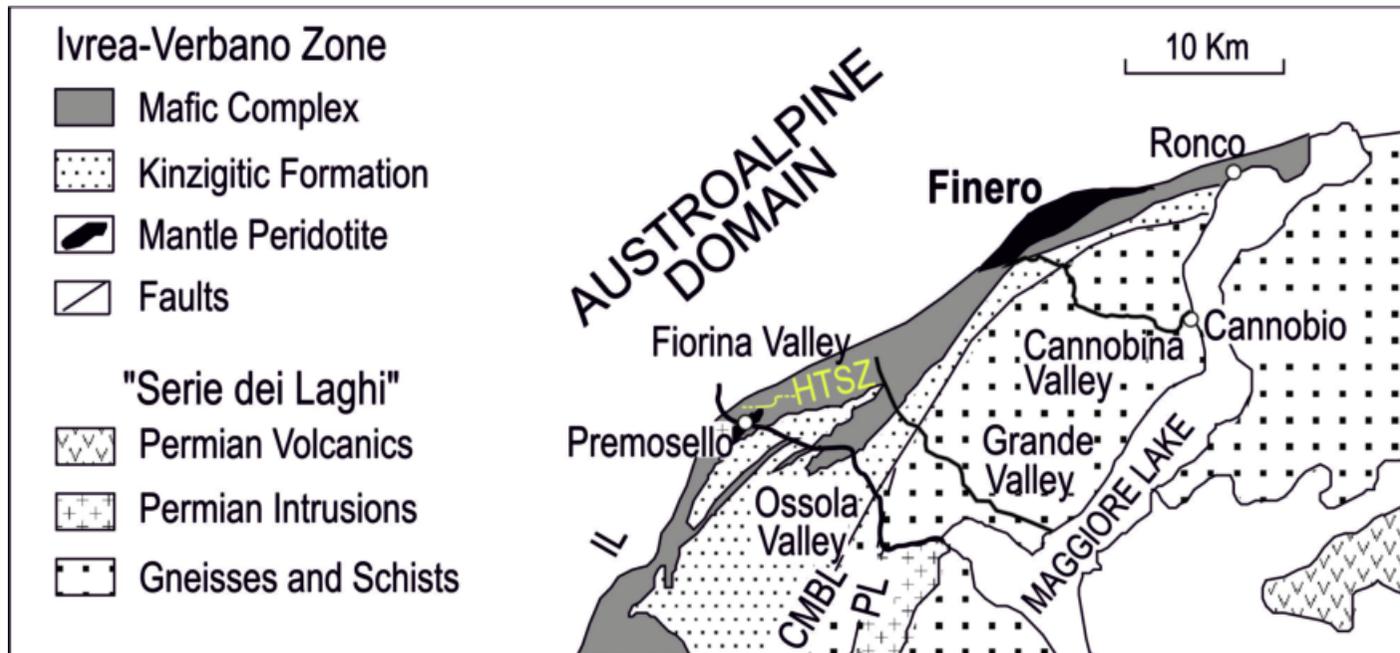
Fig. 48 – Sketch map of the Northern Ivrea-Verbano zone. IL = Insubric line; CMBL = Cossato-Mergozzo-Brissago line; PL = Pogallo line; HTSZ = high-temperature shear zone of Anzola - Grande Valley area. The Fiorina Valley is a small lateral trough of the Grande Valley, being is approximately located at 46°3'15" N, 8°27'00" E.

revised. Unfortunately, insufficient information is presently available about the petrochemistry and age of the metamorphic basement of the Finero area and its thermal state and thickness in Permian-Triassic time to adequately explore these issues.

Crucial for the reconstruction of the geodynamic evolution of the Finero region appears also a better definition of i) the possible presence of a Permian mafic intrusion in the area, ii) the timing of the pervasive metasomatism experienced by the Finero peridotite, as well as iii) the age and the structural scenario in which the Finero peridotite and the mafic complex were placed in contact. In particular, the Triassic emplacement age of the Finero mafic complex suggests that the tectonic contact with the associated mantle peridotite could have been established in Middle Jurassic time. The emplacement likely occurred during the opening of the Ligurian-Piedmontese neo-Tethys, possibly along rift-related structures (such as lithospheric listric faults), whose record is widespread in the ocean-continent transition sequences of the Western Alps (e.g. Beltrando et al., 2010).

5.1 - The mantle phlogopite peridotite unit

The Finero mantle sequence markedly differs in its mineralogical, geochemical and isotopic characteristics from the other mantle bodies of the IVZ (Balmuccia - central IVZ, Baldissero - southern IVZ). These latter are depleted spinel lherzolites showing nearly absent (Baldissero) or weak metasomatic effects (Balmuccia), which are basically limited to the regions close to pyroxenite contacts, showing positive εNd_{270} and $^{87}Sr/^{86}Sr_{270} <$ 0.704 (Voshage et al., 1988).

Conversely, the mantle sequence of Finero mainly includes harzburgites that were nearly completely recrystallised by metasomatic fluids during several episodes of pervasive to channeled porous flow migration of (mostly hydrous) melts (Fig. 49). The mantle sequence also experienced the late intrusion of mafic to sialic veins-dykes (locally characterized by the presence of sapphirine, Fig. 50), which discordantly cut the mantle foliation and the sub-concordant lithologic layering defined by harzburgite-pyroxenite alternation.

There is a sharp geochemical difference between the metasomatic melts affecting the Finero mantle unit and the parent melts of the associated mafic complex, for which it has been proposed an affinity with tholeiitic-transitional melts (Siena & Coltorti, 1989; Lu et al., 1997a, b; Zanetti et al., 1999; Stähle et al., 2001; Raffone et al., 2006; Morishita et al., 2008; Giovanardi et al., 2014). In contrast, the mantle peridotite records

Fig. 49 – Phlogopite-bearing amphibole harzburgite and phlogopite-bearing pyroxenites.

Fig. 50 – Sapphirine-bearing gabbroic dyke.
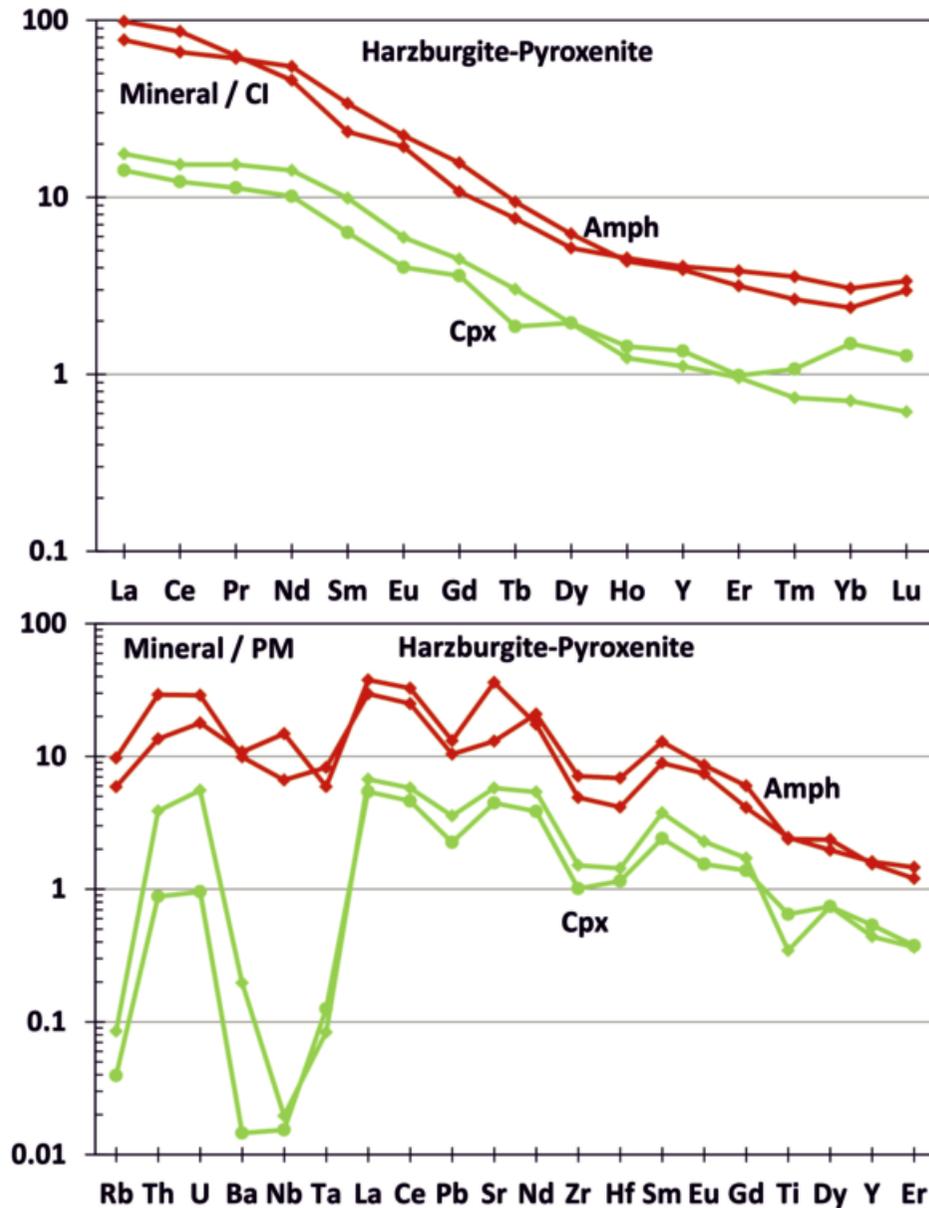
Fig. 51 – REE and incompatible trace element diagrams for amphibole and clinopyroxene of the harzburgite and pyroxenite rocks.

a multistage evolution characterized by the migration of different melts with variable geochemical affinity. Most of the mantle sequence experienced the pervasive metasomatic growth of phlogopite-amphibole-orthopyroxene-bearing mineral assemblages, associated with marked enrichment in LILE, LREE and B, and in radiogenic Sr, Pb, He, Ne and Ar, but with low HFSE concentrations. These mineralogical and compositional features are considered as the evidence of the presence of slab-derived crustal-component in the percolating melts (Hartmann & Wedepohl, 1993; Zanetti et al., 1999; Morishita et al., 2003, 2008; Matsumoto et al., 2005).

Bulk-rock incompatible trace element diagrams (Fig. 51) show that metasomatic components enriched the Finero mantle harzburgites in Rb, Ba and Sr (LILE) and LREE with respect to HREE, creating smoothly decreasing profiles from LREE to HREE (La_N/Yb_N = 8 to 17). They were also relatively depleted in Nb, as suggested by the negative Nb anomaly shown by bulk rock and mineral compositions. Available isotope data indicate that the Finero phlogopite peridotite is characterized by high radiogenic Sr ($^{87}Sr/^{86}Sr_{270}$)= 0.7055 to 0.7093; Voshage et al. 1987, Hartmann & Wedepohl 1993; Obermiller, 1994) and low radiogenic Nd (εNd_{270}) = -1 to -3, Voshage et al., 1987; Obermiller, 1994).
On the basis of the Pb isotope data ($^{206}Pb/^{204}Pb$= 18.2 to 18.8; $^{207}Pb/^{204}Pb$= 15.6 to 15.7; $^{208}Pb/^{204}Pb$= 38.3 to 38.8), Cummings et al. (1987) and Obermiller (1994) inferred the involvement of crustal Pb in the metasomatic

overprint of the Finero peridotite. The $^{207}Pb/^{204}Pb$ range overlaps the field of OIB recording EMII characteristics of the mantle source (Hofmann, 1997), which are usually considered as markers of the presence of recycled crustal rocks. Hydrogen isotope composition of amphibole and phlogopite has a variation range of δD from -29 to –44‰, interpreted as a mixture of magmatic fluids with sea water (Hartmann & Wedepohl, 1993). On the basis of the geochemical and isotope characteristics, Hartmann & Wedepohl (1993) concluded that at Finero the metasomatic agent had crustal characteristics and was probably derived from a subducted slab.

Zanetti et al. (1999) examined in detail the petrochemical features of two sections of the main lithological association made by phlogopite-harzburgite and phlogopite-bearing Cr-Di websterite, showing the virtual absence of major and trace element gradients in the mineral phases. In both rock types, pyroxenes and olivines have the most unfertile major element composition observed in IVZ peridotites. Spinel is chromite, amphibole is pargasite. Clinopyroxene shows LREE-enriched patterns (La_N/Yb_N ~16), negative Ti and Zr and generally positive Sr anomalies. The trace element compositions of the amphibole approach the chemical equilibrium with the associated clinopyroxene.

In contrast, marked geochemical gradients occur towards late apatite and carbonate-bearing domains, which are randomly distributed in both the sections examined. In these regions, pyroxenes and amphibole (edenite) are lower in Mg# and higher in Na_2O, and spinels and phlogopite are richer in Cr_2O_3. Both the mineral assemblage and the incompatible trace element characteristics of the mineral phases are the typical signatures of "carbonatite" metasomatism (HFSE depletion, Sr, LILE and LREE enrichment). Clinopyroxene has higher REE and Sr concentrations than amphibole ($^{amph/cpx}D_{REE,Sr}$ = 0.7 to 0.9) and lower Ti and Zr abundances. It was proposed that the metasomatic process that affected the Finero mantle forming the harzburgite-pyroxenite association required the permeation of a refractory mantle wedge by slab-derived H_2O-CO_2 bearing silicate melts of a subduction environment, where metasomatism occurred before peridotite incorporation in the crust (Zanetti et al., 1999). The authors suggest that the lack of chemical gradients between pyroxenite and peridotite may be explained by a model in which melts derived from an eclogite-facies slab infiltrate the overlying harzburgitic mantle wedge and, because of the thermal structure of the subduction zones, become heated to the temperature of the peridotite. If the resulting temperature is above that of the incipient melting of the hydrous peridotite system, the slab-derived melt equilibrates with the harzburgite and a crystal mush consisting of harzburgite and a silica saturated, hydrous melt is formed. During cooling, the crystal mush crystallises producing the observed sequence of mineral phases and their observed chemical characteristics.

In this context, pyroxenites are interpreted to be regions of higher concentration of the melt in equilibrium with the harzburgite and not conduits through which exotic melts percolated. The apatite, dolomite-bearing wehrlitic domains were related to the presence of some CO_2 in the slab-derived melt. The CO_2/H_2O ratio in the peridotite mush increased by crystallisation of hydrous phases (amphibole and phlogopite) locally resulting in the unmixing of a late carbonate fluid (Zanetti et al., 1999). The proposed scenario was argued to be consistent with subduction of probably Variscan age and with the occurrence of modal metasomatism before peridotite incorporation in the crust. Raffone et al. (2005) concluded that the differences in LILE concentration of the minerals from phlogopite harzburgite and wehrlitic layers are more consistent with the percolation of distinct metasomatic agents. Metasomatism of a mantle slab was also invoked by Grieco et al. (2001, 2004) and Morishita et al. (2003, 2008) to explain the geochemical features of chromitite-dunite bands and apatite-rich peridotite layers, respectively. These authors also determined U-Pb zircon and apatite Triassic ages (spanning from 215 to 208 Ma), pointing to multiple episodes of melt injection. A consistent scenario was envisaged by Matsumoto et al. (2005) and Raffone et al. (2006) by comparing isotopic and LLE composition of different kind of peridotites. Stahle et al. (2001) determined U-Pb-zircon ages of 225 Ma for intrusions in the Finero mantle sequence, interpreting the parent melts as derived by a metasomatically enriched mantle source. The latter was described as an "asthenospheric" mixture of depleted (DM) and enriched (HIMU) mantle components. A carbonatite-type metasomatism related to subcontinental mantle plume was proposed by Zaccarini et al. (2004) to explain the occurrence of zirconolite and Zr-Th-U minerals in the Finero chromitites. Selverstone & Sharp (2011) combined Cl, H, and O stable isotope geochemistry with petrologic and major and trace element data to conclude that metasomatism occurred in a forearc wedge, with fluids sourced from at least two subducted components with distinct chemical and isotopic compositions.

In conclusion, at present, there is no doubt that the mantle sequence of Finero experienced a multiple injections of melts/fluids. The early metasomatic events were pervasive and resulted in the ubiquitous crystallisation of phlogopite-bearing mineral assemblages. Mineralogical and geochemical features of this metasomatic event indicate the significant presence of crustal component. Therefore, in the frame of the "mantle wedge" scenario, it is likely that the mantle sequence was close to a subducted slab, the latter undergoing partial melting and/or fluid release. After this main, pervasive metasomatism the mantle sequence experienced an exhumation stage, likely in Lower Jurassic time, during which it was emplaced at the base of the continental crust.

excursion notes

5.2 - The Finero mafic complex

The Finero mafic complex is a layered pluton intruded at the roots of the continental crust of the Adria plate, thath experienced at least three granulite-facies re-equilibration events during its cooling history. It is characterized by abundant modal amphibole in all rock types. According to Siena & Coltorti (1989), the mafic complex can be divided into the following units: a) layered internal zone (LIZ); b) amphibole peridotite (Amph-Pd); c) external gabbro (EG). Units (a) and (c) correspond to the lower and upper metagabbro units of Cawthorn (1975), respectively (Fig. 52). Siena & Coltorti (1989) interpreted the mafic complex of Finero to be the result of hydrated fractionation of a single basaltic liquid of transitional affinity. On the basis of trace element and isotopic data, Lu et al. (1997a, b) proposed a MORB *sensu lato* affinity for the parent melts, which were attributed to the partial melting of depleted to slightly enriched mantle sources.

5.3 - Geochronological data

Collectively, geochronological data for the rocks belonging to the Finero complex spread from 550 Ma to 180 Ma (Fig. 47 and Lu et al., 1997b). However, Triassic ages are by far predominant, both for mantle and crustal rocks, in contrast to the mainly Permo-Carboniferous ages of the rest of the Ivrea-Verbano mafic complex (e.g. the mafic complex in the Balmuccia sector, Peressini et al., 2007).
Published ages of the rocks from the Finero antiform are reviewed below, with the emphasis on the Finero phlogopite peridotite and the mafic complex.
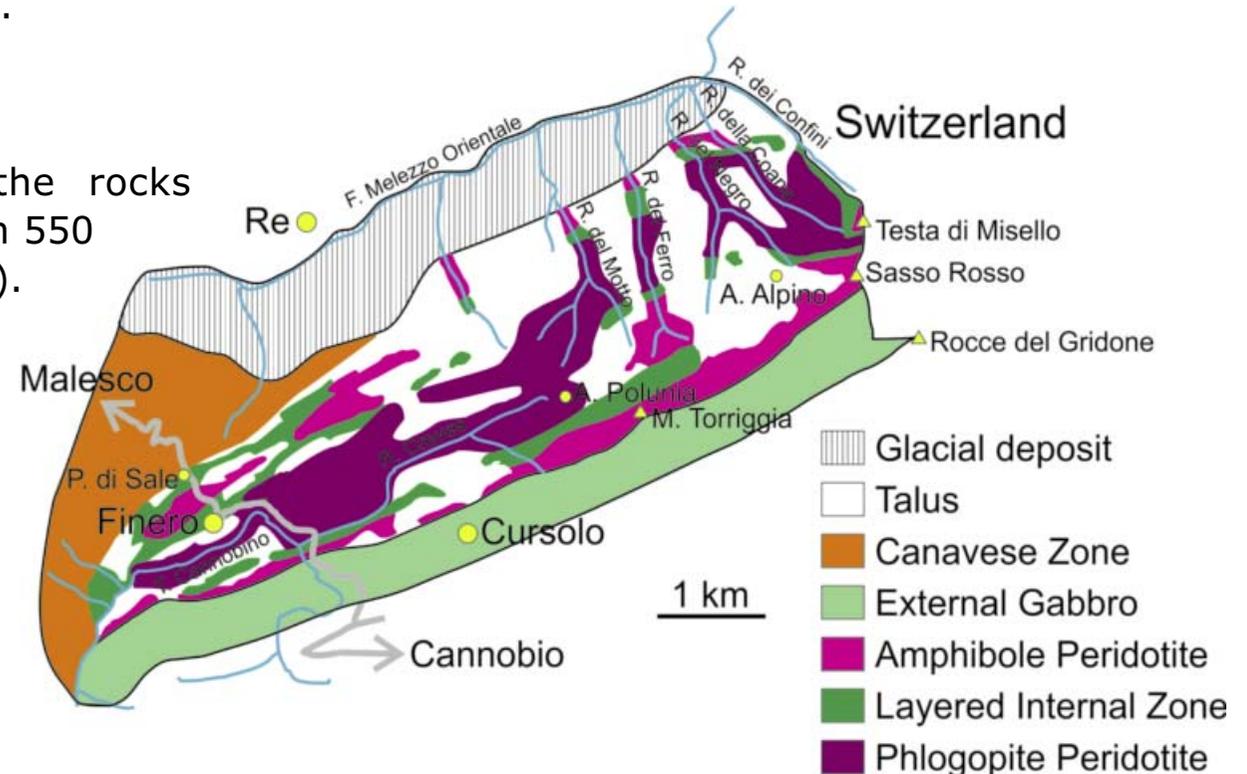
Fig. 52 – Sketch map of the Finero area after Vogt (1962), modified.

5.3.1 - Finero mantle phlogopite peridotite
U-Pb zircon and apatite ages

U-Pb age determinations (Fig. 47) were carried out on zircons from dioritic pegmatitic lenses and/or dykes (Stähle et al., 1990) or chromitite layers and/or pods (von Quadt et al., 1993; Grieco et al., 2001). Stähle et al. (1990) dated zircons from a Na-alkaline dioritic pegmatitic dyke at 225±13 Ma with the Pb-Pb evaporation technique. For the chromitites, conventional multigrain dating gave, for one of four grain fractions, a concordant age of 204±4 Ma, while the other fractions define discordia with an upper intercept at 207±5 Ma and a lower at 0 Ma (von Quadt et al., 1993). Analogous determinations by Grieco et al. (2001) define a lower intercept age of 208±2 Ma, with the presence of an inherited component that is reversely discordant at about 225 Ma. Grieco et al. (2001) also document U-Pb zircon ages of 195±4 Ma and 202±1 Ma for an alkali pegmatite and a pegmatitic plagioclasite, respectively. SHRIMP analyses on apatites from a peridotite layer (Fig. 47) yielded a three-dimensional isochron age of 213±35 Ma (Morishita et al., 2008).

Rb-Sr and Ar-Ar ages

Hartmann & Wedepohl (1993) determined Rb-Sr internal isochrons (Fig. 47) between 163±4 and 226±5 Ma (2-points, phlogopite-amphibole isochrons), which were interpreted to record rapid cooling by uplift. Ar-Ar stepwise heating spectra on phlogopite (Fig. 47) yielded ages from 207±3 Ma (Friedrichsen, 1989) to 220±3 Ma (Friedrichsen, as cited in Hartmann & Wedepohl, 1993). K-Ar ages for phlogopites (Fig. 47) yielded ages of 190 Ma or younger, which were interpreted as cooling ages (see Lu et al., 1997b and references therein). Stähle et al. (2001) obtained ages from 225 to 220 Ma with K-Ar and Ar-Ar on amphiboles from alkaline diorite and hornblendite dykes (Fig. 47), which are essentially the same ages obtained on zircons by Stähle et al. (1990). Matsumoto et al. (2005) obtained an age of 240±41 Ma resulting from the regression line of 4 samples of phlogopite-peridotites in a $^{40}Ar/^{36}Ar$ vs. $^{40}K/^{36}Ar$ plot (Fig. 47).

5.3.2 - Finero mafic complex
U-Pb zircon ages

Gebauer & Grünenfelder (cited in Gebauer, 1993) obtained five concordant conventional multi-grain U-Pb zircon ages at 238±1 Ma for gabbros close to the Ronco village (Switzerland), interpreted as intrusion age (Fig. 47). Vavra et al. (1999) dated two paragneisses and one gabbro from Fiorina Valley. This sample-set was collected at

the "transition" between central and northern IVZ. However, the presence of minor bodies of phlogopite-bearing mantle peridotite suggests a link of the Fiorina Valley section to the Finero area. For these samples, Vavra et al. (1999) interpreted Carboniferous single-spot ages (300 to 293 Ma) as zircon growth ages dating intrusion whereas Triassic ages spanning 214 to 199 Ma were attributed to a recrystallisation episode that affected the layered internal zone (Fig. 47). A single-grain evaporation Pb-Pb age on one zircon from the layered internal zone (Fig. 47) yielded a Lower Cambrian age of 549±12 Ma (Lu et al., 1997b). This "poor quality measurement" (Lu et al., 1997b) was likely determined on an inherited zircon.

Age determinations were also performed on zircons from late pegmatitic bodies within the mafic complex (Fig. 47). Klötzli et al. (2007, 2009) determined a LA-ICP-MS U-Pb concordia age of 226±1 Ma (with individual $^{206}Pb/^{238}U$ ages ranging from 211 to 237 Ma) for zircons from nepheline syenite-pegmatite pods crosscutting the Amph-Pd unit. Relatively young ages were determined by Oppizzi & Schaltegger (1999), who dated zircons at 213±1 Ma from a plagioclasite dyke, whereas Schaltegger et al. (2008) dated five fragments of one large zircon that yielded $^{206}Pb/^{238}U$ ages between 208 and 210 Ma. The occurrence of an "event" of zircon growth at 215±3 Ma is also supported by some other unpublished data (U. Klötzli, personal communication).

Sm-Nd and Ar-Ar ages

Lu et al. (1997b) determined 2-and 3-point internal isochrons on cumulus rocks of the layered internal zone, which yielded ages between 203±13 and 231±23 Ma. Considering only the 3-point isochrons, the age range is restricted to 223±10 to 231±23 Ma. A meta-sedimentary septum within the external gabbro yielded a similar Sm-Nd age of 228±4 Ma. Lu et al. (1997b) argued that the mafic complex in this area intruded at about 270 to 290 Ma and was affected by a regional heating event at about 215±10 Ma. Lu et al. (1997b) also determined a whole-rock "apparent isochron" of 533±20 Ma defined by 7 samples from the amphibole peridotite unit, which is best interpreted as an artefact of mixing, although close to the single zircon age acquired in the same study.

Boriani & Villa (1997) obtained an Ar-Ar age of 210±10 Ma on rocks within the external gabbro unit. Also, Lu (1994) determined an Ar-Ar age of 191±5 Ma on a sample from the amphibole peridotite unit.

excursion notes

Igneous evolutions across the Ivrea crustal section: the Permian Sesia Magmatic System and the Triassic Finero intrusion and mantle

M. Mazzucchelli - J. E. Quick - S. Sinigoi - A. Zanetti - T. Giovanardi
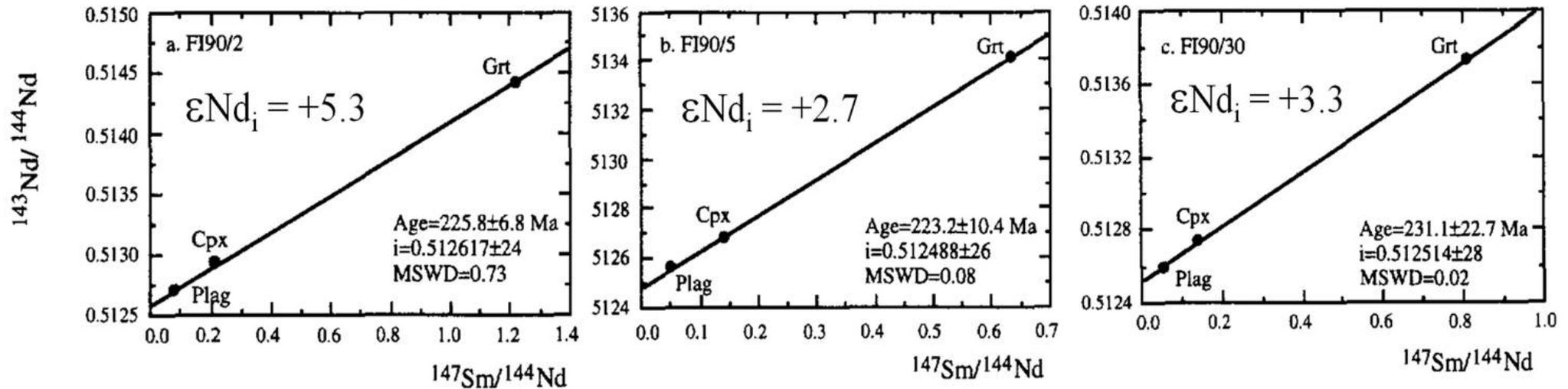
Fig. 53 – 3-point Sm/Nd internal isochrons on gabbroic rocks of the layered internal zone after Lu et al. (1997b), modified.

5.4 - The Finero-type Ivrea Verbano zone - Conclusion

The most-commonly held interpretation for the origin of the mafic complex is that intruded in the Permian and was subsequently overprinted by a Triassic thermal event (e.g. Vavra et al., 1999; Lu et al., 1997b), possibly accompanied by hydrothermal activity (Vavra et al., 1999; Oppizzi & Schaltegger, 1999), in a regional regime of slow cooling since the Late Permian. However, most of the geochronological data obtained for the metasomatised peridotite and the intrusive bodies of the phlogopite peridotite mantle unit converge towards Triassic ages, very close to that inferred for the "heating event".
Nevertheless, SHRIMP U-Pb dating of interstitial, magmatic zircons separated from a diorite of the external gabbro unit by Zanetti et al. (2013, 2014) definitely demonstrates that at least the youngest unit of the Finero mafic complex intruded the lower crust at 232±3 Ma.
This is important for the interpretation of the widespread Triassic magmatism of the Southern Alps suggesting the need for a re-evaluation of the geodynamic setting for this period.

Table 1- Two different "Types" of Ivrea-Verbano zone ?

		Val Sesia - Type	**Finero - Type**
MANTLE BODIES	Lithologies	Spinel Lherzolite, with Depleted Mantle affinity	Spinel Phlogopite Harzburgite, strongly metasomatised
MAFIC COMPLEX		Gabbros, Diorites, subordinate Pyroxenite and Anorthosites, rare Peridotites	Garnet Hornblendites, Garnet gabbros, Cumulus Amphibole Peridotites, Pyroxenites, Gabbros
MAFIC COMPLEX		Strong	modest, if any
Crustal assimilation			
MAFIC COMPLEX		Gabbro glacier	layered, strongly deformed
Internal structure			
MANTLE BODIES & MAFIC COMPLEX		Lower Permian or older	Triassic to Lower Jurassic
Magmatic/Metamorphic ages			
Contact between MANTLE BODIES and MAFIC COMPLEX		locally, Magmatic	always Tectonic

Field Trips
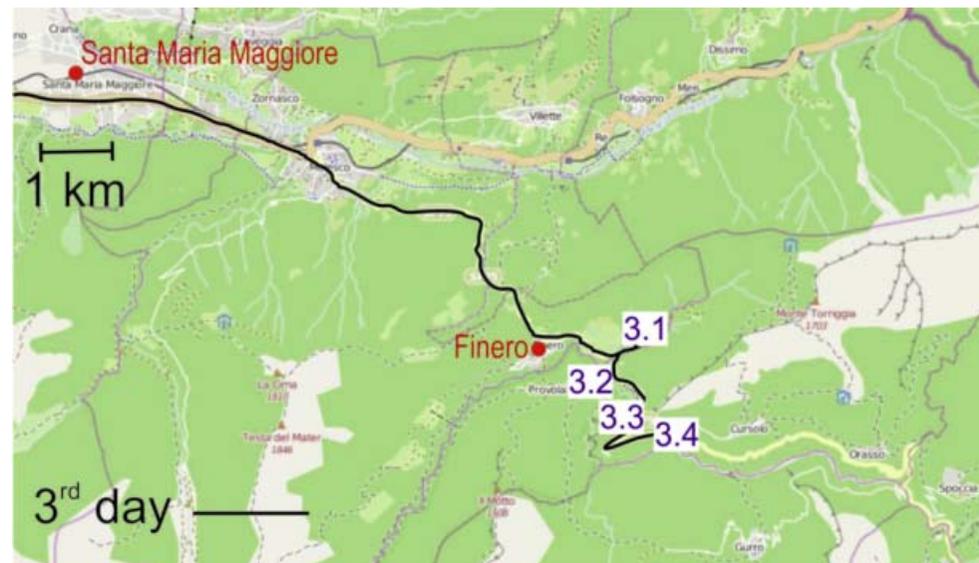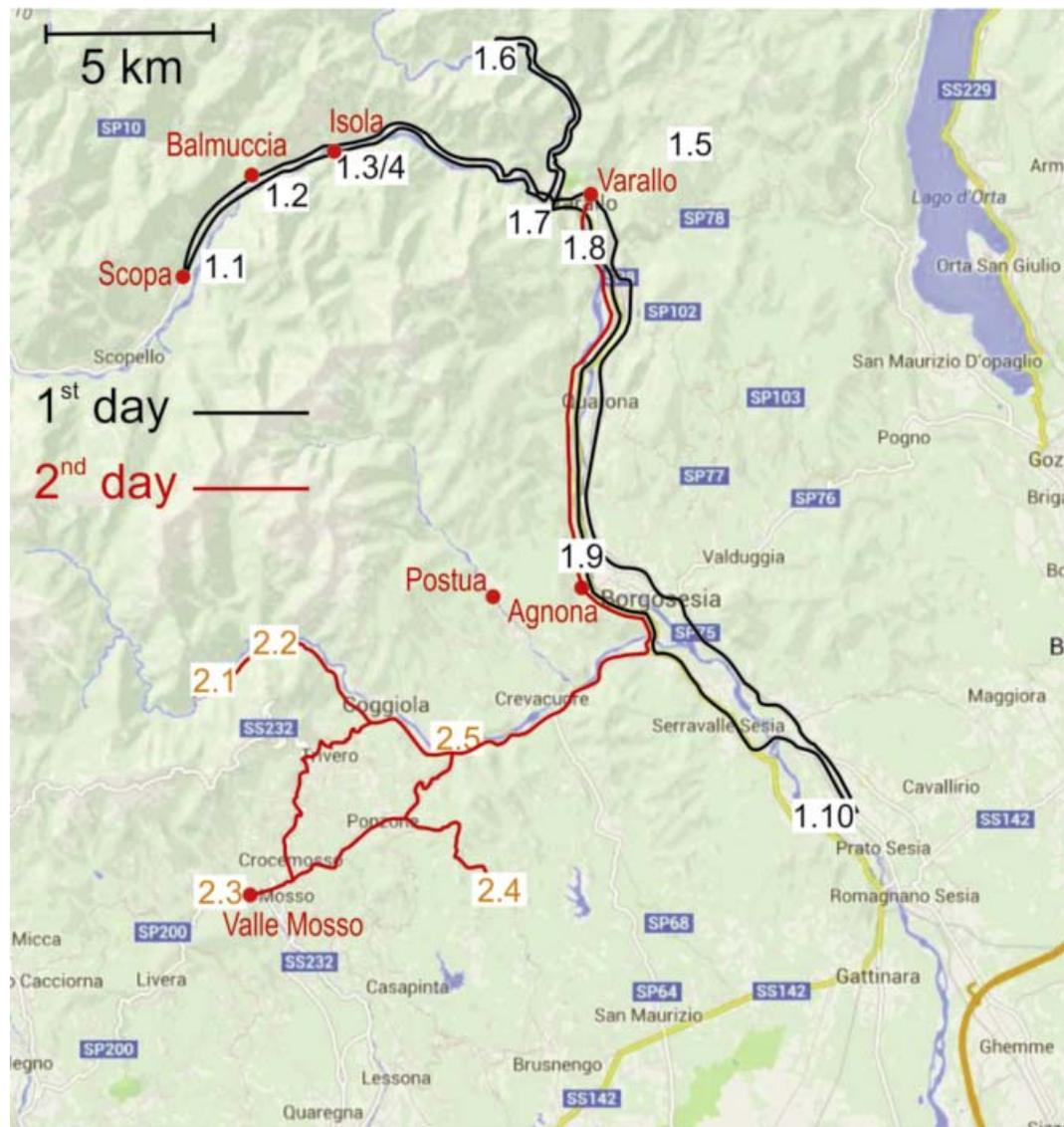
Fig. 54 - Geographical location of the field trips area (days 1, 2 and 3) with itineraries and Stops.

Day 1
The Sesia magmatic system

The first two days the trip will lead participants across the Sesia magmatic system, starting from the deepest exposure of the crustal section and moving progressively up-section to the volcanic rocks at the surface (Fig. 55). The excursion begins with a traverse across the mafic complex in the Sesia River, starting at the Insubric line, followed by stops in the Balmuccia area and ending in the upper mafic complex in the vicinity of Varallo up to the roof contact with the Kinzigite formation. The excursion continues, cross-cutting the Kinzigite formation to see ortho- and paragneisses in anatectic facies, and mingling of mafic and acidic magmas at the base of the large granitic pluton of Roccapietra. After crossing the Cremosina line (see Fig. 1, for its location), the excursion ends in the area of Prato Sesia to see the best outcrops of megabreccia filling the caldera.

Stops in the Balmuccia area

STOP 1.1: Mylonite of the Insubric line

Leave the car at the locality Dinelli (45°48′25″ N; 8°7′26″ E) and follow a short path to reach an old bridge over the Sesia river where the mylonites of the Insubric line are well exposed (45°48′21.3″ N; 8°7′32.8″ E). The geomorphology, in this segment of the valley, is strongly controlled by the Insubric fault.
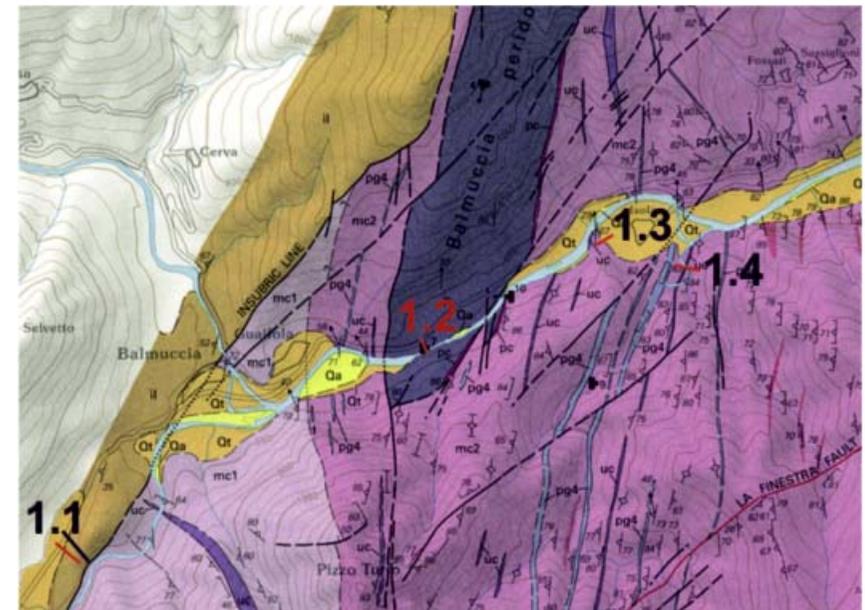
Fig. 55 – The Balmuccia area.

STOP 1.2: Balmuccia peridotite
(45°49'12.6" N; 8°09'11.5" E)

Once thought to be the mantle basement above which the mafic complex was underplated at the crust-mantle boundary, this lens of mantle rocks was interfingered within the Kinzigite formation before the Permian mafic intrusion. Even though it does not present a true petrologic Moho and is not directly involved in the igneous evolution of the Sesia magmatic system, it is worth a look because it is one of the best preserved mantle peridotites in the world. The peridotite experienced a number of partial melting events which are recorded by networks of Cr-diopside and Al-augite dikes and bands (Fig. 56).

STOP 1.3: Deformation of ultramafic cumulates
(45°49'31" N; 8°09'55" E)
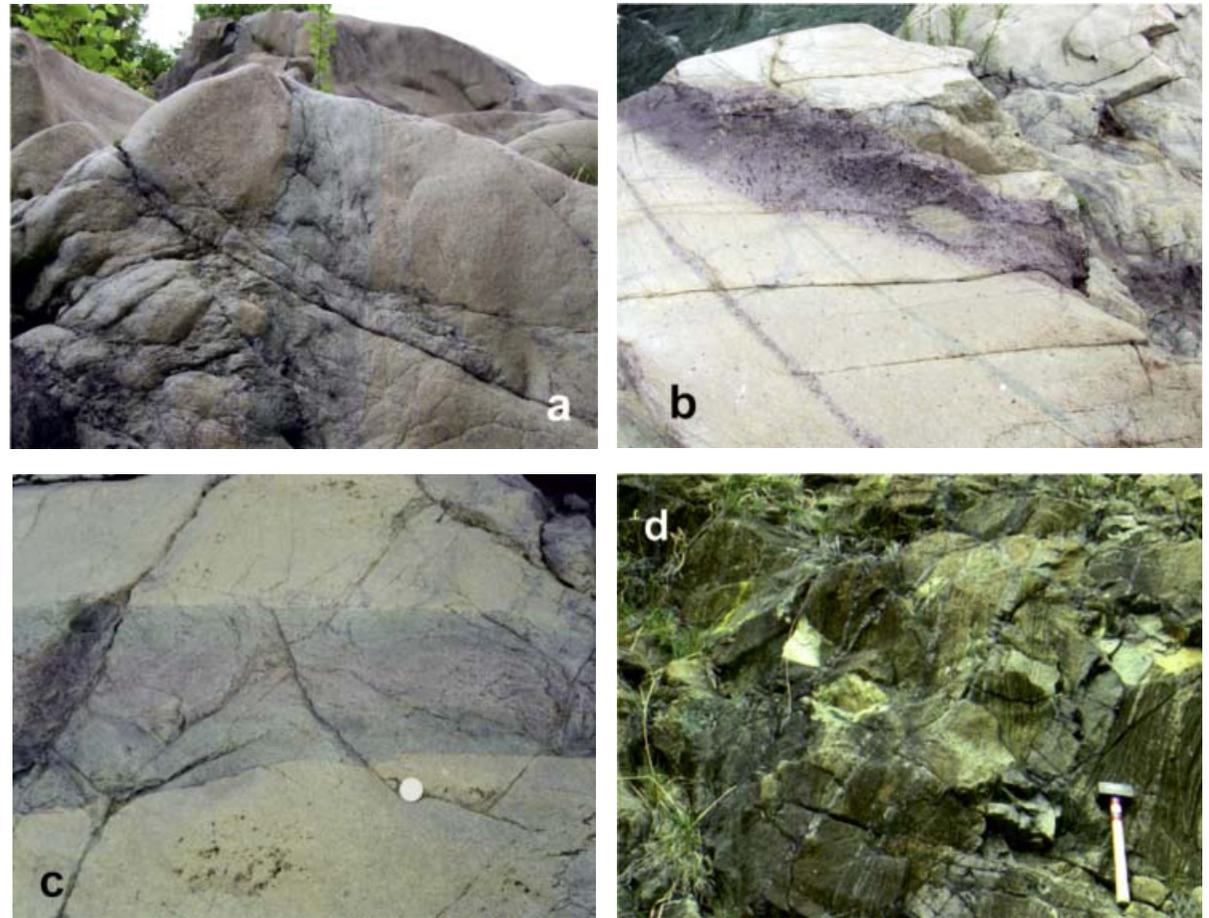
Fig. 56 – **a**, **b**, **c** - Cr-diopside and Al-augite bands in the Balmuccia peridotite: **d** - advanced spinel foliation.

On a large outcrop on the river, gabbros show advanced stretching foliation, isoclinal folds and boudinage of ultramafic cumulates, which are common at this structural level in the mafic complex. This high-T deformation is better exposed uphill on the opposite side of the valley (shown in Fig. 29).

STOP 1.4: Paragneiss septum
(45°49'24" N; 8°10'18" E)

Fig. 57 – **a, b** paragneiss septum, Isola, Stop 1.4.

Follow a trail from Isola to the south toward the "croso della Gavala". Within a few minutes, you will reach a bridge crossing the stream above a paragneiss septum. The rock is a metapelitic granulite with strongly parallel fabric and abundant garnet, quartz, plagioclase ± graphite, sillimanite and very rare biotite (Fig. 57). The septum is in primary contact with foliated norite. At a distance of about 20 meters, it is possible to observe the entrance of an abandoned nickel mine, from which Fe/Ni sulphides in cumulus pyroxenite were mined up to WWII.

Stops in the Varallo area

STOP 1.5: "Diorites" of the upper mafic complex
(45°49'28" N; 8°14'52" E)

From Varallo, take the road to Val Mastallone until locality Aniceti where you may park beside the road (Fig. 58). Exposed in the stream is a swarm of mafic enclaves in the "Diorites". The enclaves are fine-grained, porphyritic gabbro with plagioclase xenocrysts derived from the intruded crystal mush (Fig. 59a).

Fig. 58 – The Varallo area.

STOP 1.6: Stretched mafic enclaves
(45°51'11" N; 8°14'17" E)

In the stream at locality Bocciolaro, an example of mingled diorite and mafic enclaves crops out at the transition between "Main Gabbro" and "Diorites". More advanced stretching of mingled rocks (Fig. 59b) is visible about 100 meters upstream, at (45°51'11.6" N; 8°14'12.8" E).

STOP 1.7: Mafic complex – Kinzigite formation contact
(45°48'38" N; 8°15'25" E)

Take the bridge from Varallo to Crevola, and within 100 meters of crossing the bridge, you may enter a drive way on the right for a parking lot for tennis courts on the south bank of the Sesia River. Along the river there is one of the best exposures of the contact between mafic complex and the Kinzigite formation. Amphibolite-facies migmatite,

Fig. 59 – **a)** Enclaves, Aniceti, Stop 1.5; **b)** Stretched enclaves, Bocciolaro, Stop 1.6 (after Sinigoi et al., 2010, modified).

Fig. 60 – Stop 1.7, **a)** Migmatite, Crevola, **b)** Boudinage.

(Fig. 60) with chaotic deformation, is in primary contact with garnet-bearing diorite (following upstream about 200 meters).

STOP 1.8: Granite dike cutting the Kinzigite formation

(45°47'46" N; 8°16'19" E)

Along the road from Varallo to Borgosesia, the Kinzigite formation is cross-cut by a dike of fine-grained granite (Fig. 61) that is similar, both petrologically and chemically, to microgranite mingled with granodiorite in the Roccapietra pluton.

Stop in the Agnona - Postua area

Fig. 61 – Fine-grained granite dyke; Stop 1.8 (after Sinigoi et al., 2010, modified).

Fig. 62 – The Agnona - Postua area.

STOP 1.9: Deep levels of the Roccapietra pluton

(45°43'24" N; 8°15'44" E)

69

Following the road from Varallo to Borgosesia on the right bank of the Sesia (Fig. 62), park the car immediately after having passed beneath an old bridge connecting Agnona and Borgosesia towns. This Stop is within the deepest levels of the Roccapietra pluton, where mingled dioritic and granitic rocks, with locally abundant inclusions of the country rock, are exposed in a good outcrop on the river (Fig. 63).

itinerary

Fig. 63 – Granitoid with inclusions, Postua (Stop 1.9).

Stop in the Prato Sesia area
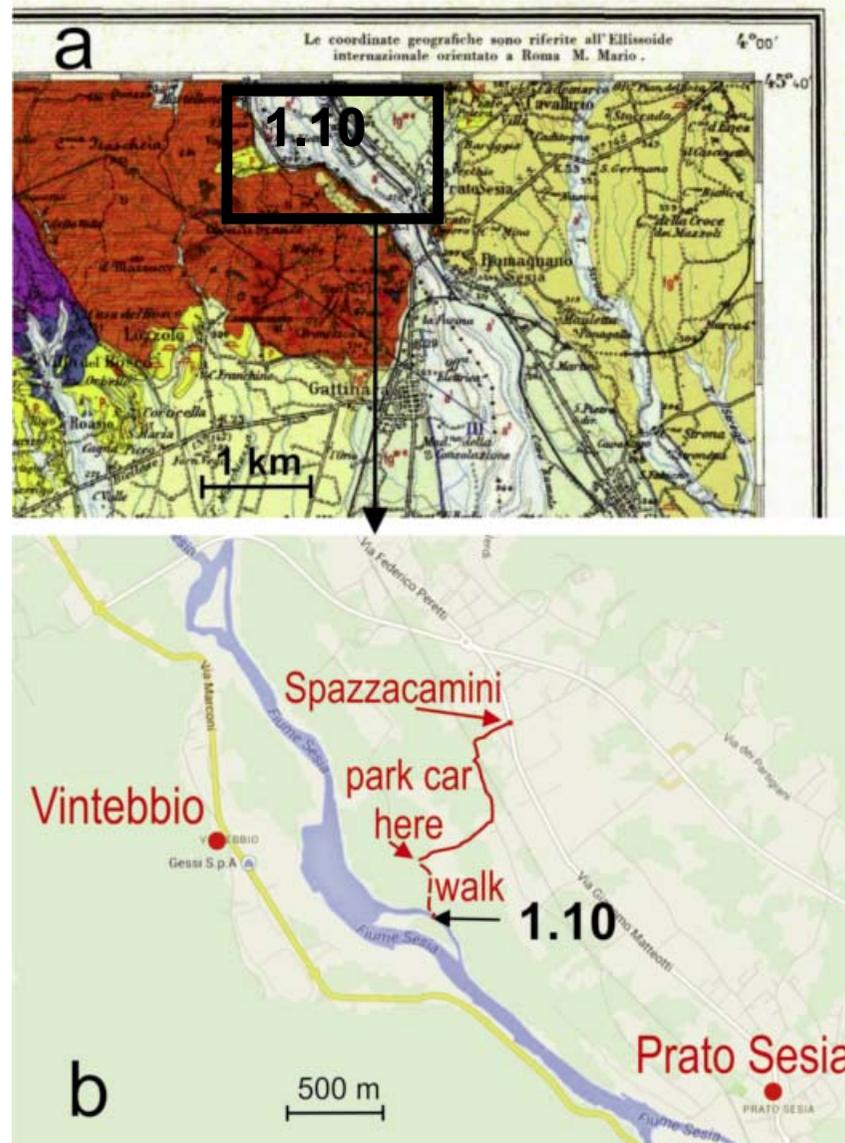
Fig. 64 – The Prato Sesia area: **a** – the Geological map of Italy, 1:100.000 scale, "Sheet 43 Biella"; **b** – road map with stop position.

STOP 1.10: Caldera megabreccia

This area is located with in the caldera fill, and exposes one of the better outcrops of megabreccia.

From Borgosesia, follow the the Sesia River downstream, taking the left bank south of Serravalle. Three kilometers after the bridge over the Sesia (immediately after "La Pipa", at 45°39′31″ N; 8°21′32″ E) turn to the right following the indication "Spazzacamini" (Fig. 64).

After crossing the railway, continue along the dirt road, turn to the left at the crossing and continue for about 2 km. Park the car close to the bridge over a drainage canal (45°39'10" N; 8°21'23" E). From here walk west to the bed of the Sesia (45°39'09" N; 8°21'10" E) arriving within a few minutes to outcrops of megabreccia (Fig. 65). Outcrops on the river are reachable only when water levels are low in the river. If the stream conditions do not allow reaching the outcrop, an alternative may be a stop on the opposite side of the river, following the road on the right bank. South of Vintebbio, after "Regione Cave", park the car at 45°39'07" N, 8°21'06" E, and descend to the river, where megablocks included in welded tuff are exposed.

Fig. 65 – a, b) Megabreccia.

DAY 2
The Sesia magmatic system

Stops in the Val Sessera area

The second day of the field trip provides another transect across the Sesia magmatic system, starting from outcrops of the lower mafic complex and paragneiss bearing belt in the Sessera Valley (Fig. 66). Subsequent stops are at the Valle Mosso granitic pluton and the contact between the Valle Mosso granite and volcanic rocks (see Fig. C in General Info).

Fig. 66 – The Val Sessera area.

Igneous evolutions across the Ivrea crustal section: the Permian Sesia Magmatic System and the Triassic Finero intrusion and mantle

M. Mazzucchelli - J. E. Quick - S. Sinigoi - A. Zanetti - T. Giovanardi
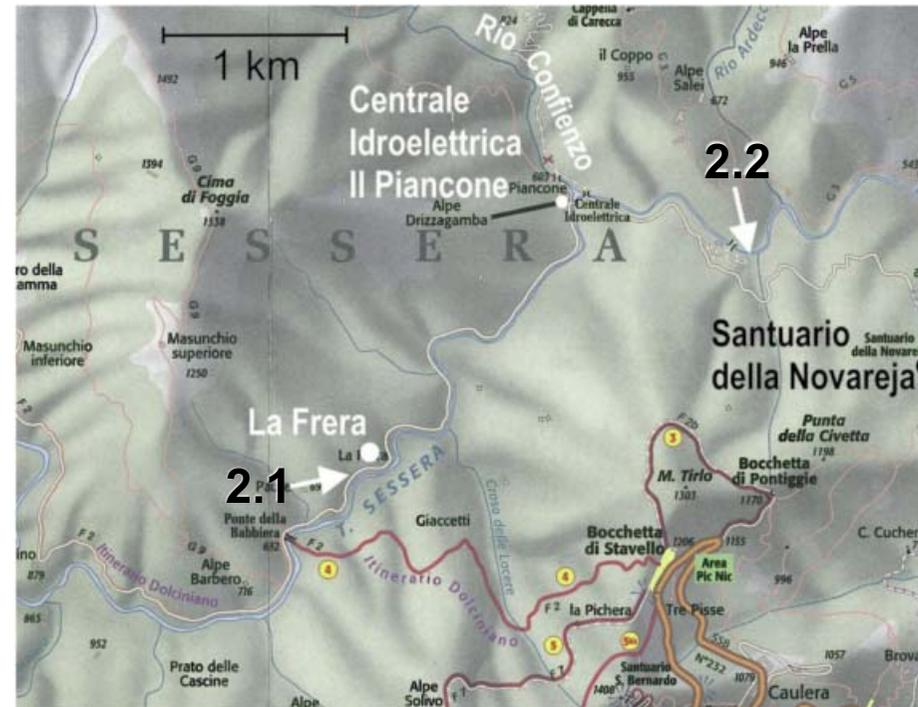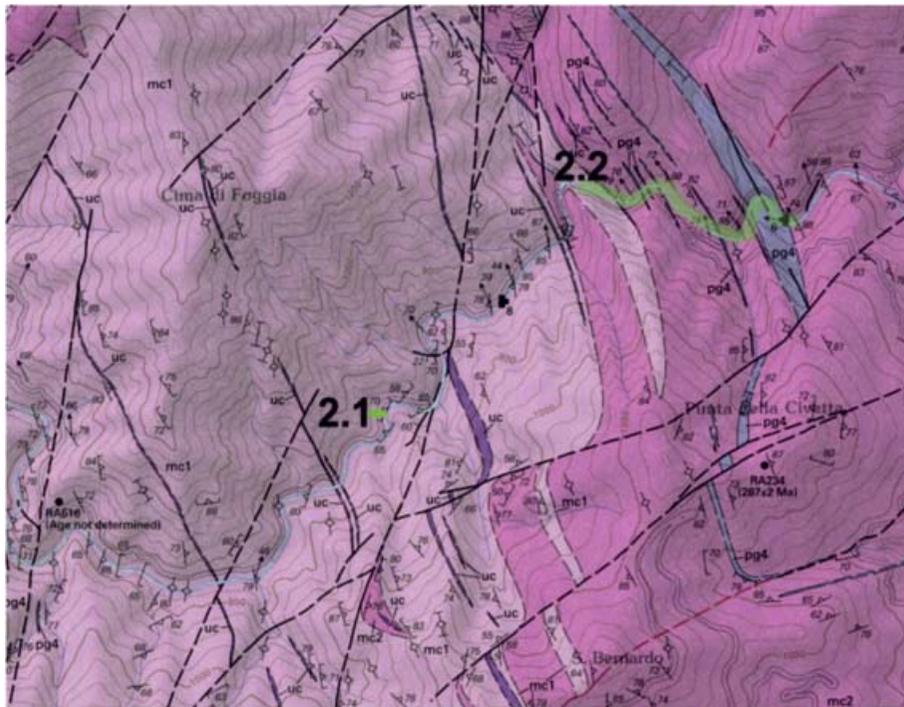
STOP 2.1: Sin-magmatic deformation in gabbro

From Trivero, follow the asphalt road to Castagnea and then continue along a dirt road for about 7 km into the Sessera Valley. Park the car about 300 m before the only house in proximity to Stop 2.1 (45°41'22" N; 8°07'30" E, locality "La Frera"), and descend to the stream to look at small synmagmatic normal faults cross-cutting recrystallised and foliated amphibole gabbro of the lower mafic complex (Fig. 67), and other high-temperature deformation structures.
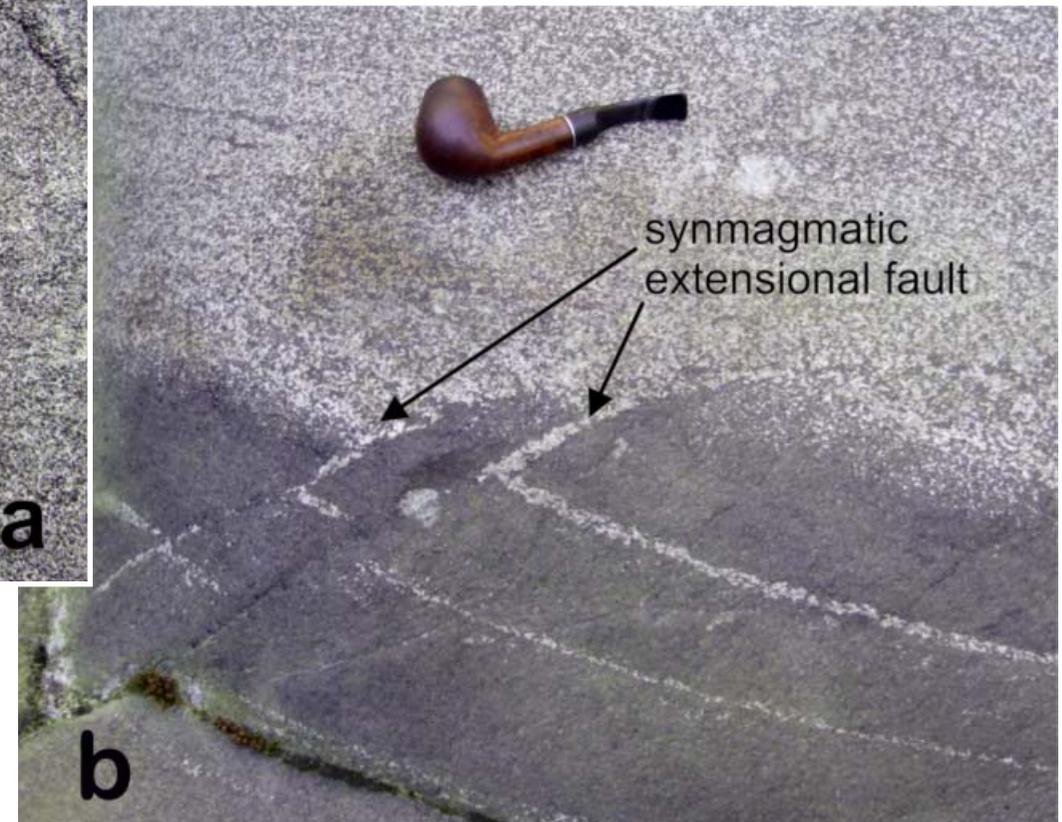
Fig. 67 – **a**, **b**) Lower mafic complex, Sessera Valley; Stop 2.1 (after Sinigoi et al., 2010, modified).

Fig. 68 – **a**) Bands of norite and amphibole gabbro (after Sinigoi et al., 2010, modified); **b**) Restitic paragneiss; Stop 2.2.

STOP 2.2: Traverse across a large paragneiss septum

This is a hike of about 1.3 km along the riverbed, which is feasible only if the water in the stream it is low. Descend to the stream in proximity to the Piancone power station, underneath the confluence of the Sessera and Confienzo streams, and continue downstream. After the first outcrops of amphibole gabbro, noritic rocks become more abundant approaching the first septum of the paragneiss bearing belt (45°42'01" N; 8°08'20" E). From here downward, the stream cross-cuts the paragneiss bearing belt, where norites, quartz-norites and charnockites are abundant and interlayered with restitic paragneiss septa and minor amphibole gabbros (Figs. 68 and 69).

Fig. 69 – **a**) thin septa; **b**) quartz-norite and charnockite; Stop 2.2 (after Sinigoi et al., 2010, modified).

At the end of the traverse is the thickest paragneiss septum, which is about 100 m across (45°41′59″ N; 8°09′03″ E). Before arriving at this septum, smaller septa of paragneiss are included in norite and cut by small normal faults filled by fine-grained gabbro (Fig. 70). In the septum, charnockite is present either as bands or discordant

Fig. 70 – **a, b**) Stop 2.2, thin paragneiss fragments in norite; a - after Sinigoi et al., 2010, modified.

Fig. 71 – Charnockitic dike.

dikes (Fig. 71) within a garnet-rich metasediment. Biotite is present, although rare. At the eastern contact of the septum, garnet-bearing norites are present. Immediately above, bands of charnockite mingled with norite are transposed into the foliation. The composition of these granitoids is very similar to that of leucosomes observed at the roof of the mafic complex (Fig. 60a), suggesting that the last septum incorporated in the mafic complex was as fertile as the roof Kinzigite (Sinigoi et al., 2011).

charnockitic dike

Stops in the Valle Mosso – San Bononio area

STOP 2.3: Granite – migmatite contact

At the western end of Valle Mosso village, park the car close to a small church (45°38'17" N, 8°07'43" E) and descend to the stream beneath the bridge on the main road. Walking downstream, ortho- and paragneiss in migmatite facies (Fig. 73a) are in primary contact with the base of the granitic pluton, where faintly foliated granodiorite is cross cut by aplitic and mafic dikes (Fig. 73b and c). The outcrop is continuous for more than 200 m.
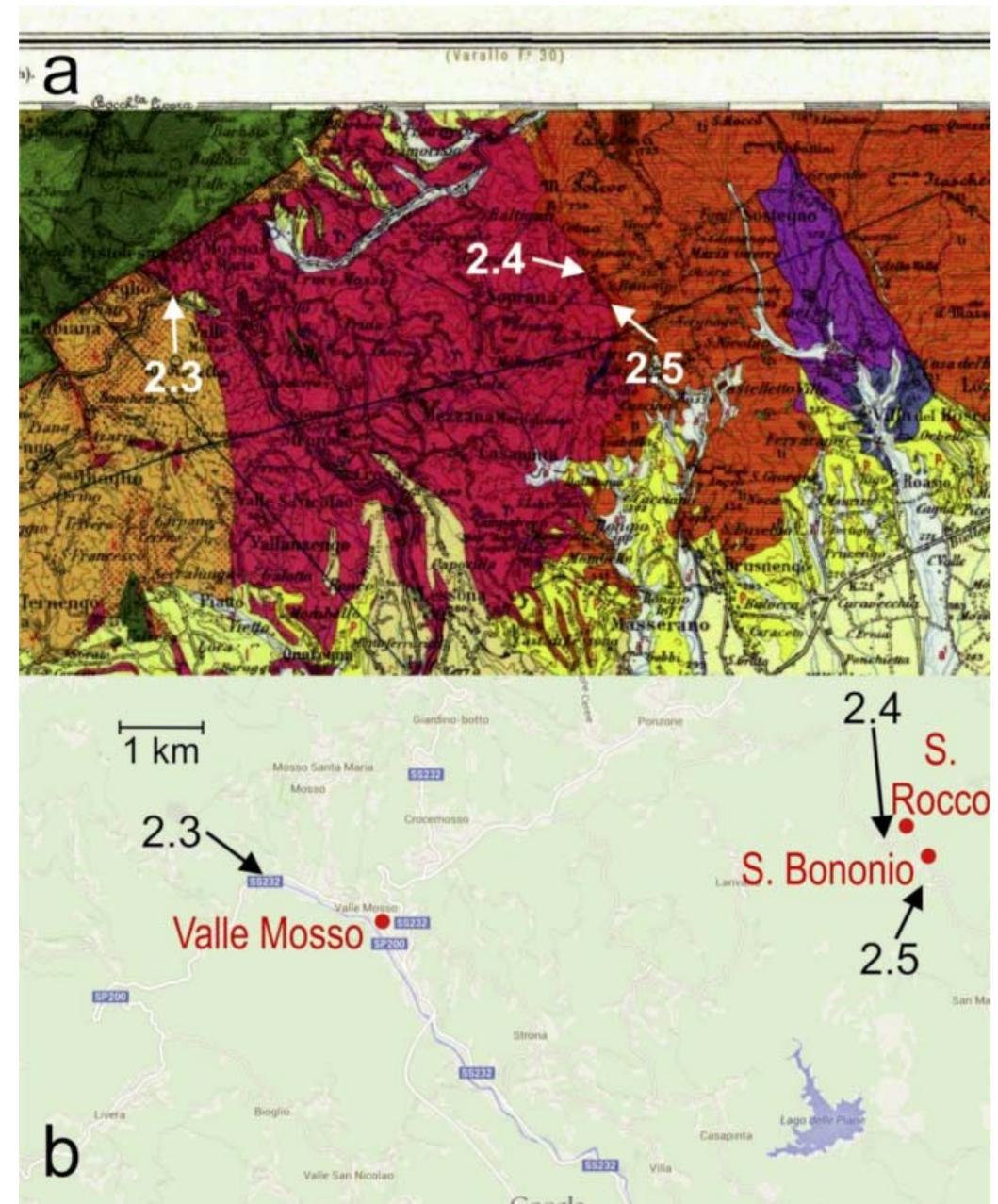
Fig. 72 – The Valle Mosso area: **a)** the Geological map of Italy, 1:100.000 scale, "Sheet 43 Biella"; **b)** road map with Stops position.

Fig. 73 – **a)** Orthogneiss; **b)** aplite; **c)** mafic dyke; Stop 2.3.

STOP 2.4: The upper Valle Mosso granite

After Stop 2.3, the excursion will traverse the Valle Mosso pluton to reach its roof, where it is intruding volcanic rocks. The granite is monotonous, and the distinction between lower and upper Valle Mosso, defined solely on the basis of chemistry, is hardly detectable in the field. Follow the road to Ponzone (en route an easy brief stop may be made in a small quarry inside the town, at 45°39′08.9″ N; 8°10′59.2″ E, to see an aplitic dike cross-cutting the granite), then turn to the right in direction of Baltigati and continue towards San Bononio. Here (45°38′30″ N; 8°13′13″ E), the granite becomes granophyric approaching the contact with volcanic rocks.

STOP 2.5: Granite – Volcanic rock contact

After San Bononio, stop the car at the hairpin turn (45°38′13″ N; 8°13′36″ E) and follow the path to the west towards an abandoned quarry (less than 100 meters). Immediately after a small valley, volcanic rocks, here represented by an aphyric dacite, are clearly intruded by granite with granophyric patches. From here to the east we reenter the caldera fill.

Igneous evolutions across the Ivrea crustal section: the Permian Sesia Magmatic System and the Triassic Finero intrusion and mantle

M. Mazzucchelli - J. E. Quick - S. Sinigoi - A. Zanetti - T. Giovanardi

DAY 3
The Finero-type IVZ

Stops in the Finero area

The third day the fieldtrip will lead participants across the Finero area, starting from the core of the antiform (i.e. the Finero Mantle unit) looking at the Finero mafic complex by crossing the southern flank of the antiform and rising progressively up-section to the country rocks of the Kinzigite formation. Stops are indicated in Fig. 74.
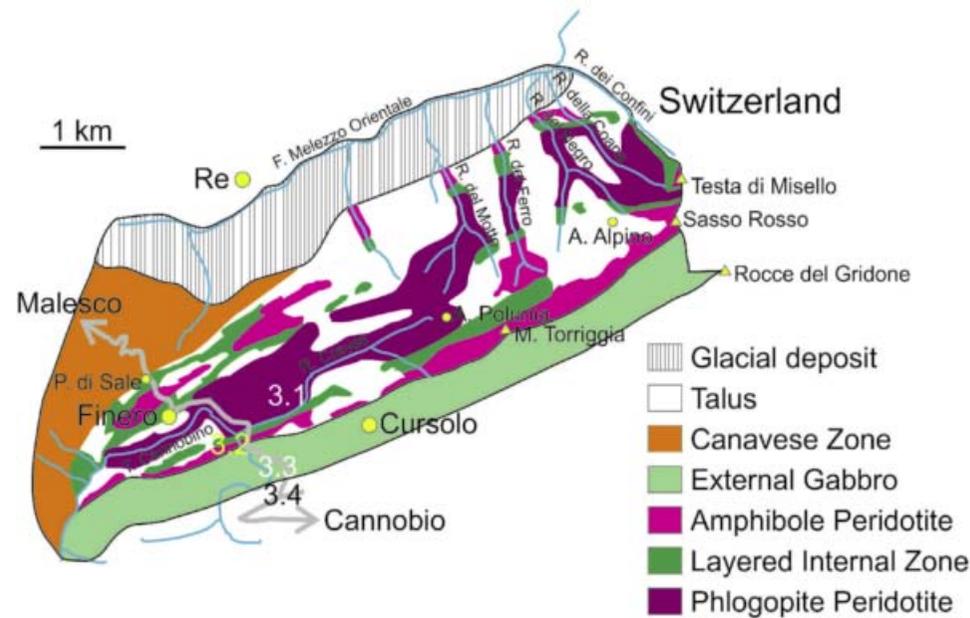
Fig. 74 - Geographical location of the field trip area and Stops.

78

itinerary

STOP 3.1: Val Creves Stop, the Finero mantle phlogopite peridotite unit

The first Stop will be held along a road cutting the right flank of the Rio Creves valley. Here, the typical sequence of the Finero mantle unit is exposed. The sequence includes phlogopite-harzburgite intercalated with websterites (containing emerald green clinopyroxene, orthopyroxene, phlogopite, amphibole, spinel and, in places, olivine) and subordinately orthopyroxenites.

Dunite layers (Fig. 75), up to 60 cm thick, concordant with the main mantle foliation, randomly occur (46°06'22" N; 8°32'46" E). These layers contain (i) thin, one-grain-thick, trails of chromite that strike nearly parallel to the mantle foliation and (ii) discordant veins and pockets filled by phlogopite flakes, up to 10 cm large. Half-way up (46°06'27" N; 8°33'10" E) late sapphirine-bearing amphibole gabbro veins (Fig. 76) crosscut at variable, but usually high, angle the main peridotite-pyroxenite layering and the mantle foliation (Giovanardi et al., 2013). These veins show a banded structure consisting of various melanocratic zones towards to the contact with the host peridotite, and a leucocratic zone forming the dyke core. Moving from the mantle peridotite to the dyke core, the following layers can be recognized: 1) an orthopyroxenite zone, established within the host peridotite as a result of the melt-peridotite interaction inducing formation of secondary orthopyroxene and dissolution of peridotite olivine; 2) a melanocratic zone formed by large, primary dark-brown amphibole (up to 1 cm long) including apatite, small plagioclase grains and phlogopite lamellae; 3) a reaction zone: here, the reaction between the primary amphiboles and a melt (similar to the parent melt of the minerals in zone 4), produced secondary patches consisting of secondary light-brow amphibole, green spinel, sapphirine and phlogopite. Sapphirine
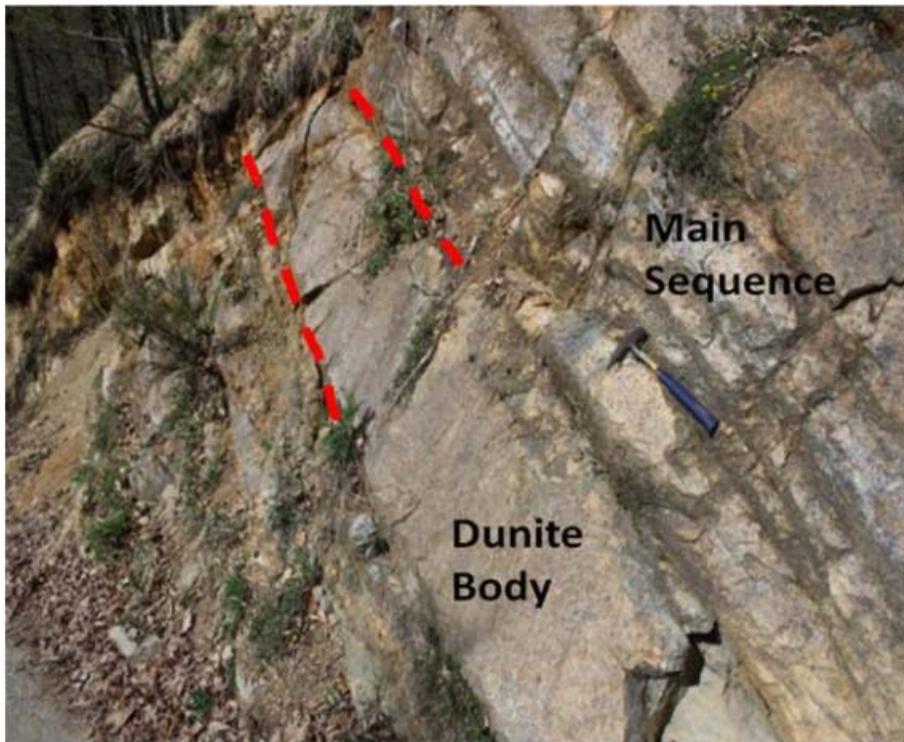
Fig. 75 - Dunite layers.

79

itinerary
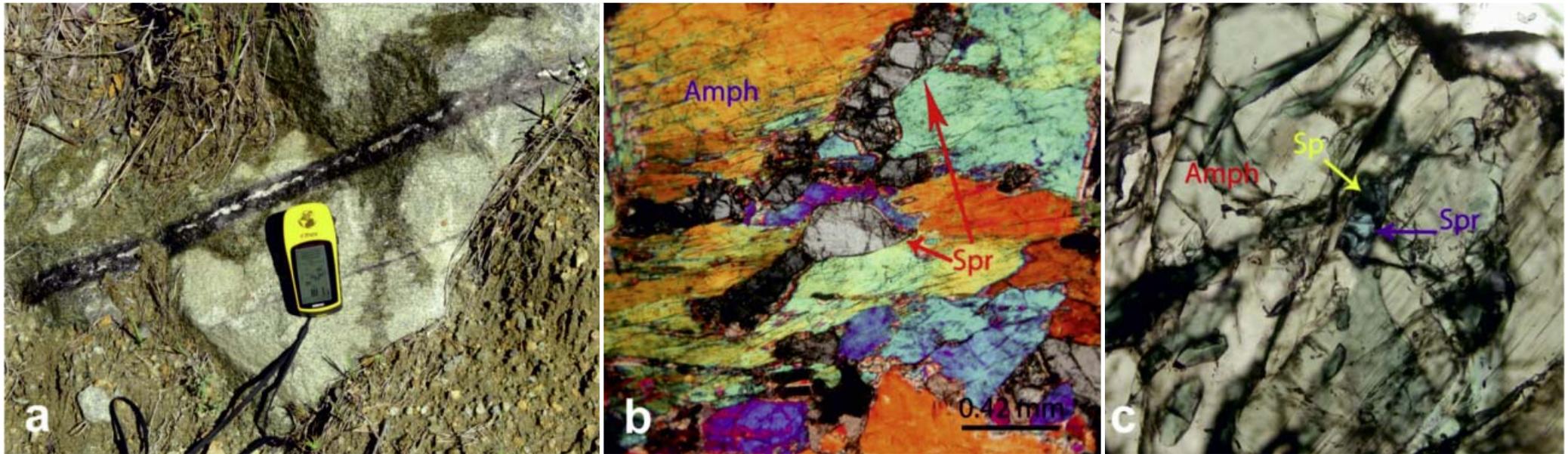
Fig. 76 – **a)** Late sapphirine-bearing amphibole gabbro vein. Sapphirine is present in association with titanian pargasite. It may be found in two different microtextural occurrences: **b)** as an envelope around green spinel grains, which are sometimes elongated to vermicular in shape; **c)** as prismatic grains isolated or in aggregates. Amph = amphibole, Sp = spinel, Spr = sapphirine.

crystals occur in this reaction zone as interstitial grains, inclusions within late amphiboles and as coronas rimming spinel; 4) a leucocratic zone formed by plagioclase and subordinate light-brown amphibole. In places, concentrations of apatite grains occur.

Phlogopite mainly occur in the sapphirine-bearing veins as late, interstitial flakes apparently in equilibrium with other magmatic phases. In addition, phlogopite forms monomineralic, very late intrusions and patches that crosscut the melanocratic zones (in particular, the zone 2).

Near the entrance to a huge quarry (46°06'29" N; 8°33'12" E), there is a sequence enriched in pyroxenites. Here, it is still visible the Section II studied by Zanetti et al. (1999), which intersected two Cr-Di websterites, phlogopite harzburgite and a dolomite-apatite-bearing wehrlite. Apatite in wehrlitic layers is Cl-rich (Cl ~2 wt.%). The wehrlitic layers are surrounded by metasomatic haloes, which indicate that their crystallisation was related to a relatively late event of melt migration.

Recently, the progression of the quarry activities has (sadly) destroyed the largest Cr-Di websterites, which were up to 1.5 m thick. However, the quarry development has exposed a ~10 m-thick dunite body (Fig. 77, 46°06'31" N; 8°33'12" E) made by coarse-grained olivine ubiquitously associated with small chromite grains. Isolated phlogopite flakes, some mm large, are also present throughout the dunite body, especially along micro-shear planes. This large dunite body shows sharp contact with the harzburgite-pyroxenite associations, that are virtually parallel to the strike of the hazburgite-pyroxenite banding. Several bands of magmatic origin suggest a multistage evolution of melt migration through the dunite body after its formation.

The first magmatic layers (up to 20 cm thick) to be segregated are chromitites, running broadly parallel to the main mantle foliation (Fig. 78). In these layers, chromite is associated with orthopyroxene,

81

itinerary

Fig. 77 - The Rio Creves quarry: large dunite body.

Fig. 78 - The Rio Creves quarry: chromitite layer.

with subordinate clinopyroxene and amphibole: in the most recrystallised layers only very few relics of rounded olivine can be found. The chromitites segregation was followed by the crystallisation of a complex sequence of pyroxenite layers and pockets, basically formed by clinopyroxene, orthopyroxene, amphibole, phlogopite and spinel. The early pyroxenite layers include phlogopite-bearing websterites showing nearly parallel strike, which is also nearly parallel to the main foliation.

Late pyroxenite layers (Fig. 79) show instead curvilinear strike and a progressive increase of the modal amount of amphibole and phlogopite with respect to the pyroxenes. The highest modal concentration of the hydrous minerals is shown by pegmatoidal pockets (Fig. 80), with grain size up to 10 cm. All the magmatic layers are cut at variable angle by mm-thick veins filled by very large phlogopite flakes.
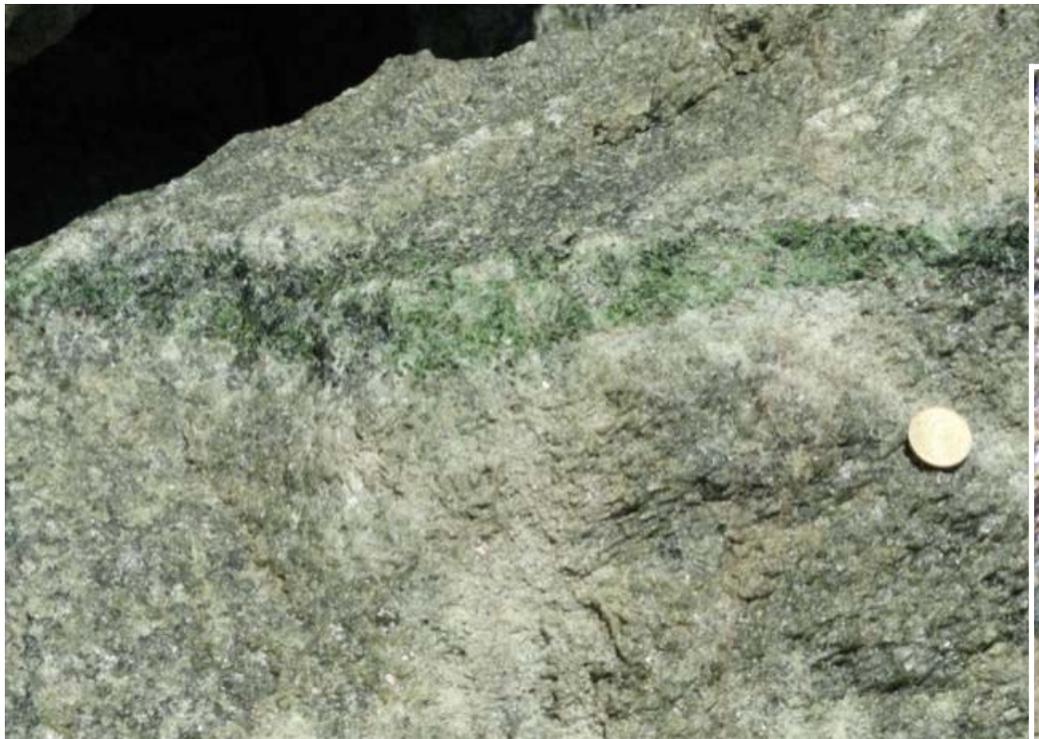
Fig. 79 - The Rio Creves quarry: late pyroxenite layer.

Fig. 80 - The Rio Creves quarry: pegmatoidal pocket.

Geochemical data (Fig. 81) indicate that the parent melts of the chromitites and websterites segregated into the huge dunite have a cognate origin with those forming the harzburgite-pyroxenite association.

Owing to the advancement of the quarry front, the huge dunite above described is presently nearly exhausted, leaving the place to a rather amphibole-rich phlogopite harzburgite.
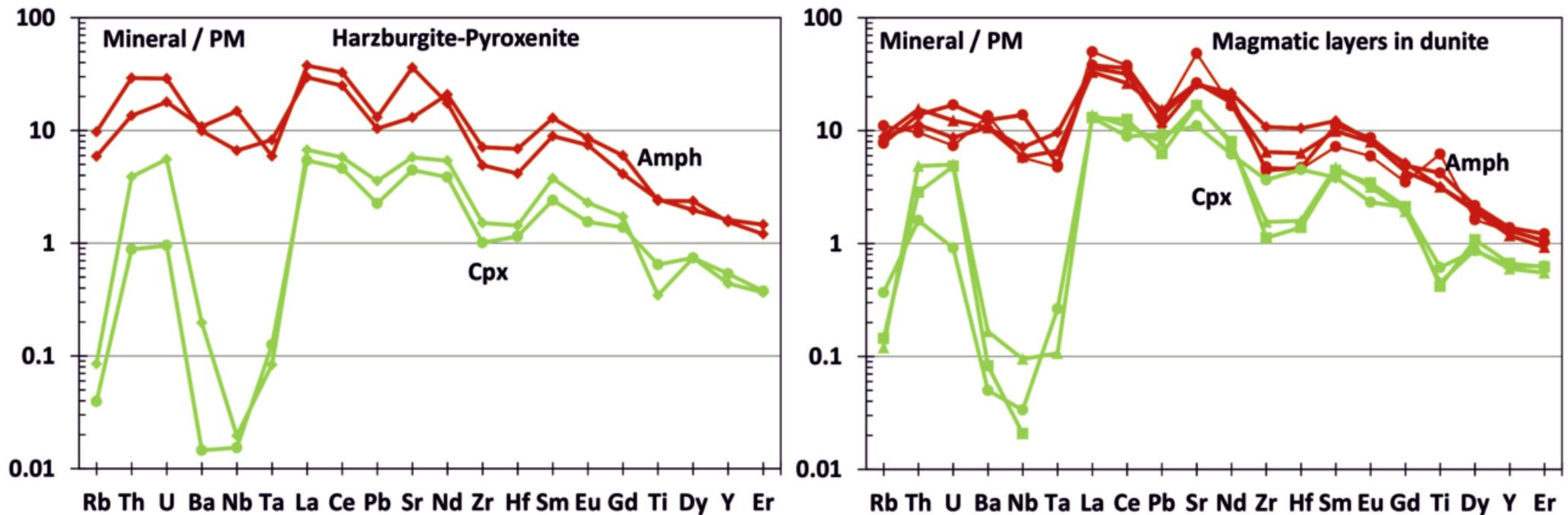
Fig. 81 - Incompatible element spidergram of clinopyroxene and amphibole: **a)** harzburgite-pyroxenite association; **b)** magmatic layers (chromitites and websterites) in dunite.

STOP 3.2: Cannobino River Stop, the Finero mafic complex

The valley of the Cannobino River allows to study a relatively short, but rather complete, section of the Finero mafic complex. From the bridge on the Cannobino River (46°06'17" N; 8°32'40" E), situated close to the confluence with the Creves creek, it is possible to see the tectonic contact between the phlogopite peridotite mantle unit and the layered internal zone (LIZ) of the Finero mafic complex, consisting of a decimeters-thick mylonite (Fig. 44).

The LIZ is typically 70 to 120 m thick (Siena & Coltorti, 1989) mainly consisting of garnet gabbros, garnet hornblendite (Fig. 82), anorthosites and pyroxenites (Fig. 84). Near the structurally lower tectonic contact with the phlogopite peridotite, the LIZ rocks are made of up to 30% garnet (e.g. Cawthorn, 1975).

Along the Cannobino River (46°06'16" N; 8°32'41" E), the gabbroic sequence is about 10 m thick, consisting of garnet-bearing amphibole gabbros (made by plagioclase, clinopyroxene, amphibole, garnet and orthopyroxene) intercalated with garnetiferous hornblendite, anorthosites, pyroxenites (mainly, clinopyroxenites) in decreasing order of abundance (Fig. 83). The pyroxenites are always rimmed by

Fig. 82 - Garnet hornblendite.
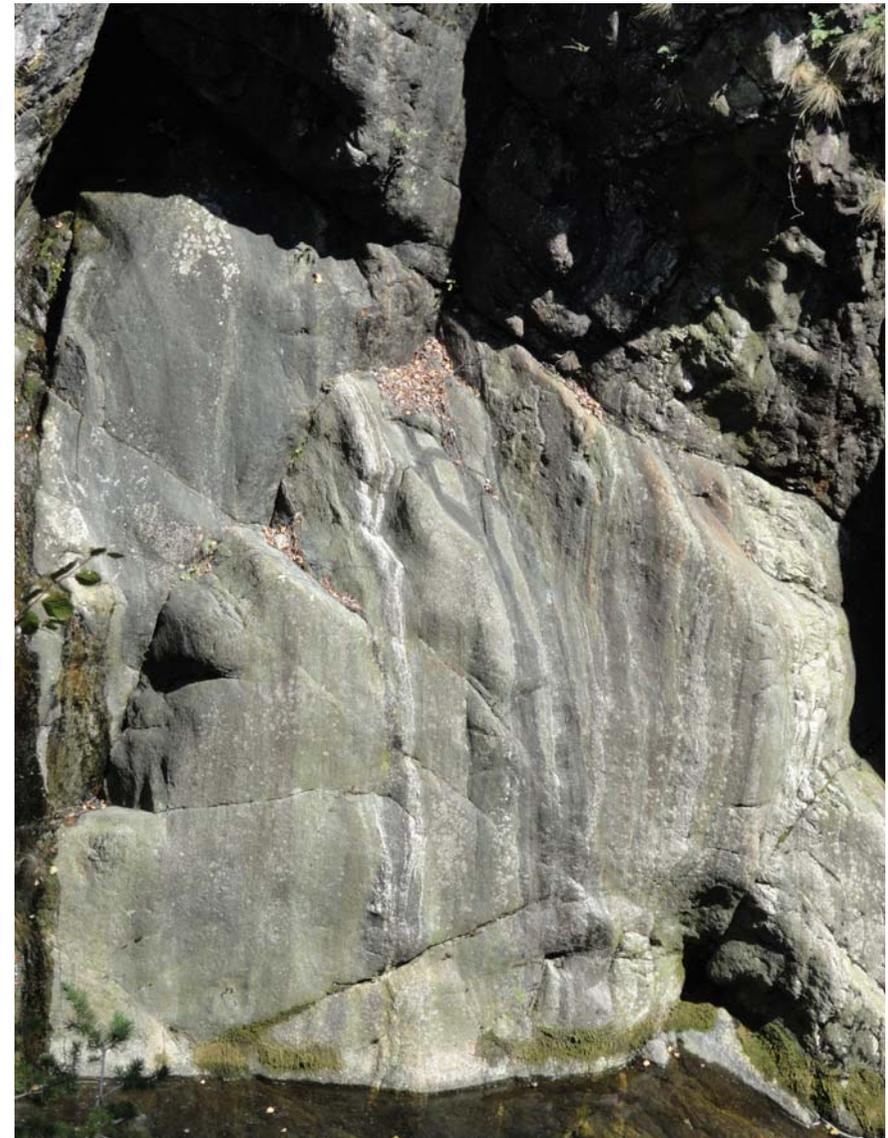
Fig. 83 - Gabbroic sequence of the layered internal zone (LIZ).

hornblendite selvages (Fig. 84). Discrete cm-to m-scale lenses and pods of peridotite are randomly included.

The stratigraphic upper contact of LIZ with the amphibole peridotite unit (46°06'15" N; 8°32'42" E) presents a transition zone ~20 m thick, mainly formed by amphibole websterites (with Cpx and Opx) and orthopyroxenites embedded by garnet hornblendites. In places, these pyroxenites are rich in phlogopite, as well as in amphibole.

Fig. 84 - Anorthosite and pyroxenite rimmed by hornblendite selvages.

Fig. 85 - Amphibole-bearing cumulus peridotite.

The amphibole peridotite unit is ~400 m thick. It includes amphibole-bearing cumulus peridotites (mainly dunites, with subordinate harzburgites, wehrlites and lherzolites), pyroxenites and hornblendites (Fig. 85). The latter occurs as bands,

lenses and pods, sometimes showing pegmatoidal texture (Fig. 86), with amphibole crystals up to 1 m long. In the Cannobino section, field and petrochemical data suggest that the pervasive amphibole occurrence is mainly related to the late injection of amphibole-saturated melts, which reacted and recrystallised the former cumulus peridotite.

Fig. 86 - Hornblendite with pegmatoidal texture. The hexagon highlights the basal section of an amphibole crystal. Stop 3.2.
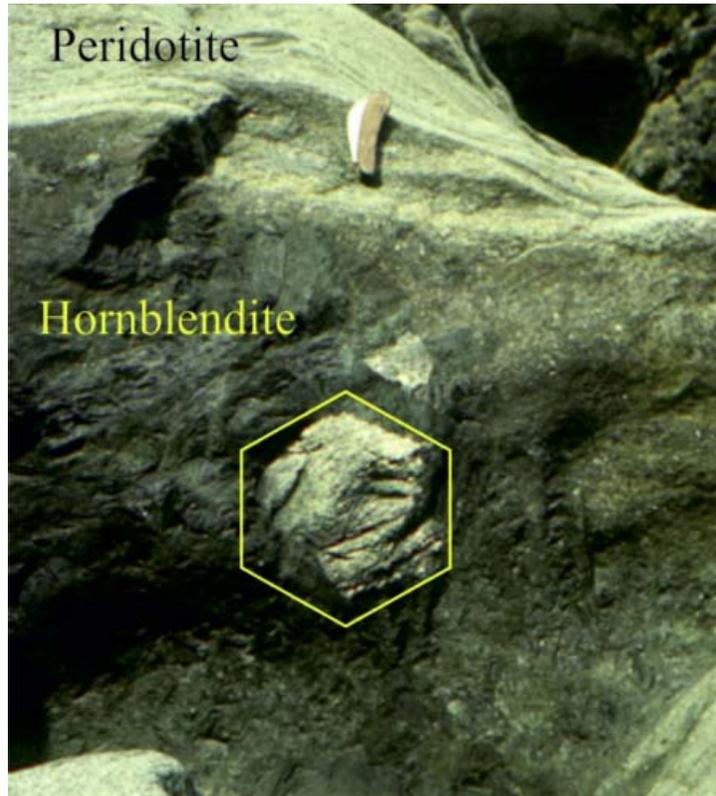
STOP 3.3: Road Finero - Cannobio, the Finero mafic complex
(46°06'08" N; 8°32'56" E)

The external gabbro unit is 400 to 500 m thick and mainly consists of amphibole gabbros and diorites (plagioclase, clinopyroxene, amphibole, orthopyroxene, ilmenite, magnetite, ±garnet, ±apatite, ±zircon, Fig. 87), with minor pyroxenite and anorthosite bands. Along the Cannobino River the contact between amphibole peridotite and external gabbro is tectonic. Where primary, it is defined by a close alternation of layers of peridotite,

Fig. 87 - Amphibole-bearing gabbro in the external gabbro unit.

86

itinerary

hornblendite and gabbro, 20 cm to 1 m thick (Siena & Coltorti, 1989; Hingerl et al., 2008; Palzer et al., 2012). Hingerl et al. (2008) completed a detailed profile through the external gabbro along the Cannobino Valley. They have found several metapelitic septa of the Kinzigite formation with partial melting evidence in the contact zones. According to their observations, contact melting of the metapelitic septa decreases towards the top of the mafic complex. The rocks of the external gabbro (and of the metapelitic septa) are strongly deformed in the Cannobino Valley area. Late alkaline pegmatitic dykes and pods crosscut the gabbroic rocks and their fabrics (Klötzli et al., 2007; Hingerl et al., 2008).

STOP 3.4: Road Finero - Cannobio Stop, the upper contact of the Finero mafic complex

After the second tunnel of the Finero – Cannobio road outcrops of the country rocks of the Kinzigite formation (46°05'53" N; 8°32'60" E). Here the rocks are represented by locally highly deformed amphibolites and migmatitic paragneisses. Their strike is parallel to sub-parallel to the layering of the mafic complex.
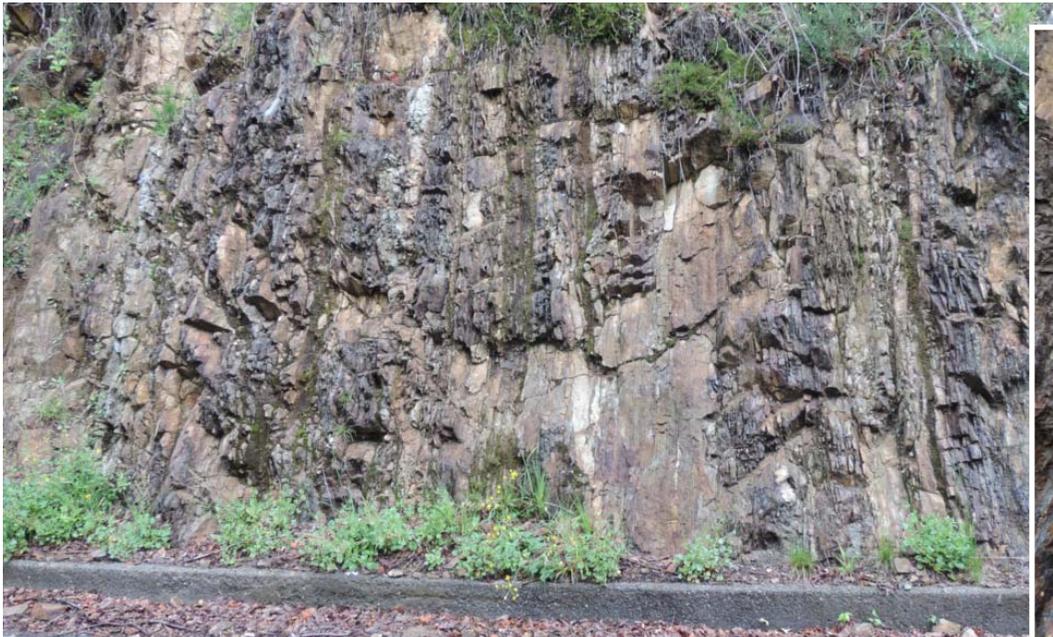
Fig. 88 – Rocks of the Kinzigite formation in the Val Cannobina area, along the road Finero - Cannobio.

Fig. 89 – Rocks of the Kinzigite formation in the Val Cannobina area: a detail of the migmatitic paragneisses.

Igneous evolutions across the Ivrea crustal section: the Permian Sesia Magmatic System and the Triassic Finero intrusion and mantle

M. Mazzucchelli - J. E. Quick - S. Sinigoi - A. Zanetti - T. Giovanardi

geological field trips 2014 - 6(2.2)

89

memorandum

References

Barbey P., Macaudiere J. & Nzenti J.P. (1990) - High-pressure dehydration melting of metapelites: evidence from migmatites of Yaounde (Cameroon). Journal of Petrology, 31, 401-427.

Barbieri M.A. (1996) - Petrologia dei corpi peridotitici minori in Val Grande (zona Ivrea-Verbano Settentrionale). Translated Title: Petrology of minor peridotite bodies in Val Grande (northern IVZ). Atti Ticinesi di Scienze della Terra, 4, 121-128.

Beltrando M., Rubatto D. & Manatschal G. (2010) - From passive margins to orogens: The link between ocean-continent transition zones and (ultra)high-pressure metamorphisim. Geology, 38, 559-562.

Berckhemer H. (1968) - Topographie des ''Ivrea-Koerpers'' abgeleitet aus seismischen und gravimetrischen daten. Schweizerische Mineralogische und Petrographische Mitteilungen, 48, 235-246.

Bodinier J.L. (1988) - Geochemistry and petrogenesis of the Lanzo peridotite body, Western Alps. Tectonophysics, 149, 67–88.

Boriani A., Burlini L. & Sacchi R. (1990a) - The Cossato-Mergozzo-Brissago Line and the Pogallo Line (Southern Alps, Northern Italy) and their relationships with the late-Hercynian magmatic and metamorphic events. Tectonophysics, 182, 91-102.

Boriani A., Giobbi-Origoni E., Borghi A. & Caironi V. (1990b) - The evolution of the "Serie dei Laghi" (Strona-Ceneri and Scisti dei Laghi): the upper component of the Ivrea-Verbano crustal section; Southern Alps, North Italy and Ticino, Switzerland. Tectonophysics, 182, 103-118.

Boriani A. & Sacchi R. (1973) - Geology of the junction between the Ivrea-Verbano and Strona-Ceneri Zones (southern Alps). Memorie degli Istituti di Geologia e Mineralogia dell' Università di Padova, 28, 1-36.

Boriani A. & Villa I.M. (1997) - Geochronology of regional metamorphism in the IVZ and Serie dei Laghi, Italian Alps. Schweizerische Mineralogische Petrographische Mitteilung, 77, 381-401.

Brodie K.H. & Rutter E.H. (1987) - Deep crustal extensional faulting in the Ivrea Verbano Zone of Northern Italy. Tectonophysics, 140, 193-212.

Brodie K.H., Rutter E.H. & Evans P.J. (1992) - On the structure of the IVZ (N Italy) and its implications for present day lower continental crust geometry. Terra Nova, 4, 34-40.

Brodie K.H., Rex D. & Rutter E.H. (1989) - On the age of deep crustal extensional faulting in the Ivrea Zone, Northern Italy. In: Coward M. P., Dietrich D., Park R. G. (eds) Alpine Tectonics, Geological Society London, Special Publications, 45, 203-210.

Bryan S.E., Ferrari L., Reiners P.W., Allen C.M., Petrone C.M., Ramos-Rosique A. & Campbell I.H. (2008) - New insights into crustal contributions to large-volume rhyolite generation in the mid-Tertiary Sierra Madre Occidental Province, Mexico, revealed by U-Pb geochronology. Journal of Petrology, 49, 47-77.

Cawthorn R.G. (1975) - The amphibole peridotite - metagabbro complex, Finero, northern Italy. Journal of Geology, 83, 437-454.

Charlier B.L.A., Wilson C.J.N., Lowenstern J.B., Blake S., Van Calsteren P.W. & Davidson J.P. (2004) - Magma generation at a large, hyperactive silicic volcano (Taupo, New Zealand) revealed by U-Th and U-Pb systematic in zircons. Journal of Petrology, 46, 3-32.

Coleman D.S., Gray W. & Glazner A. F. (2004) - Rethinking the emplacement and evolution of zoned plutons: geochronologic evidence for incremental assembly of the Tuolumne Intrusive Suite, California. Geology, 32, 433-436.

Correia C.T., Sinigoi S., Girardi V.A.V., Mazzucchelli M., Tassinari C.C.G. & Giovanardi T. (2012) - The growth of large mafic intrusions: Comparing Niquelândia and Ivrea igneous complexes. Lithos, 155, 167-182.

Cummings G.L., Koepper V. & Ferrario A. (1987) - A lead study of the northeastern Ivrea Zone and the adjoining Ceneri Zone (N Italy): evidence for a contaminated subcontinental mantle. Contributions to Mineralogy and Petrology, 97, 19-30.

Demarchi G., Quick J.E., Sinigoi S. & Mayer A. (1998) - Pressure gradient and original orientation of a lower-crustal intrusion in the IVZ, Northern Italy. Journal of Geology, 106, 609-622.

Fountain D. M. (1976) - The Ivrea-Verbano and Strona-Ceneri Zones, northern Italy: A cross-section of the continental crust – New evidence from seismic velocities of rock samples. Tectonophysics, 33, 145-165.

Friedrichsen H. (1989) - Hydration of the Finero Ultramafic body: Its origin and age. C.N.R. - D.F.G. Workshop "On the composition and structure of the lower continental crust", Varallo Sesia (VC, Italy), May, 17th-20th 1989, Abstracts Volume.

Garuti G., Bea F., Zaccarini F. & Montero P. (2001) - Age, geochemistry and petrogenesis of the ultramafic pipes in the Ivrea Zone, NW Italy. Journal of Petrology, 42, 433-457.

Gebauer D. (1993) - The Pre-Alpine evolution of the continental crust of the Central Alps: an overview. In: von Raumer J.F., Neubauer F. (eds): Pre-Mesozoic Geology in the Alps. Springer-Verlag.

Giovanardi T., Mazzucchelli M., Zanetti A., Langone A., Tiepolo M. & Cipriani A. (2014) - Occurrence of Phlogopite in the Finero Mafic Layered Complex. Central European Journal of Geosciences, 6, 588-613.

Giovanardi T., Morishita T., Zanetti A., Mazzucchelli M. & Vannucci R. (2013) - Igneous sapphirine as a product of melt-peridotite interactions in the Finero Phlogopite-Peridotite Massif, Western Italian Alps. European Journal of Mineralogy, 25, 17–31.

Grieco G., Ferrario A. & Mathez E.A. (2004) - The effect of metasomatism on the Cr-PGE mineralization in the Finero Complex, Ivrea Zone, Southern Alps. Ore Geology Reviews, 24, 299–314.

Grieco G., Ferrario A., von Quadt A., Köppel V. & Mathez A. (2001) - The zircon-bearing chromitites of the phlogopite peridotite of Finero (Ivrea Zone, Southern Alps): evidence and geochronology of a metasomatized mantle slab. Journal of Petrology, 42/1, 89-101.

Guidarelli M., Zille A., Sarao A., Natale M., Nunziata C. & Panza G.F. (2006) - Shear-wave velocity models and seismic sources in Campanian volcanic areas: Vesuvius and Phlegraean Fields. In: Vesuvius: Education Security and Prosperity (edited by Dobran F.). Developments in Volcanology, 8. Elsevier Science Publications, Amsterdam, 287–310.

Handy M.R. (1987) - The structure, age and kinematics of the Pogallo fault zone, southern Alps, northwestern Italy. Eclogae Geologicae Helvetiae, 80, 593-632.

Handy M.R. & Stünitz H. (2002) - Strain localization by fracturing and reaction weakening – a mechanism for initiating exhumation of subcontinental mantle beneath rifted margins. In: De Meer S., Drury M.R., De Bresser J.H.P. & Pennock G.M. (eds). Deformation Mechanisms, Rheology and Tectonics: Current Status and Future Perspectives. Geological Society Special

Publications, 200, 387–407.

Handy M.R. & Zingg A. (1991) - The tectonic and rheological evolution of an attenuated cross-section of the continental crust: Ivrea crustal section, southern Alps, northwestern Italy and southern Switzerland. Geological Society of America Bulletin 103, 236-253.

Harris N.B.W., Pearce J.A. & Tindle A.G. (1986) - Geochemical characteristics of collision-zone magmatism. In: Collision Tectonics (edited by Coward M.P. & Ries A.C.), Geological Society of London, Special Publications 19, 67-81, London.

Hartmann G. & Wedepohl K.H. (1993) - The composition of peridotite tectonites from the Ivrea Complex, northern Italy: Residues from melt extraction. Geochimica et Cosmochimica Acta, 57, 1761-1782.

Henk A., Franz L., Teufel S. & Oncken O. (1997) - Magmatic underplating, extension, and crustal reequilibration: insights from a cross-section through the Ivrea Zone and Strona-Ceneri Zone, northern Italy. Journal of Geology, 105, 367-377.

Henstock T.J., Woods A.W. & White R.S. (1993) - The accretion of oceanic crust by episodic sill intrusion. Journal of Geophysical Research, 98, 4143-4161.

Hingerl F., Kloetzli U., Steuber C. & Kleinschrodt R. (2008) - New results from the mafic complex in the Finero area. 33th International Geological Congress, Oslo 6-14th, August 2008, CD-ROM abstracts, X-CD Technologies, http://www.cprm.gov.br/33IGC/1344964.html

Hofmann A.W. (1988) - Chemical differentiation of the Earth: the relationship between mantle, continental crust and oceanic crust. Earth and Planetary Science Letters, 90, 297-314.

Hofmann A.W. (1997) - Mantle geochemistry: the message from oceanic volcanism. Nature, 385, 219-229.

Kelemen P.B. & Dick H.J.B. (1995) - Focused melt flow and localized deformation in the upper mantle: juxtaposition of replacive dunite and ductile shear zones in the Josephine peridotite, SW Oregon. Journal of Geophysical Research, 100, 423-438.

Kelemen P.B., Hirth G., Shimizu N., Spiegelman M. & Dick H.J.B. (1997) - A review of melt migration processes in the adiabatically upwelling mantle beneath oceanic spreading ridges. Philosophical Transactions of the Royal Society of London, Series A, 355, 283-318.

Kelemen P.B., Whitehead J.A., Ahranov E. & Jordahl K.A. (1995) - Experiments on flow focusing in soluble porous media, with applications to melt extraction from the mantle. Journal of Geophysical Research, 100, 475-496.

Klötzli U., Hochleitner R. & Kosler J. (2007) - Lower Triassic mantle-derived magmatism in the IVZ: evidence from laser ablation U-Pb dating of a pegmatite from the eastern Finero Complex (Switzerland). Mitteilungen der Österreichischen Mineralogischen Gesellschaft, 153, 65.

Klötzli U., Klötzli E., Günes Z. & Kosler J. (2009) - Accuracy of Laser Ablation U-Pb Zircon Dating: Results from a Test Using Five Different Reference Zircons. Geostandards and Geoanalytical Research, 33/1, 5-15.

Lensch G. (1968) - Die Ultramafitite der Zone von Ivrea und ihre geologische Interpretation. Schweizerische Mineralogische Petrographische Mitteilung, 48, 91-102.

Lensch G. (1971) - Die Ultramafitite der Zone von Ivrea. Annales Universitatis Saraviensis, 9, 5-146.

Lu M. (1994). Geochemistry and geochronology of the mafic-ultramafic complex near Finero, IVZ, Northern Italy. Unpublished PhD Thesis, J. Gutenberg Universität, Mainz.

Lu M., Hofmann A.W., Mazzucchelli M. & Rivalenti G. (1997a) - The mafic-ultramafic complex near Finero (IVZ), I. Chemistry of MORB-like magmas. Chemical Geology, 140, 207-222.

Lu M., Hofmann A.W., Mazzucchelli M. & Rivalenti G. (1997b) - The mafic-ultramafic complex near Finero (IVZ), II. Geochronology and isotope geochemistry. Chemical Geology, 140, 223-235.

Marchesi M., Mazzucchelli M., Bottazzi P., Ottolini L. & Vannucci R. (1992) - Rocce subcrostali nella zona di Ivrea (Italia): i "corpi minori" della Val Strona. Atti Ticinesi di Scienze della Terra, 35, 97-106.

Marocchi M., Morelli C., Mair V., Klotzli U. & Bargossi G.M. (2008) - Evolution of large silicic magma systems: New U-Pb zircon data on the NW Permian Athesian Volcanic Group (Southern Alps, Italy). Journal of Geology, 116, 480-498.

Matsumoto T., Morishita T., Masuda J., Fujioka T., Takebe M., Yamamoto K. & Arai S. (2005) - Noble gases in the Finero Phlogopite–Peridotites, Italian Western Alps. Earth and Planetary Science Letters, 238, 130–145.

Mayer A., Mezger K. & Sinigoi S. (2000) - New Sm-Nd ages for the IVZ, Sesia and Sessera Valleys (Northern Italy). Journal of Geodynamics, 30, 147-166.

Mazzucchelli M. & Barbieri M.A. (1997) - Geochemical and isotopic characteristics of the mafic rocks of the north-eastern IVZ: The gabbro of Finero and the amphibolites. Atti Ticinesi di Scienze della Terra, Serie Speciale 5, 139-146.

Mazzucchelli M., Marchesi M., Bottazzi P., Ottolini L. & Vannucci R. (1992a) - The Premosello Chiovenda peridotitic body in Ossola Valley (IVZ, Itay). Atti Ticinesi di Scienze della Terra, 35, 75-81.

Mazzucchelli M., Rivalenti G., Brunelli D., Zanetti A. & Boari E. (2009) - Formation of highly-refractory dunite by focused percolation of pyroxenite-derived melt in the Balmuccia peridotite massif (Italy). Journal of Petrology, 50, 1205-1233.

Mazzucchelli M., Rivalenti G., Vannucci R., Bottazzi P., Ottolini L., Hofmann A.W. & Parenti M. (1992b) - Primary positive Eu anomaly in clinopyroxenes of low-crust gabbroic rocks. Geochimica et Cosmochimica Acta, 56, 2363-2370.

Mazzucchelli M., Rivalenti G., Vannucci R., Bottazzi P., Ottolini L., Hofmann A.W., Sinigoi S. & Demarchi G. (1992c) - Trace element distribution between clinopyroxene and garnet in gabbroic rocks of deep crust: an ion microprobe study. Geochimica et Cosmochimica Acta, 56, 2371-2386.

Mazzucchelli M., Zanetti A., Rivalenti G., Vannucci R., Correia C.T. & Tassinari C.C.G. (2010) - Age and geochemistry of mantle peridotites and diorite dykes from the Baldissero body: Insights into the Paleozoic-Mesozoic evolution of the Southern Alps. Lithos, 119, 485-500.

Mehnert K.R. (1975) - The Ivrea Zone. A model of the deep crust. Neues Jahrbuch für Mineralogie Abhandlungen, 125, 156-199.

Morgan Z. & Liang Y. (2005) - An experimental study of the kinetics of lherzolite reactive dissolution with applications to melt channel formation. Contributions to Mineralogy and Petrology, 150, 369-385.

Morishita T., Arai S., Tamura A. (2003) - Petrology of an apatite rich layer in the Finero Phlogopite-Peridotite massif, Italian Western Alps: implications for evolution of a metasomatizing agent. Lithos, 69, 37–49.

Morishita T., Hattori K.H., Terada K., Matsumoto T., Yamamoto K., Takebe M., Ishida Y., Tamura A. & Arai S. (2008) - Geochemistry of apatite-rich layers in the Finero phlogopite–peridotite massif (Italian Western Alps) and ion microprobe dating of apatite. Chemical Geology, 251, 99–111.

Mukasa S.B. & Shervais J.W. (1999) - Growth of subcontinental lithosphere: evidence from repeated dike injections in the Balmuccia lherzolite massif, Italian Alps. Lithos, 48, 287-316.

Nicolas A. (1989) - Structures of Ophiolites and Dynamics of Oceanic Lithospheres. Kluwer Academic Publishers, Hingham, Massachusetts, USA.

Nicolas A. (1992) - Kinematics in magmatic rocks with special reference to gabbros. Journal of Petrology, 33, 891-915.

Nicolas A., Hirn A., Nicolich R., Polino R. & Group E.-C.W. (1990) - Lithospheric wedging in the Western Alps inferred from the ECORS-CROP traverse. Geology, 18, 587-590.

Obermiller W.A. (1994) - Chemical and isotopic variations in the Balmuccia, Baldissero and Finero peridotite massifs (Ivrea Zone, N-Italy). PhD thesis. Max Planck Institut Mainz. 192pp.

O'Hara M.J. (1968) - The bearing of phase equilibria studies in synthetic and natural systems on the origin and evolution of basic and ultrabasic rocks. Earth Sciences Review, 4, 69-133.

Oppizzi P. & Schaltegger U. (1999) - Zircon bearing plagioclasites from the Finero complex (Ivrea zone): dating a Late Triassic mantle hic-cup?. Schweizerische Mineralogische Petrographische Mitteilung, 79, 330-331.

Palzer M., Österle J. & Klötzli U. (2012) - Lithological and structural investigations of the Finero back thrust. Geophysical Research Abstracts, 14, EGU2012-13857.

Peressini G., Quick J.E., Sinigoi S., Hofmann A.W. & Fanning M. (2007) - Duration of a Large Mafic Intrusion and Heat Transfer in the Lower Crust: a SHRIMP U/Pb Zircon Study in the IVZ (Western Alps, Italy). Journal of Petrology 48, 1185-1218.

Phipps Morgan J. & Chen Y.J. (1993) - The genesis of oceanic crust: Magma injection, hydrothermal circulation, and crustal flow. Journal of Geophysical Research 98, 6283-6297.

Piccardo G.B., Zanetti A. & Müntener O. (2007) - Melt/peridotite interaction in the Southern Lanzo peridotite: Field, Textural and geochemical evidence. Lithos, 94, 181-209.

Pin C. (1986) - Datation U-Pb sur zircons à 285 M.a. du complexe gabbro-dioritique du Val Sesia- Val Mastallone et âge tardi-hercynien du métamorphisme granulitique de la zone Ivrea-Verbano (Italie). Académie des Sciences Comptes Rendus, Paris, 303 (II - 9), 827-830.

Presnall D.C. (1976) - Alumina content of enstatite as a geobarometer for plagioclase and spinel lherzolites. American Mineralogist, 61, 582-588.

Pride C. & Muecke G.K. (1982) - Geochemistry and origin of granitic rocks, Scourian Complex, NW Scotland. Contributions to Mineralogy and Petrology, 80, 379-385.

Quick J.E. & Denlinger R.P. (1992) - The possible role of ductile deformation in the formation of layered gabbros in ophiolites. Ofioliti, 17, 249-253.

Quick J. E. & Denlinger R.P. (1993) - Ductile deformation and the origin of layered gabbro in ophiolites. Journal of Geophysical Research, 98, 14015-14027.

Quick J. E., Sinigoi S. & Denlinger R.P. (1992b) - Large-scale deformation and evolution of the underplated ingeous complex of the IVZ. In: IVZ Workshop, 1992 (Quick J. E. & Sinigoi S. eds). U.S. Geological Survey Circular 1089, Varallo, Italy, 14-15.

Quick J. E., Sinigoi S. & Mayer A. (1994) - Emplacement dynamics of a large mafic intrusion in the lower crust, IVZ, northern Italy. Journal of Geophysical Research, 99/B11, 21,559-21,573.

Quick J. E., Sinigoi S. & Mayer, A. (1995) - Emplacement of mantle peridotite in the lower continental crust, IVZ, northwest Italy. Geology, 23/8, 739-742.

Quick J.E., Sinigoi S., Negrini L., Demarchi G. & Mayer A. (1992a) - Synmagmatic deformation in the underplated igneous complex of the IVZ. Geology, 20, 613-616.

Quick J.E., Sinigoi S., Peressini G., Demarchi G., Wooden J.L. & Sbisà A. (2009) - Magmatic plumbing of a large Permian caldera exposed to a depth of 25 km. Geology, 37, 603-606.

Quick J.E., Sinigoi S., Snoke A.W., Kalakay T.J., Mayer A. & Peressini G. (2003) - Geologic map of the Southern IVZ, Northwestern Italy. U.S. Geological Survey, Reston, Virgina, VA.

Raffone N., Le Fèvre B.L., Ottolini L., Vannucci R. & Zanetti A. (2006) - Light-lithophile element metasomatism of Finero peridotite (W Alps): A secondary-ion mass spectrometry study. Microchimica Acta, 155, 251–255.

Raffone N., Le Fèvre B., Zanetti A., Ottolini L., Vannucci R., Rivalenti G. & Mazzucchelli M. (2005) - Slab-related mantle metasomatism: a SIMS investigation of LLE composition of Finero phlogopite-peridotite. Ofioliti, 30/2, 283-284.

Rivalenti G., Garuti G. & Rossi A. (1975) - The origin of the Ivrea-Verbano basic formation (western Italian Alps): Whole rock geochemistry. Bollettino della Società Geologica Italiana, 94, 1149-1186.

Rivalenti G., Garuti G., Rossi A., Siena F. & Sinigoi S. (1981) - Existence of different peridotite types and of a layered igneous complex in the Ivrea Zone of the Western Alps. Journal of Petrology, 22, 127-153.

Rivalenti G. & Mazzucchelli M. (2000) - Interaction of mantle derived magmas and crust in the IVZ and the Ivrea mantle peridotites. In: Ranalli G., Ricci C.A. & Trommsdorff V. (eds) - "Crust Mantle Interactions, Proceedings of the International School Earth and Planetary Sciences", 153-198.

Rivalenti G., Mazzucchelli M., Barbieri M.A., Parenti M., Schmid R. & Zanetti A. (1997) - Garnetite-forming processes in the deep crust: the Val Fiorina case study (IVZ, NW Alps). European Journal of Mineralogy, 9, 1053-1071.

Rivalenti G., Mazzucchelli M., Vannucci R., Hofmann A.W., Ottolini L., Bottazzi P. & Obermiller W. (1995) - The relationship between websterite and peridotite in the Balmuccia peridotite massif (NW Italy) as revealed by trace element variations in clinopyroxene. Contributions to Mineralogy and Petrology, 121, 275-288.

Rivalenti G., Rossi A., Siena F. & Sinigoi S. (1984) - The layered series of the Ivrea-Verbano Igneous Complex, Western Alps, Italy. Tschermaks Mineralogische und Petrographische Mitteilungen, 33, 77-99.

Rutter E.H., Brodie K.T. & Evans P.J. (1993) - Structural geometry, lower crustal magmatic underplating and lithospheric stretching in the IVZ, northern Italy. Journal of Structural Geology, 15, 647-662.

Rutter E., Brodie K., James T. & Burlini L. (2007) - Large-scale folding in the upper part of the IVZ, NW Italy. Journal of Structural Geology, 29, 1-17.

Rutter E.H., Khazanehdari J., Brodie K.H., Blundell D.J. & Waltham D.A. (1999) - Synthetic seismic reflection profile through the Ivrea Zone-Serie dei Laghi continental crustal section, northwestern Italy. Geology, 27, 79-82.

Ryan M.P. (1993) - Neutral buoyancy and structure of mid-ocean ridge magma reservoir. Journal of Geophysical Research, 98, 22321-22338.

Schaltegger U., Antognini M., Girlanda F., Wiechert U. & Müntener O. (2008) - Alkaline mantle melts in the southern Alpine lower crust mark the initiation of late Triassic rifting. 6th Swiss Geoscience Meeting, Abstract Volume, 99-100.

Schaltegger U. & Brack P. (2007) - Crustal-scale magmatic systems during intracontinental strike-slip tectonics: U, Pb and Hf isotopic constraints from Permian magmatic rocks of the Southern Alps. International Journal of Earth Sciences, 96, 1131-1151.

Schmid S.M., Zingg A. & Handy M. (1987)- The kinematics of movements along the Insubric Line and the emplacement of the Ivrea Zone. Tectonophysics, 135, 47-66.

Schnetger B. (1988) - Geochemische untersuchungen an den kinzigiten und stronaliten der Ivrea-zone, Norditalien. Unpublished Ph.D. thesis. University of Göttingen, Germany, pp. 116.

Seitz H.M. & Woodland A.B. (2000) - The distribution of lithium in peridotitic and pyroxenitic mantle lithologies — an indicator of magmatic and metasomatic processes. Chemical Geology, 166, 47–64.

Selverstone J. & Sharp Z.D. (2011) - Chlorine isotope evidence for multicomponent mantle metasomatism in the Ivrea Zone. Earth and Planetary Science Letters, 310, 429–440.

Shervais J.W. (1979) - Thermal emplacement model for the Alpine lherzolite massif at Balmuccia, Italy. Journal of Petrology 20, 795-820.

Siena F. & Coltorti M. (1989) - The petrogenesis of a hydrated mafic - ultramafic complex and the role of amphibole fractionation at Finero (Italian Western Alps). Neues Jahrbuch für Mineralogie Monatshefte, 6, 255-274.

Sills J.D. & Tarney J. (1984) - Petrogenesis and tectonic significance of amphibolites interlayered with metasedimentary gneisses in the Ivrea Zone, Southern Alps, northwest Italy. Tectonophysics, 107, 187-206.

Sinigoi S., Quick J.E., Clemens-Knott D., Mayer A., Demarchi G., Mazzucchelli M., Negrini L. & Rivalenti G. (1994) - Chemical evolution of a large mafic intrusion in the lower crust, IVZ, northern Italy. Journal of Geophysical Research, 99, 21575-21590.

Sinigoi S., Quick J.E., Demarchi G. & Peressini G. (2010) - The Sesia magmatic system. In: Beltrando M., Peccerillo A., Mattei M., Conticelli S., Doglioni C. (eds), The Geology of Italy: tectonics and life along plate margins. Journal of the Virtual Explorer, 36, 1–33, doi: 10.3809/jvirtex.2009.00218

Sinigoi S., Quick J.E., Demarchi G. & Klötzli U. (2011) - The role of crustal fertility in the generation of large silicic magmatic systems triggered by intrusion of mantle magma in the deep crust. Contribution to Mineralogy and Petrology, 162, 691-707.

Sinigoi S., Quick J.E., Mayer A. & Budhan J. (1996) - Influence of stretching and density contrasts on the chemical evolution of continental magmas: an example from the IVZ. Contributions to Mineralogy and Petrology, 123, 238-250.

Sinigoi S., Quick J.E., Mayer A. & Demarchi G. (1995) - Density-controlled assimilation of underplated crust, IVZ, Italy. Earth and Planetary Science Letters, 129, 183-191.

Souquière F. & Fabbri O. (2010) - Pseudotachylytes in the Balmuccia peridotite (Ivrea Zone) as markers of the exhumation of the southern Alpine continental crust. Terra Nova, 22, 70-77.

Stähle V., Frenzel G., Hess J.C., Saupé F., Schmidt S.Th. & Schneider W. (2001) - Permian metabasalt and Triassic alkaline dykes in the Northern Ivrea Zone: clues to the post-Variscan geodynamic evolution of the Southern Alps. Schweizerische Mineralogische Petrographische Mitteilung, 81, 1-21.

Stähle V., Frenzel G., Kober B., Michard A., Puchelt H. & Schneider W. (1990) - Zircon syenite pegmatites in the Finero peridotite (Ivrea Zone): evidence for a syenite from a mantle source. Earth and Planetary Science Letters, 101, 196-205.

Steck A. & Tieche J.C. (1976) - Carte géologique de l'antiforme péridotitique de Finero avec des observations sur les phases de déformation et de recristallisation. Bulletin Suisse de Minéralogie et de Pétrographie, 56, 501-512.

Stolper E. (1980) - A phase diagram for mid-ocean ridge basalts: preliminary results and implications for petrogenesis. Contributions to Mineralogy and Petrology, 74, 13-27.

Suhr G. (1999) - Melt migration under oceanic ridges: inferences from reactive transport modelling of upper mantle hosted dunites. Journal of Petrology, 40, 575-599.

Suhr G., Hellebrand E., Snow J.E., Seck H.A. & Hofmann A.W. (2003) - Significance of large, refractory dunite bodies in the upper mantle of the Bay of Islands Ophiolite. Geochemistry Geophysics Geosystems, 4. doi: 1029/2001GC000277.

Tarantino S.C., Zanetti A., Mazzucchelli M., Zema M., Heidelbach F., Miyajima N., Ghigna P., Olivi L. & Gasparini E. (2012) - Diopside-titanian pargasite intergrowth in magmatic pockets and metasomatic haloes from Balmuccia mantle peridotite. European Mineralogical Conference 2012 (Frankfurt am Main, 02-06/09/2012), Vol. 1, EMC2012-391-1.

Vavra G., Schmid R. & Gebauer D. (1999) - Internal morphology, habit and U-Th-Pb microanalysis of amphibolite-to-granulite facies zircons: geochronology of the Ivrea Zone (Southern Alps). Contributions to Mineralogy and Petrology, 134, 380-404.

Vogt P. (1962) - Geologish-petrographische Untersuchungen im Peridotitstock von Finero. Schweizerische Mineralogische Petrographische Mitteilung, 42, 59-125.

von Quadt A., Ferrario A., Diella V., Hansmann W., Vavra G. & Köppel V. (1993) - U-Pb ages of zircons from chromitites of the phlogopite peridotite of Finero, Ivrea Zone, N-Italy. Schweizerische Mineralogische Petrographische Mitteilung, 73, 137-138.

Voshage H., Hofmann A.W., Mazzucchelli M., Rivalenti G., Sinigoi S., Raczek I. & Demarchi G. (1990) - Isotopic evidence from the Ivrea Zone for a hybrid lower crust formed by magmatic underplating. Nature, 347, 731-736.

Voshage H., Hunziker J. C., Hofmann A.W. & Zingg A. (1987) - A Nd and Sr isotopic study of the Ivrea zone, Southern Alps, N-Italy. Contributions to Mineralogy and Petrology, 97, 31-42.

Voshage H., Sinigoi S., Mazzucchelli M., Demarchi G., Rivalenti G. & Hofmann A.W. (1988) - Isotopic constraints on the origin of ultramafic and mafic dikes in the Balmuccia peridotite (Ivrea Zone). Contributions to Mineralogy and Petrology, 100, 261-267.

Wedepohl K.H., Hartmann G. & Schnetger B. (1989) - Chemical composition of ultramafic rocks and metasediments of the Ivrea Zone. In: Varallo Conference on the Lower Continental Crust. Consiglio Nazionale delle Ricerche, Varallo, Italy.

Zaccarini F., Stumpfl E.F. & Garuti G. (2004) - Zirconolite and Zr–Th–U minerals in chromitites of the Finero complex, western Alps, Italy: evidence for carbonatite-type metasomatism in a subcontinental mantle plume. Canadian Mineralogist, 42, 1825-1845.

Zanetti A., Mazzucchelli M., Rivalenti G. & Vannucci R. (1999) - The Finero phlogopite-peridotite massif: an example of subduction-related metasomatism. Contributions to Mineralogy and Petrology, 134, 107-122.

Zanetti A., Mazzucchelli M., Sinigoi S., Giovanardi T., Peressini G. & Fanning M. (2013) - SHRIMP U-Pb zircon Triassic intrusion age of the Finero Mafic Complex (IVZ, Western Alps) and its geodynamic implications. Journal of Petrology, 54, 2235-2265.

Zanetti A., Mazzucchelli M., Sinigoi S., Giovanardi T., Peressini G. & Fanning M. (2014) – Erratum. SHRIMP U-Pb zircon Triassic intrusion age of the Finero Mafic Complex (IVZ, Western Alps) and its geodynamic implications. Journal of Petrology, 55, 1239-1240.

Zingg A. (1983) - The Ivrea and Strona-Ceneri zones (Southern Alps, Ticino and N-Italy) - A review. Schweizerische Mineralogische und Petrographische Mitteilungen, 63, 361-392.